

ANALYSIS OF PROCESS-INDUCED DEFECTS ON STEERED-FIBER PANELS FOR AERONAUTICAL APPLICATIONS

Olben Falcó Salcines

Dipòsit legal: Gi. 1951-2014
<http://hdl.handle.net/10803/284334>

ADVERTIMENT. L'accés als continguts d'aquesta tesi doctoral i la seva utilització ha de respectar els drets de la persona autora. Pot ser utilitzada per a consulta o estudi personal, així com en activitats o materials d'investigació i docència en els termes establerts a l'art. 32 del Text Refós de la Llei de Propietat Intel·lectual (RDL 1/1996). Per altres utilitzacions es requereix l'autorització prèvia i expressa de la persona autora. En qualsevol cas, en la utilització dels seus continguts caldrà indicar de forma clara el nom i cognoms de la persona autora i el títol de la tesi doctoral. No s'autoritza la seva reproducció o altres formes d'explotació efectuades amb finalitats de lucre ni la seva comunicació pública des d'un lloc aliè al servei TDX. Tampoc s'autoritza la presentació del seu contingut en una finestra o marc aliè a TDX (framing). Aquesta reserva de drets afecta tant als continguts de la tesi com als seus resums i índexs.

ADVERTENCIA. El acceso a los contenidos de esta tesis doctoral y su utilización debe respetar los derechos de la persona autora. Puede ser utilizada para consulta o estudio personal, así como en actividades o materiales de investigación y docencia en los términos establecidos en el art. 32 del Texto Refundido de la Ley de Propiedad Intelectual (RDL 1/1996). Para otros usos se requiere la autorización previa y expresa de la persona autora. En cualquier caso, en la utilización de sus contenidos se deberá indicar de forma clara el nombre y apellidos de la persona autora y el título de la tesis doctoral. No se autoriza su reproducción u otras formas de explotación efectuadas con fines lucrativos ni su comunicación pública desde un sitio ajeno al servicio TDR. Tampoco se autoriza la presentación de su contenido en una ventana o marco ajeno a TDR (framing). Esta reserva de derechos afecta tanto al contenido de la tesis como a sus resúmenes e índices.

WARNING. Access to the contents of this doctoral thesis and its use must respect the rights of the author. It can be used for reference or private study, as well as research and learning activities or materials in the terms established by the 32nd article of the Spanish Consolidated Copyright Act (RDL 1/1996). Express and previous authorization of the author is required for any other uses. In any case, when using its content, full name of the author and title of the thesis must be clearly indicated. Reproduction or other forms of for profit use or public communication from outside TDX service is not allowed. Presentation of its content in a window or frame external to TDX (framing) is not authorized either. These rights affect both the content of the thesis and its abstracts and indexes.



Universitat de Girona

DOCTORAL THESIS

ANALYSIS OF PROCESS-INDUCED DEFECTS ON
STEERED-FIBER PANELS FOR AERONAUTICAL
APPLICATIONS

OLBEN FALCÓ SALCINES

2014



Universitat de Girona

DOCTORAL THESIS

ANALYSIS OF PROCESS-INDUCED DEFECTS ON
STEERED-FIBER PANELS FOR AERONAUTICAL
APPLICATIONS

OLBEN FALCÓ SALCINES

2014

TECHNOLOGY DOCTORATE PROGRAM

ADVISORS

DR. JOAN ANDREU MAYUGO MAJÓ

DR. NARCIS GASCON CLARIO

Universitat de Girona

DR. CLÁUDIO SAÚL LOPES

IMDEA Materials, Madrid

A thesis submitted for the degree of Doctor by the
University of Girona

To whom it might concern,

Dr. Joan Andreu Mayugo Majó, Dr. Narcis Gascons Clario Assistant Professors at the *Universitat de Girona* of the Department of *Enginyeria Mecànica i de la Construcció Industrial*, and Dr. Cláudio Saúl Lopes, Researcher at the *IMDEA Materials Institute, Madrid*

WE DECLARE:

That the thesis entitled *Analysis of Process-induced Defects on Steered-Fiber Panels for Aeronautical Applications*, presented by Olben Falcó Salcines to obtain a doctoral degree, has been completed under our supervision. We also certify that Olben Falcó Salcines was a full time graduate student at *Universitat de Girona, Spain*, from October 2009 to present.

For all intents and purposes, we hereby sign this document.

Dr. Joan Andreu Mayugo Majó
Universitat de Girona,

Dr. Cláudio Saúl Lopes
IMDEA Materials, Madrid

Dr. Narcis Gascons Clario
Universitat de Girona

Girona, February 2014.

To my Father and my brothers

Acknowledgements

First of all, I would like to express my gratitude to my supervisors Dr. Joan Andreu Mayugo, Dr. Claudio Saúl Lopes and Narcis Gascons Clario, for their leadership, guidance and contribution to this in this thesis. A very special personal thank you goes to Dr. Claudio Lopes, for his constant support, despite the distance, and especially for the time dedicated to sharing his knowledge and experience in the challenging field of advanced composite materials. I would like to thank all of them for being by my side all this time treating me not only in a professional manner but rather, in one of sincere friendship.

I also wish to thank Dr. Josep Costa Balanzat, for making me part of the VLANCO project (MAT2009-07918) under which the thesis was conducted. I thank you for your continued support and for encouraging me to publish the results obtained. Thank you very much Dr. Albert Turon, for always passing by near my desk and giving me the confidence to ask questions and clear up any doubts.

I would like to thank Dr. Norbert Blanco Villaverde and all those who taught the Master in Analysis of Advanced Material in Structural Design, who brought back memories of my days as a student. I am deeply grateful to all my colleagues and members of the AMADE research group. Having them by my side, has meant that the doctoral burden has been lighter as it was shared during these last few years. I want to make special mention of Yunior Adolfo Batista and the members of the laboratory who contributed to the realization of the tests in this paper. Thanks to all my distant and close friends, Raul Cruz, Tamer Sebaey and Eduardo Martin for the moments we shared.

Finally, my most sincere gratitude to the Mayugo Family, for treating me and making me feel like one of them. To all my family and brothers for their unconditional support and patience with me during this time.

To all of you, I hold very dear, thank you very much!

Funding

The period of research has been funded within the framework of the Doctorate Technology Program by the Comissionat per a Universitats i Recerca del Departament d'Innovació, Universitats i Empresa de la Generalitat de Catalunya, under FI pre-doctorate Grant 2010FI_B00658, started in May of 2010 until present. Also, the present work has been partially funded by the Spanish Government through the (*Ministerio de Economía y Competitividad*) under the Project MAT2009-07918.

List of Symbols

Symbol	Description	
ε_{ij}	strain tensor	
θ_i	fiber angle mismatch	deg
ν	Poisson's ratio	
ρ	radius of curvature	mm
σ_c	residual compression strength	MPa
φ	fiber angle orientation	deg
ϕ	orientation of the axis of fiber angle variation in a VSP	deg
σ_{ij}	stress tensor	
A_d	normalized delamination area	mm ²
C_w	course width	mm
d	distance	mm
E	Young's modulus	MPa
E_i	impact energy	J
\bar{E}_a	normalized dissipate energy	
F_d^{stat}	threshold delamination load	kN
F_p^{stat}	peak impact load	kN
FI_{FC}	Fiber compression failure index	
FI_{FT}	Fiber tensile failure index	
FI_{MC}	Matrix compression failure index	
FI_{MT}	Matrix cracking failure index under tensile loading	
G	shear elasticity modulus	MPa
H_i	impactor drop height	mm
L	length	mm

Symbol	Description	
M_i	impactor mass	kg
n	course identifier	
n_t	number of tows per course	
S^L	unidirectional shear strength	MPa
S^T	transverse shear strength	MPa
t	ply thickness	mm
T_0	fiber angle at the centre of a VSP	deg
T_1	fiber angle at a characteristic distance, d , in a VSP	deg
t_w	tows width	
t_n	nominal thickness	mm
u, v, w	displacements	mm
V	velocity	m/s
W	width	mm
W_e	effective course width in the direction of shift	mm
x, y, z	global coordinate axis	mm
x', y', z'	local coordinate axis	mm
X^C	unidirectional Compressive strength in the fiber direction	MPa
X^T	unidirectional tensile strength in the fiber direction	MPa
Y^C	unidirectional Compressive strength in the transverse to fiber direction	MPa
Y^T	unidirectional tensile strength in the transverse to fiber direction	MPa

Subscripts

c	center
is	in-situ
max	maximum
min	minimum

Constants

g	acceleration due to gravitational force	9.81 m/s ²
-----	---	-----------------------

List of Acronyms

Acronym	Description
AFP	Automated Fiber Placement
AITM	Airbus Industries Test Method
ASTM	American Society for Testing Materials
ATL	Automated Tape Laying
CAI	Compression After Impact
CDT	Critical Damage Threshold
CFRP	Carbon Fiber Reinforced Plastic
CLT	Classical Lamination Theory
CTS	Continuous Tow Shearing
DIC	Digital Image Correlation
DTL	Delamination Threshold Load
DFP	Dry Fiber Placement
FE	Finite Element
LaRC	Langley Research Center
LEFM	Linear Elastic Fracture Mechanics
LVI	Low Velocity Impact
NDI	Non-Destructive Inspection
NCLs	Non-Conventional Laminates
NLR	National Aerospace Laboratory
OHT	Open Hole Tensile
PFA	Progressive Failure Analyses
UNT	Un-Notched tensile
VSP	Variable Stiffness Panels

Publications

This doctoral thesis has been presented as a compendium of papers according to the regulations of the University of Girona (*Normativa d'ordenació dels ensenyaments universitaris de doctorat de la Universitat de Girona Aprovada pel Consell de Govern en la sessió 3/12, de 26 d'abril de 2012*). The transcription of the articles and the references to the journals in which they have been published, accepted or submitted for publication are presented in the main body of this thesis.

The complete references of the papers during the development of this thesis with their corresponding impact factors, quartile and category of the journals are listed below:

1. **O. Falcó**, J.A. Mayugo, C.S. Lopes, N. Gascons, A. Turon and J. Costa. Variable-stiffness composite panels: As-manufactured modeling and its influence on the failure behavior. *Composites Part B: Engineering*, Vol. 56: pp. 660-669, 2014. **doi:** 10.1016/j.compositesb.2013.09.003
(Impact Factor: 2.143, Journal 5 of 24, *Quartile 1*, Category: *Material Science, Composites*)
2. **O. Falcó**, J.A. Mayugo, C.S. Lopes, N. Gascons and J. Costa. Variable-stiffness composite panels: Defect tolerance under in-plane tensile loading. *Composites Part A: Applied Science and Manufacturing*, Submitted Nov. 2013.
(Impact Factor: 2.744, Journal 2 of 24, *Quartile 1*, Category: *Material Science, Composites*)
3. **O. Falcó**, C.S. Lopes, J.A. Mayugo, N. Gascons and J. Renart. Effect of tow-drop gaps on the damage resistance and tolerance of Variable Stiffness Panels. *Composite Structures*, Submitted Feb. 2014.
(Impact Factor: 2.231, Journal 4 of 24, *Quartile 1*, Category: *Material Science, Composites*)

The present work has also resulted in the following conferences presentations:

- **O. Falcó**, J.A. Mayugo, C.S. Lopes, N. Gascons and J. Costa. Variable Stiffness Panels: Modeling Methodology, Prediction of the Failure Behavior, and Experimental Study of Tow-Drop Defects. MATCOMP-13, ISBN 978-84-616-4681-4. Jul-2013, Algeciras, Spain.
- **O. Falcó**, C.S. Lopes and J. Costa. Variable stiffness composite panels. Modeling methodology and prediction of the failure behaviour. ICCS17-17th International Conference on Composite Structures Porto, Portugal, June 17-21, 2013
- **O. Falcó**, C.S. Lopes, N. Gascons and J. Costa. Variable Stiffness panels: Compression and Buckling response. MATCOMP-11, ISBN 978-84-8458-352-3. Jul-2011, Girona, Spain.
- **O. Falcó**, N. Gascons, C.S. Lopes, and J. Juliá. Variable Stiffness panels: Definition and virtual test. XVIII National congress of Mechanical Engineering, ISSN 0212-5074. Nov-2010, Ciudad Real, Spain.

Dr. Joan Andreu Mayugo Majó, Dr. Narcis Gascons Clario, Dr. Cláudio Saúl Lopes, Dr. Josep Costa Balanzat, Dr. Albert Turon Travesa and Dr. Jordi Renart Canalias as co-authors of the following articles:

- O. Falcó, J.A. Mayugo, C.S. Lopes, N. Gascons, A. Turon and J. Costa. Variable-stiffness composite panels: As-manufactured modeling and its influence on the failure behavior. *Composites Part B: Engineering*, Vol. 56: pp. 660-669, 2014. **doi:** 10.1016/j.compositesb.2013.09.003
- O. Falcó, J.A. Mayugo, C.S. Lopes, N. Gascons and J. Costa. Variable-stiffness composite panels: Defect tolerance under in-plane tensile loading. *Composites Part A: Applied Science and Manufacturing*, Submitted Nov. 2013.
- O. Falcó, C.S. Lopes, J.A. Mayugo, N. Gascons and J. Renart. Effect of tow-drop gaps on the damage resistance and tolerance of Variable Stiffness Panels. *Composite Structures*, Submitted Feb. 2014.

accept that and agree to Mr. Olben Falcó Salcines presenting the above cited articles as principal author and as part of his doctoral thesis and that said articles cannot, therefore any part of any other doctoral thesis and as such, for all intents and purposes they hereby sign this document.

Dr. Joan Andreu Mayugo Majó
Universitat de Girona

Dr. Cláudio Saúl Lopes
IMDEA Materials, Madrid

Dr. Narcis Gascons Clario
Universitat de Girona

Dr. Josep Costa Balanzat
Universitat de Girona

Dr. Albert Turon Travesa
Universitat de Girona

Dr. Jordi Renart Canalias
Universitat de Girona

Girona, February 2014.

Table of Contents

List of Symbols	xi
List of Acronyms	xiii
Summary / Resumen / Resum	xxi
1 Introduction and Objectives	1
1.1 Introduction	1
1.2 Objectives	3
1.3 Thesis Outline	4
2 State of the Art	7
2.1 Introduction	7
2.2 Automated Fiber Placement	7
2.2.1 AFP process description	8
2.2.2 Applications in the Aerospace Industry	9
2.3 Manufacturing Restrictions and Process-induced Defects	11
2.3.1 Process-induced Defects	11
2.3.2 Strategies for minimization of defects and their influence	14
2.4 Variable Stiffness Composites Panels	16
2.4.1 Variable-Stiffness Laminate Definition	17
2.4.2 Development of modeling for VSP	19
2.5 Experimental works in VSP	23
References	26

3	Variable-stiffness composite panels: As-manufactured modeling and its influence on the failure behavior	33
4	Variable-stiffness composite panels: Defect tolerance under in-plane tensile loading	45
5	Effect of tow-drop gaps on the damage resistance and tolerance of Variable Stiffness Panels	71
6	Conclusions and Future Work	93
6.1	Introduction	93
6.2	Conclusions	94
6.2.1	Methodology for modeling variable stiffness panels taking into account manufacturing constraint	94
6.2.2	Manufacturing and experimental testing	95
6.3	Future Work	97

Summary

The use of laminated composites for structural applications has increased significantly in the aerospace industry. Recently, the capacity for large-scale automation of the laminated composite production process added to its high performance as a material for the design of lightweight, has made it even more attractive. Currently, the use of Automated Fiber Placement technology allows, for example, large composite aircraft components to be manufactured with high quality materials while, at the same time, offering scope to introduce new laminate concepts. Among such concepts are the tow-steered panels with curved fibers which stand out thanks to their improved structural efficiency and their ability to obtain variable stiffness and load redistribution. However, despite these advantages, conventional laminates with straight fiber architectures are still preferred by designers. The main reason that limits the use of variable stiffness laminates is the incomplete knowledge of the effect of process-induced defects and the response to damage and structural failure mechanisms.

The study of the influence of the defects induced in varying stiffness panel manufacture is still in its early days. The work presented in this thesis focuses on analyzing this influence. To fulfill this objective, initially a methodology for modeling numerical simulation, which takes into account the manufacturing constraints, has been developed. This pre-processing tool enables unconventional laminates to be delineated and allows for progressive damage (from inception to final breakdown) to be simulated for such designs. In the second part of this thesis, experimental tests have been carried out to study the effects on the mechanical response of manufacturing defects due to tow-drops. The impact of these defects on laminates with discontinuities in the angle between courses was investigated in samples with and without a hole. Tests have also been conducted on the influence of such defects on low-velocity impact damage tolerance.

In general, the experimental results show that the influence of induced defects in manufacturing is more significant in samples without holes, where the defects themselves are acting as the initiators of the damage, while in the samples with a hole, failure mechanisms are primarily driven by the stress concentration due to the discontinuity that the hole itself causes. A similar conclusion is obtained in the analysis of the residual resistance compression after impact. The results reveal that resin rich areas (gap-defects) are relevant only in low values of impact energy. This indicates that the residual strength reduction is mainly caused by impact damage, rather than manufacturing-induced defects.

Future research should be focused on the influence of other types of defects not studied in this work. In addition, progressive damage simulation of variable-stiffness laminates could be addressed and the numerical results could be validated with experimental campaigns.

Resumen

El uso de compuestos laminados para aplicaciones estructurales ha aumentado notablemente en la industria aeroespacial. A su elevado rendimiento como material para la concepción de estructuras ligeras, se le ha añadido la capacidad de automatización a gran escala del proceso de producción. Actualmente, el uso de la tecnología de 'Automated Fiber Placement' permite, por ejemplo, la fabricación de grandes componentes de material compuesto para aviones con una elevada calidad y, a la vez, brinda la posibilidad de introducir nuevos conceptos de laminados. Entre estos conceptos están los 'tow-steered panels' con fibras curvas que resaltan por una mejora de la eficiencia estructural debido a su capacidad de obtener rigidez variable y de redistribución de las cargas. Sin embargo, a pesar de estas ventajas, los laminados convencionales con arquitecturas de fibra rectas son aún preferidos por los diseñadores. Las principales razones que limitan el uso de los laminados de rigidez variable es el incompleto conocimiento del efecto de los defectos inducidos en su fabricación y su respuesta a los mecanismos de daño y fallo estructural.

El estudio de la influencia de los defectos inducidos en la fabricación en los paneles de rigidez variable se encuentra en una etapa temprana de investigación. El trabajo presentado en esta tesis está enfocado en el análisis de esta influencia. Para el cumplimiento de este objetivo, inicialmente ha sido desarrollada una metodología de modelado para la simulación numérica que tiene en cuenta las limitaciones de fabricación. Esta herramienta de pre-proceso permite definir los laminados no convencionales y permitirá la simulación del daño progresivo desde su inicio hasta el fallo final de este tipo de diseños. En la segunda parte de esta tesis, se han llevado a cabo ensayos experimentales para el estudio de los efectos sobre la respuesta mecánica de los defectos de fabricación debido a los 'tow-drop'. Se han investigado su efecto en laminados con discontinuidad en el ángulo entre 'courses' en probetas con y sin agujero. También se han realizado pruebas sobre la influencia de los defectos mencionados en la tolerancia al daño bajo eventos de impacto a baja velocidad.

En general los resultados experimentales muestran que la influencia de los defectos inducidos en la producción es más significativa en probetas sin agujero, donde son los propios defectos que actúan como iniciadores del daño. Mientras, en las probetas con agujero los mecanismos de fallo son primordialmente conducidos por la concentración de tensiones debido a la discontinuidad que provoca el propio agujero. Una conclusión similar se obtiene en el análisis de la resistencia residual a compresión después del impacto. Los resultados revelan que las zonas ricas de resina ('gap-defects') tiene relevancia solamente para valores bajos de energía de impacto. Esto indica que la reducción de resistencia es llevada a cabo principalmente por el daño causado por el impacto, más que los defectos inducidos por la fabricación.

Investigaciones futuras deben centrarse en la influencia de otros tipos de defectos no estudiados en este trabajo. Además, se deberían realizar simulaciones de daño progresivo en laminados de rigidez-variable y validar los resultados numéricos mediante campañas experimentales.

Resum

L'ús de materials compostos laminats en aplicacions estructurals ha augmentat notablement a la indústria aeroespacial. Al seu elevat rendiment com a material per a la concepció d'estructures lleugeres, se l'hi ha afegit la capacitat d'automatització del procés de producció a gran escala. Actualment, l'ús de la tecnologia de 'Automated Fiber Placement' permet, per exemple, la fabricació de grans components de compòsit per a avions amb una elevada qualitat i, a la vegada, ens dóna la possibilitat d'introduir nous conceptes de laminats. Entre aquests conceptes hi ha els 'tow-steered panels' amb fibres corbes que destaquen per la millora de l'eficiència estructural donada la seva capacitat d'obtenir rigidesa variable i de redistribució de càrregues. Tanmateix, malgrat aquestes avantatges, els laminats convencionals amb arquitectures de fibres rectes són encara la solució preferida pels dissenyadors. Les principals raons que limiten l'ús dels laminats de rigidesa variable és l'incomplet coneixement de l'efecte dels defectes induïts durant la seva fabricació i la seva resposta als mecanismes de dany i de fallada estructural.

L'estudi de la influència dels defectes induïts en la fabricació en els panells de rigidesa variable es troba en una fase inicial de recerca. El treball presentat en aquesta tesi està enfocat en l'anàlisi d'aquesta influència. Pel compliment d'aquest objectiu, primer ha estat desenvolupada una metodologia de modelat per a la simulació numèrica que té en compte les limitacions de fabricació. Aquesta eina de pre-procés permet definir els laminats no convencionals que permetrà la simulació del dany progressiu des del seu inici fins a la fallada final d'aquest tipus de dissenys. A la segona part d'aquesta tesi, s'han portat a terme assaigs experimentals per a l'estudi dels efectes sobre la resposta mecànica dels defectes de fabricació deguts als 'tow-drop'. S'ha investigat el seu efecte en laminats amb discontinuïtat en l'angle entre els 'courses' en provetes amb i sense forat. També s'han realitzats proves sobre la influència dels defectes de producció sobre la tolerància al dany sota esdeveniments d'impacte a baixa velocitat.

En general els resultats experimentals mostren que la influència dels defectes induïts en al producció és més significativa en provetes sense forat, on són els propis defectes que actuen com iniciadors del dany. Mentre, en les provetes amb forat els mecanismes de fallada són principalment conduïts per la concentració de tensions degut a la discontinuïtat que provoca el propi forat. Una conclusió similar s'obté en l'anàlisi de la resistència residual a compressió després de l'impacte. Els resultats revelen que les zones riques de resina ('gap defects') tenen rellevància només per a valors baixos d'energia d'impacte. Això indica que la reducció de resistència es porta a terme principalment pel dany causat amb l'impacte, més que pels defectes induïts per la fabricació.

Futures investigacions han de centrar-se en la influència d'altres tipus de defectes no estudiats en aquest treball. A més, s'haurien de realitzar simulacions de dany progressiu en laminats de rigidesa variable i validar els resultats numèrics amb campanyes experimentals.

Chapter 1

Introduction and Objectives

1.1 Introduction

The use of laminated composites made of epoxy resins, and reinforced with carbon fibers for lightweight structural applications, has increased notably in recent decades. Thanks to this composite material's in terms of specific stiffness (stiffness/density) and specific strength (strength/density) its application has been extended to the aerospace industry. In addition, with the Automated Fiber Placement (AFP) technology, it is possible to manufacture large structures while still ensuring high quality, reliability and production. This technology can be used to design specific components, by tailoring the direction and placement of fiber laminates; also known as tow-steered composites.

Steered laminates Variable Stiffness Panels (VSP) are noted for greatly improving the structural efficiency of composites. They are very effective when buckling and post-buckling responses, caused by transferring the applied loads, are considered, and they are more tolerant to notches and stress concentration effects. In a variable-stiffness composite, where the fibers follow curved paths, the stiffness can be tailored to create more efficient load redistribution, resulting in weight savings that cannot be achieved using conventional laminates. However, despite the potential benefits of the AFP and VSP, traditional straight-fiber laminates based on 0° , 90° and -45° ply angles are still predominantly used.

Meanwhile, some of the crucial issues related to VSP concerning manufacturing viability, structural performance or design complexity have been under investigation. The full details of the mechanisms that lead to failure and the mechanical response of a VSP are not yet fully understood. In particular, it is unclear just what the influence of embedded defects is. These defects are mainly gaps, overlaps and the fiber angle discontinuities induced by the manufacturing constraints of the AFP system.

While introducing VSP may demand an advanced level of automated technology or analytical optimization tools, due to the complexity of the design, it also provides reliable methodologies to simulate the mechanical response. Therefore, it would firstly be beneficial to develop virtual testing tools that analyze the mechanical response in terms of stiffness or buckling modes (elastic behavior of the material). Then, the capabilities of these tools could be used to predict structural behavior until failure. Damage modeling under quasi-static and the impact loads in VSP is a novel field of research. In addition, these computational tools would reduce the time and cost associated with experimental testing.

All in all, VSP certification will be the most critical and imperative issue to introducing VSP into aerospace engineering. Certification involves an extensive test program which could in fact be unfeasible because of the large number of design possibilities for a VSP and the multiple variables of study. In the past, experimental tests were carried out in order to study the structural behavior of VSP as to stiffness and strength response. Although the advantages of VSP in comparison with conventional laminates have been demonstrated by experimental test programs under in-plane and thermal loading condition. However, the influence of the process-induced defects under different loading conditions needs to be analyzed on a reduced sub-level scale. Theoretical and numerical investigations on the influence of the tow-drop fiber-free areas and staggering on the stiffness and strength of VSP laminates have been developed. However, for a better comprehension of the mechanical response, failure and damage mechanisms that occur in a VSP need to be addressed within the framework of test programs. Defect tolerance analyses of VSP under in-plane and (out-of-plane) Low-Velocity Impact (LVI) loads is a new field that requires investigation.

The aim of this thesis is to contribute to the study of questions that remain, for the moment, as unresolved stage and need to be addressed. For instance, what are the features that will need to be added to the existing computational tools to study damage mechanism

and the occurrence of delaminations in VSP? Is it possible to quantify the effect of the manufacturing-induced defects in a VSP by taking into account the different failure and damage mechanisms that occur in a real environment? How can we evaluate the impact damage resistance as well as the residual strength, or damage tolerance, in a representative sub-domain of a real VSP?

In order to answer these questions, experimental work should be carried out to validate the results predicted for the VSP, as well as to validate the numerical analysis of the influence of tow-drops on panel strength. This study attempts to provide some insight into these issues. The objectives established are explained as follows:

1.2 Objectives

The main goal of this thesis is to investigate the influence of the process-induced defects on the damage resistance and damage tolerance of Variable Stiffness Panels. In order to evaluate the mechanical behavior of these non-conventional laminates and to achieve this objective, a novel numerical simulation tool is developed and experimental tests are carried out under in-plane and out-of-plane loading. A brief description of these two tasks and their relationship are presented in the following statements:

- To develop a pre-processing framework in order to obtain parametric VSP models with different configurations and modeling strategies. In this partial objective a modeling methodology is developed to simulate and predict the mechanical response from damage onset to structural collapse, taking into account the manufacturing constraints and process-induced defects.
- To study the effect of manufacturing tow-drop defects in VSP. For this investigation, two experimental test campaigns are carried out. Firstly, the defect tolerance for notched and open-hole specimens under tensile loading is tested. Secondly, the effect of tow-drop gaps under drop-weight impact events is studied. For damage tolerance analysis, the residual compressive strengths are obtained through compression after impact tests.

1.3 Thesis Outline

As stated in the objectives, the thesis outline is structured as follows.

In Chapter 2, a survey of the literature provides an overview of the the state-of-the-art research in three relevant areas. These include Automated Fiber Placement technology, Variable Stiffness tow-steered laminates and a review of process-induced defects. In this chapter, the technological development of the tow steered system and its impact on the aeronautical industry is presented. In addition, the most relevant aspects of VSP, which can only be produced with this technology, are presented. This section includes the main characteristics of these non-conventional laminates compared with their conventional counterpart in terms of design, manufacture and mechanical response. Particular attention has been given to the different studies and modeling approaches of VSP. Finally, a detailed review is carried out on the main defects originated during the manufacturing process and their influence on the strength reduction of the laminates.

The main body of the thesis, presented in Chapters 3, 4 and 5, is structured as a compendium of papers. All of which refer to the partial objectives defined in this thesis. In Chapter 3, a numerical analysis tool has been developed for structural simulations in a three-dimensional domain. This tool contains structured mesh generator possibilities, thus allowing advanced FE models for reliable analyses of progressive damage and delaminations. The proposed methodology takes into account the effect of the discontinuities of the fiber orientation between the courses, as well as the effect of the fiber-free areas. In this paper, a comparison between different configurations and modeling approaches for VSP under tensile loading is presented. This work also includes post-process analyses which stimulate the mechanical response of panels with steered fibers and include predicting of first-ply failure.

The influence of several manufacturing parameters is discussed in Chapter 4. The results of an experimental work on the un-notched and open-hole tensile strength of the steered laminates are presented. This paper investigates the effects resulting from the manufacturing process such as fiber angle discontinuities between different tow courses in a ply and the process-induced defects. In order to carry out this experimental campaign, some specific test matrices were developed to reproduce an equivalent sub-domain of VSP with defects included. The manufacturing parameter tow-drop gap-coverage and the staggering technique are discussed.

In the third paper, in Chapter 5, an experimental study of the effect of tow-drop gaps in Variable Stiffness Panels under drop-weight impact events is presented. The results indicate that the influence of the gap defects is only relevant under small-impact energy values.

This thesis is concluded in Chapter 6 with an exposition of its main accomplishments, and suggests issues that deserve future research.

Chapter 2

Automated Fiber Placement and Variable Stiffness Panels

2.1 Introduction

An overview of the development of Automated Fiber Placement technology and Variable Stiffness Panels will be presented in this chapter. The chapter begins with a brief description of the development of Fiber Placement and its application in the aerospace industry in the past decade is discussed. In addition, the limitations to steered tow-drop composite manufacture and the principal process-induced defects that take place are presented. Furthermore, the current improvement in the fiber placement machine head in order to reduce these defects and enhance reliability and productivity is addressed. Finally, the Variable-Stiffness design concepts applied in this thesis are introduced along with the development of the Finite Element Method for modeling.

2.2 Automated Fiber Placement

Automated Fiber Placement (AFP) is a major advance in the state-of-the-art of automated processes for the production of fiber-reinforced composites of exceptional quality with high accuracy and repeatability. AFP technology is a hybrid process that combines the advantages of both filament winding and Automated Tape Laying (ATL) systems. The payout capability of filament winding is used mainly for rotational structures. However, the major geometric restriction is that concave contours cannot be wound, because the

fibers are under tension and will bridge across the cavity [1]. Whereas, ATL stands out because of achievable high productivity rates for large flat laminates such as wing skins. Its main disadvantages are related with high initial capital expenditure, limited geometric complexity capability and higher material wastage rates [2]. The AFP was developed to allow the automated fabrication of large parts that could not be fabricated by either tape laying or filament winding [3].

2.2.1 AFP process description

AFP machines automatically place multiple individual pre-impregnated tows onto a mandrel at high speed, using a numerically controlled head with multiple degrees of freedom (DOF) to dispense, clamp, cut and restart each tow during placement. Its advantages are variable bandwidth of material, localized build-ups and cutouts, constant thickness on tapered shapes, in-process compaction, no limitation on ply orientations and low material scrap rates of only 2-5%. The adjustable tension employed during the manufacturing process allows the machine to lay tows into concave contours, limited only by the diameter of the roller mechanism in the head. This allows the manufacture of complicated ply shapes, similar to those that can be obtained by hand lay-up [1]. In addition, AFP technology permits the manufacture of advanced composite structures, in which the fiber orientation angle is allowed to vary continuously throughout the structure and also following curvilinear paths [4, 5]. The use of this technology permits the manufacture of larger and complex structures, providing more strength and stiffness where needed, opening a future branch for optimizing tailored smart structures. Currently, increases in productivity and reliability are the main goals of the AFP systems for industrial applications.

The main improvements to inventions with the AFP in the past decade, have been focused on the machine head. The productivity is able to be achieved by not only using multiple placement heads, replaceable creels and replaceable placement heads [6], but also by increasing the material lay-down rates (2000 in/min) with the introduction of High-Speed AFP systems [7, 8]. In addition, the ability to perform high-speed events "on-the-fly" during fabrication needs to be guaranteed. These are all related to the capabilities for cutting or adding tows (cut/add), changing tension, temperature or pressure applied to a tow or the material band, along with the real time inspection of a composite structure during the steering process [9, 10].

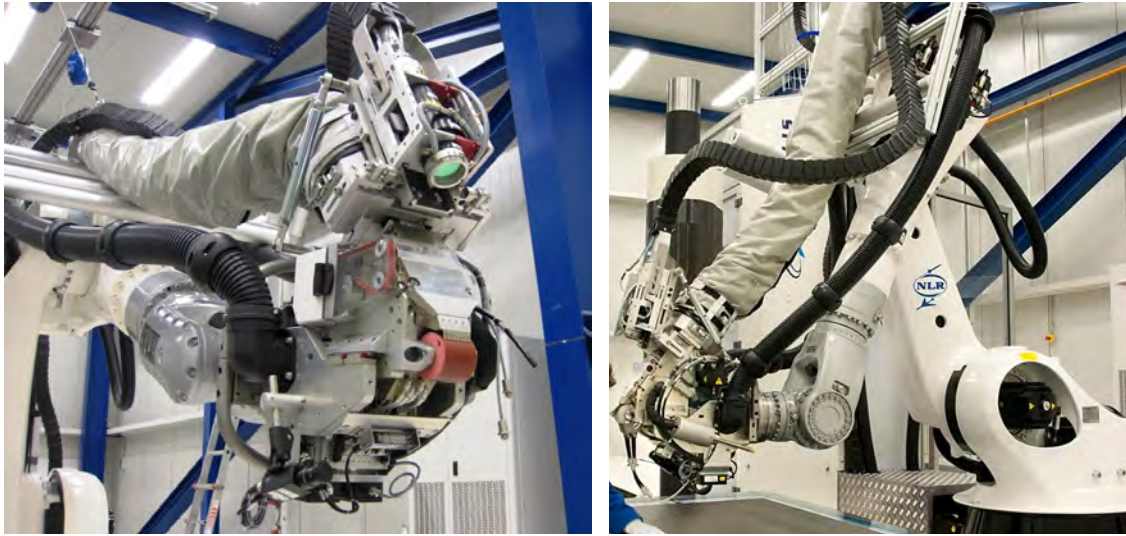


Figure 2.1: Coriolis Fibre Placement Machine. (Courtesy of NLR)

Nowadays, robotic AFP systems make the AFP more affordable. The steering process has been enhanced by combining the technologies of an accurate articulated robotic system with a modular AFP head. These new systems are presently cheaper than comparable gantry AFP systems. As an example, the test specimens mentioned in this thesis were manufactured with a KUKA-Robot developed by Coriolis Composites [11] (see Fig 2.1). This AFP system combines the heating from an Infrared lamp (525 W) for thermoset materials with a 6 kW diode laser for thermoplastic materials, and dry fiber placement. In addition, the design programming and simulation tools are integrated and embedded in the multi-platform CATIA developed by the French company Dassault Systèmes.

2.2.2 Applications in the Aerospace Industry

The high cost of carbon fiber laminates (associated with the complexity of the design and of the manufacturing process) can only be reduced/made cheaper/made more economic by using AFP control systems that ensure high quality and shorter production times. These are the characteristics that mean AFP systems are a widely applied technology in the aerospace industry.

The first European research project to consider Full-Barrel Composite Fuselage manufacturing viability was (FUBACOMP) [12]. In that project a Viper 1200 CNC fiber

placement system and off-line composite programming system supplied by Cincinnati Machine (Hebron, Kentucky) were used to successfully produce a one-piece carbon fiber fuselage. In addition, the first large scale civil application of AFP was for the manufacture of section 19 of the A380 manufactured by Airbus at Illescas, Madrid. The same section for the Airbus A350 XWB (Extra Wide Body) rear spar and trailing edge assembly was developed with AFP (see Fig. 2.2). This plane is in response to Boeing's 787 Dreamliner, which is built of fully closed fuselage section barrels produced by AFP. In both cases, composite materials and AFP technology were a key components in reducing production costs and part weight, thus increasing the overall structural performance [13, 14]. Hawker Beechcraft Corp has also employed automated advanced fiber placement techniques in its personal/business jets, and has particularly focused on reducing the weight of parts required in the assembly of its aircraft.

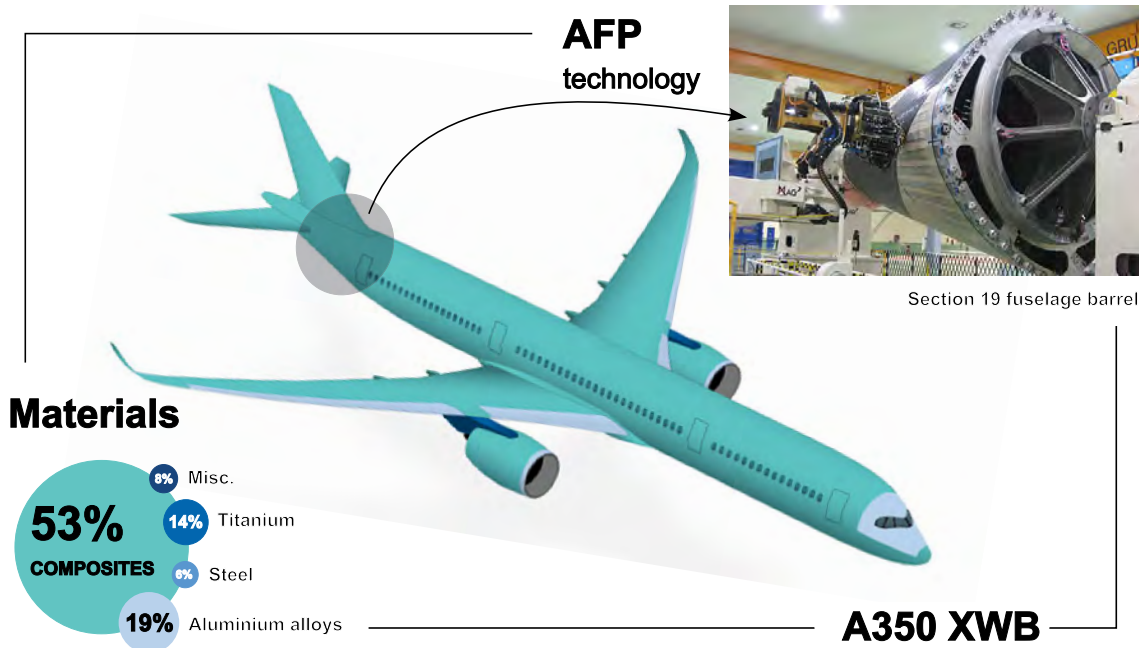


Figure 2.2: Airbus A350 XWB, Materials and AFP technology.

In the military aircraft sector, the increasing use of composites can be directly attributed to AFP systems which reduce production costs while maintaining quality. One of most successful programs is with the F-35 Joint Strike Fighter aircraft [15]. In this project, AFP processes were employed to manufacture large-scale, complex composite parts such as wing skins, ducts, nacelles, fuselage skins and other classified stealth tech-

nologies. Some other programs also use the AFP system in large aerospace composite products [16]. They include Unmanned Aerial Vehicles, the F/A-18E/F Super Hornet and F/A-22 Raptor Stealth Fighters, the V-22 Osprey multi-mission aircraft aft fuselage [17], the Apache Longbow Helicopter and satellite launch vehicles.

2.3 Manufacturing Restrictions and Process-induced Defects

Although the AFP technology allows the introduction of tow-steered fibers along curved paths with high efficiency, there are realistic manufacturing limitations which produce significant undesirable defects that need to be addressed in order to guarantee the structural reliability of the products. In this section some of these limitations and process-induced defects are discussed.

2.3.1 Process-induced Defects

During the fiber placement process, tows of slit prepreg tape are steered on the surface in bands of parallel fibers, called courses. Depending on the AFP system, these courses might include up to 32 tows. The most common tow widths are 3.175 mm, 6.35 mm and 12.7 mm, while the course width varies according to the number of tows. When manufacturing Variable Stiffness Panels or other complex shapes, misalignments at the boundaries of the courses and process-induced defects can happen. These defects are related not only with discontinuities in the orientation angle, but also with gaps and/or overlapping regions that occur in order to achieve a complete fiber coverage of a surface.

Variable Stiffness Panels can be constructed, in general, by two possible methods. The *shifted method* presented by Olmedo and Gürdal [18] and the *parallel method* introduced by Waldhart *et al.* [19]. In the shifted method, the reference course is repeatedly shifted a prescribed distance in order to fill out the complete flat surface of the panel. Whereas in the parallel method, new courses parallel to the reference path are created. As for path definition, the parallel method implies that no gaps are created between the courses, keeping the ply thickness constant. However, this method does not permit large stiffnesses like those obtained with the shifted method. Also, the parallel method is not able to redistribute the loading to the same degree as the shifted fiber in detriment to the critical

buckling load. In addition, in the parallel method the reference path is not copied from course to course, hence the fiber curvatures vary significantly within a lamina and close to the center of curvature of the reference path there is fiber kinking.

Waldhart *et al.* [20] considered that the primary manufacturing constraint in the analysis of variable-stiffness laminates was the limitation to/in fiber curvature which proved to be more restrictive for parallel fiber laminae than for shifted fiber ones. This curvature constraint is inversely proportional to the minimum turning radius (ρ_{min}) allowed by the AFP system [21]. For a turning radius lower than ρ_{min} , the inner tow-pregs in the course tend to wrinkle out-of-plane and local buckling/crimping appears. To overcome these disadvantages and achieve higher design flexibility, dry fiber bundles are applied in the steered process (DFP). However, even using dry fiber, tows will tend to wrinkle and in-plane bending deformation takes place if they are curved too much.

Depending on the parallel or shifted method chosen to construct a variable-stiffness ply, different defects can occur. Dirk *et al.* [2] resume the main tow-steered defects in three categories: tow buckling, tow pull-up and tow misalignment. Twisted tows can also occur but are less common. The authors explain that tow buckling might occur on the inside radius of a tow because of the high compressive forces. In contrast, tow pull-up tends to occur on the outside radius due to excessive tensile forces. The tow misalignment is inherent to the layup and material used. Fig. 2.3 illustrates different defects. The AFP system can lay dry tows for thermoset or thermoplastic material. However, the real deformation of the tows introduces more complex types of process-induced defect than tape placement.

Some of the process-induced defects that mainly take place when the conventional AFP techniques are applied are described by B. C. Kim *et al* [22]. These defects are described according to tow path definition and characteristic deformation. Local buckling, thickening and thinning defects appear in the laminate when curved tow paths are followed. Therefore, when the imperfections of a tow element such as the difference of the edge lengths and/or width, tension and feed length variations appear, the distortion of the tow element becomes worse. In addition, defects like missing, twisted, or spliced tows, occur during the steered process of both tape or dry placement. The main recommendation to reduce the effect of these defects is to use curvatures over the minimum turning radius. A recent study from NLR recommends a turning radius $\rho > 150$ mm for 1/8" and $\rho > 250$ mm for 1/4" of tow width [23].

2.3. MANUFACTURING RESTRICTIONS AND PROCESS-INDUCED DEFECTS 13

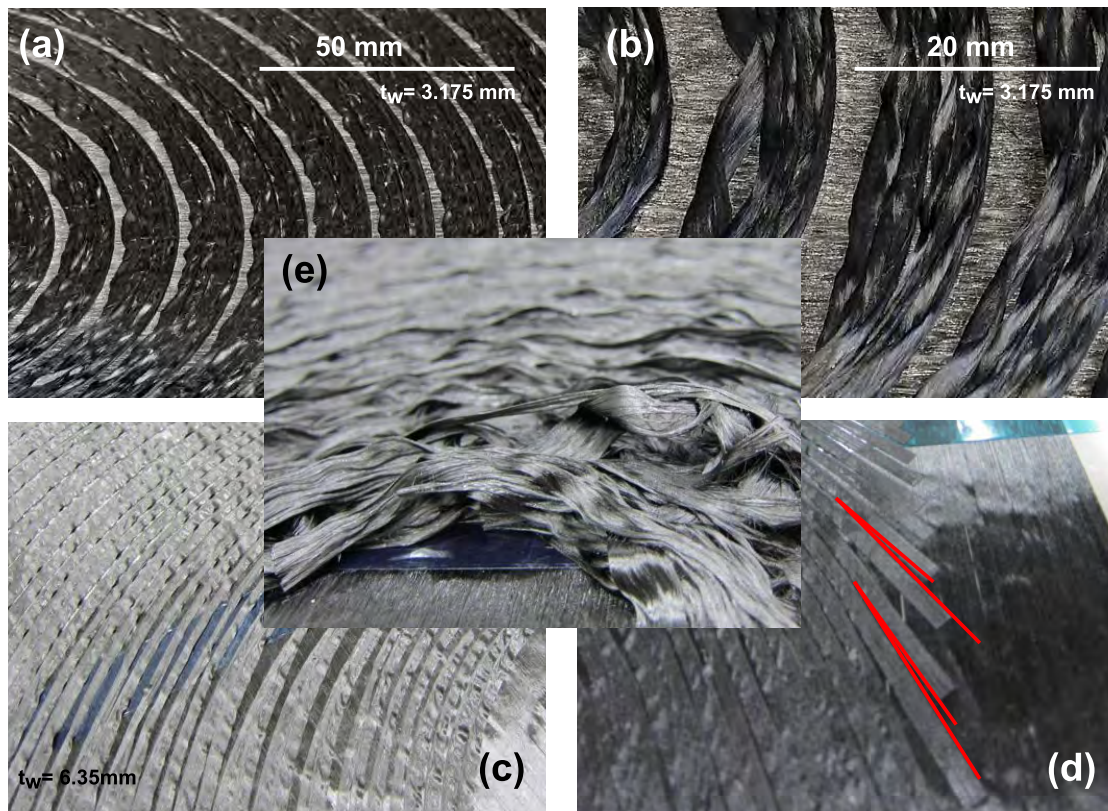


Figure 2.3: Process-induced defects, (Courtesy of NLR). (a) Wrinkling, (b) Folding, (c) Wrinkling and folding, (d) Unsupported Ends and (e) Twisted.

Although the shifted method is more efficient for manufacturing VSP, tow-overlapped regions appear because of the discrete width of the course shifting. These local thickness buildup effects create regions which can act as 'integral stiffeners' that improve the load-carrying capability of the structure [24]. However, the thicker regions are associated to a local laminate asymmetry that might not be desired. To prevent the overlapping regions, the tow-placement machine can be instructed to cut/restart (on-the-fly) the tows individually so that no thickness builds up. However, this creates small fiber-free areas in the boundaries of the courses. These resin-rich regions are in fact gap defects. A representation of the tow-drop overlap and tow-drop gap defects is illustrated in Fig. 2.4. Minimizing these gap defects is one of the challenges in the design and manufacture of variable-stiffness panels. The minimum cut length is a further limitation in manufacturing that needs to be taken into account [25]. This length is the shortest tow length the machine

can properly lay down, and is equal to the distance from the start of the lay-down point to the tow-cutting mechanism in the placement head.

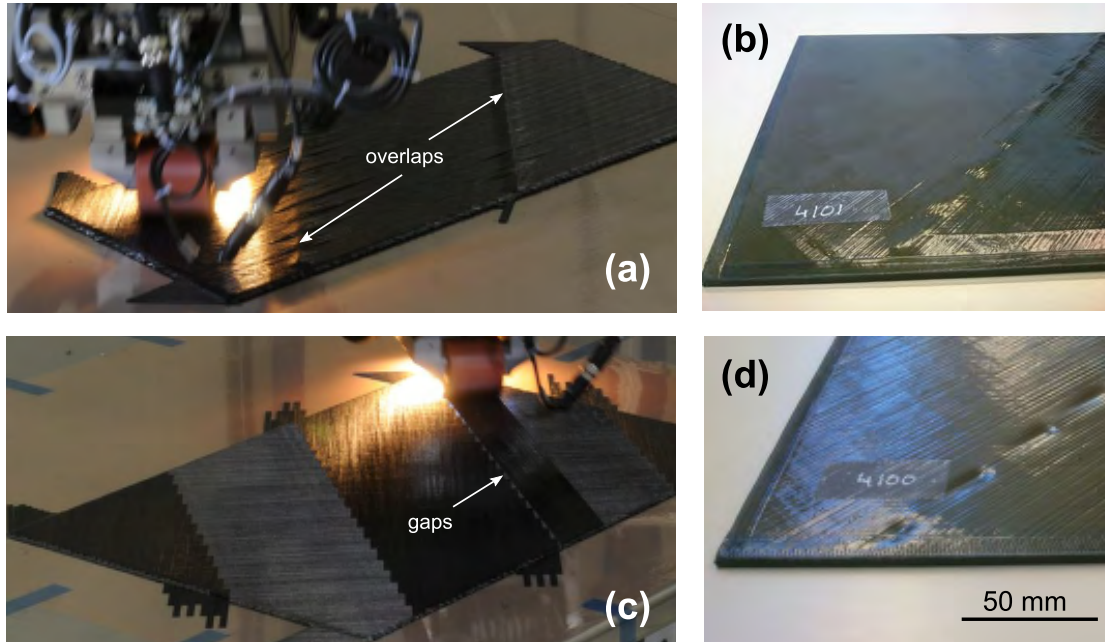


Figure 2.4: Overlaps and Gaps areas. (a) Tow-overlaps regions during the manufacturing, (b) Plate with overlap after curing, (c) Tow-drop with gaps, (d) Plate with gaps after curing.

2.3.2 Strategies for minimization of defects and their influence

Several methods such as staggering, tow-overlap and tow-drop, and the choice of the coverage parameter, have been developed to minimize the influence of defects and improve the strength and surface quality of a tow-steered laminates [26, 5, 4]. The staggering technique is useful to avoid the collocation of course edges, tow-drops or tow-overlaps that would occur at the same places through-the-thickness of a laminate in clustered plies, which might reduce the laminate strength [27]. This technique is not only applied in VSP, but also in conventional laminates with straight fibers clustered with the same fiber angle distribution, thus avoiding the collocation of the tows and consequently a smoother surface is obtained. The staggering effect for both tow-overlap and tow-drop laminates is shown in Fig. 2.5. Unfortunately, ply staggering generally causes the laminate to become

2.3. MANUFACTURING RESTRICTIONS AND PROCESS-INDUCED DEFECTS 15

locally asymmetric and unbalanced. The choice of an appropriate coverage parameter can also reduce the negative influence of the gap-defects on the strength and surface quality of a laminate, by minimizing the resin-rich areas. However, despite these methods, defects are never completely avoided and the resin-rich areas are never completely covered. On top of that, the influence of such defects in the mechanical performance of tow-steered structures is not yet well understood.

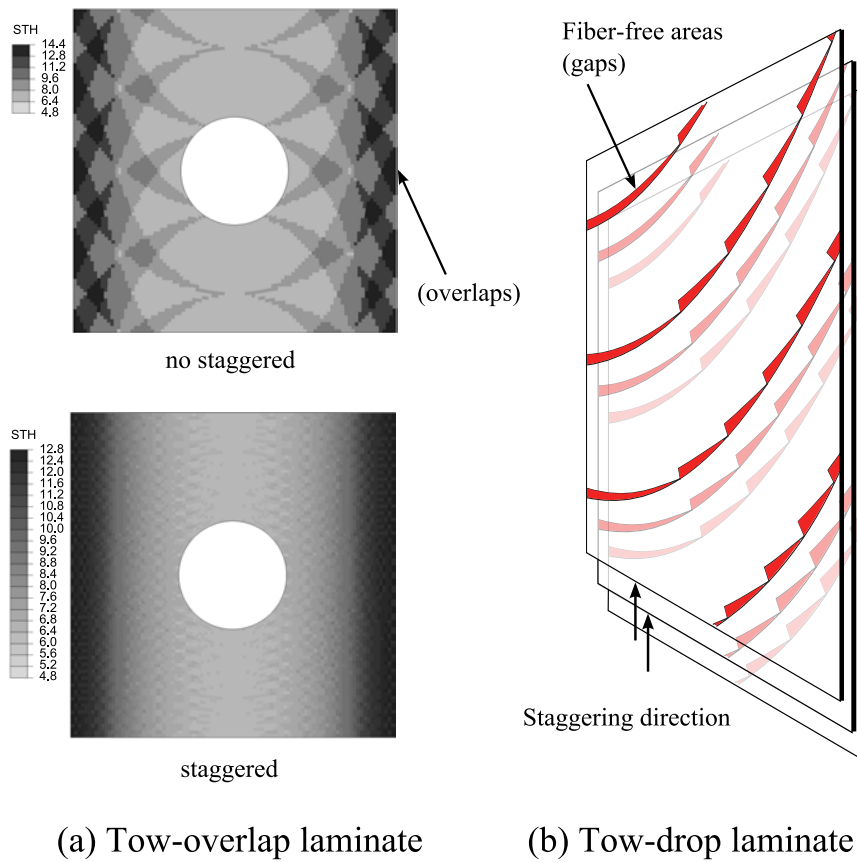


Figure 2.5: (a) Thickness distributions for variable stiffness laminates with tow-overlaps. (b) Laminate with tow-drop staggered

Recently, a novel continuous tow shearing method (CTS) for manufacturing variable-stiffness laminates has been suggested [22]. The idea behind this method is to replace the current AFP conventional method which was developed in the late 1980s. The defects mentioned above due to the in-plane bending deformation can be reduced by the in-plane shear deformation of the tows.

The CTS method might be an option for futures composites manufacturing technology as it seems to significantly reduce the defects. However, the CTS method does not avoid all the problems and in fact presents some limitations. These problems and limitations are all to do with a 90° shear angle is impossible to reach. In addition, the shear deformation creates critical variations in the thickness of the tows. A further drawback is associated with the limited speed of the in-situ impregnation process, which decreases productivity. Finally, in those parts with complex geometries, like Tapered Channel Sections (TCS), gaps or overlaps still can happen [28].

2.4 Variable Stiffness Composites Panels

Chapter 1 provides some insights concerning the introduction of variable stiffness laminates through AFP technology. Since the 90s, manufacturing capabilities have reached a far more advanced technological level than the actual laminate concepts used by engineers. The development of Non-conventional Laminates (NCL's) represents a step forward to fully exploit the possibilities of AFP, and with the ultimate outcome being to improve the mechanical performance of composite structures (see Fig. 2.6.)

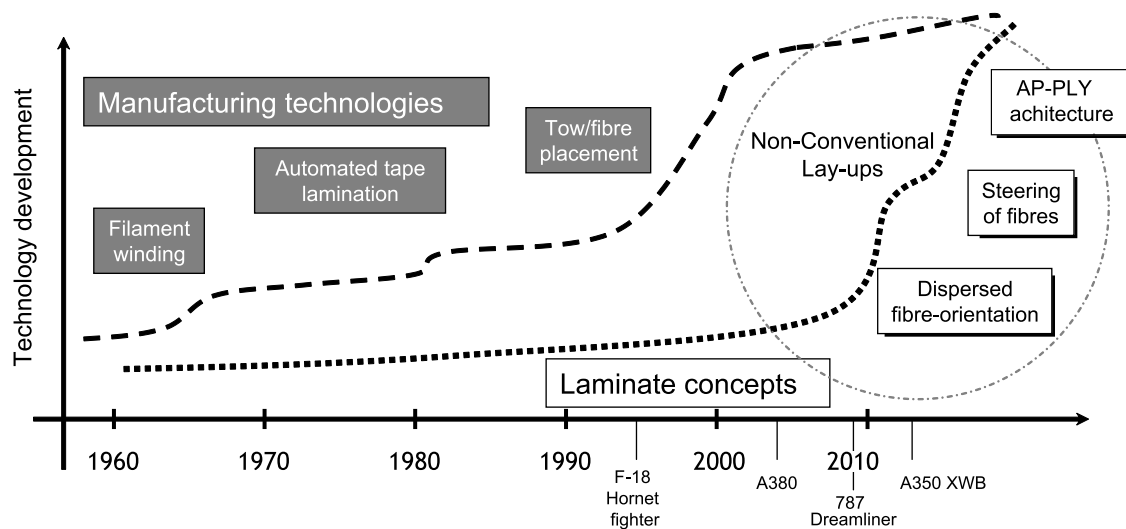


Figure 2.6: Automated manufacturing technologies vs. laminate concepts.

Non-conventional layout includes laminates with dispersed stacking sequences tow-steered laminates and, more recently, the introduction of novel architectures such as APPLY [29, 30]. In this section, the variable stiffness panel definition used in the present work is described.

2.4.1 Variable-Stiffness Laminate Definition

The name of the steered-fiber composite, Variable Stiffness Panels (VSP), refers to variable stiffness properties as opposed to conventional straight-fiber laminates which present constant in-plane stiffness properties. These laminates not only have variable in-plane stiffness properties, but also acquire variable bending and coupling stiffness properties as well [31]. Such variability can be obtained because the material orientation follows curvilinear steered paths. Traditionally, the stiffness and strength properties of conventional laminates could be changed by designing the laminate stacking sequence of layers with different orientation angles. However, the orientation angles in each ply remained constant and did not use the full potential of directional material properties, which can be useful for non-uniform stress distribution, in panels with holes and notches. Thanks to the AFP's capability of placing the tows while varying fiber orientation angle and the curvature of the fibers, the applied loads can redirect the applied loads to the supported edges of the panel, hence avoiding the central sections which are critical in a buckling event [24], for example.

The variable stiffness panel definition adopted in this work was developed by Gurdal and Olmedo [30, 18]. Their first implementation of Variable Stiffness Panels (VSP) used the linear variation of the orientation angle as the basis for the reference path variation. In those early works, closed-form solutions were proposed for rectangular plates with simple boundary conditions. By adopting a linear variation of the orientation angle, the laminate global stiffness could be analytically deduced. This definition is formulated using three parameters T_0 , T_1 and d . The general equation for the linear angle variation path is:

$$\varphi(x') = \phi + (T_1 - T_0) \frac{|x'|}{d} + T_0 \quad (2.1)$$

This equation describes the reference curve path of the course in a trajectory of the AFP machine head center, and is assumed to be continuous and antisymmetric with respect to the origin. The fiber angle varies linearly from the value T_0 at the center of the

panel to T_1 at the characteristic dimension d along the x' -direction. According to this formulation, the family of curvilinear configurations can be denoted by $[\phi \pm \langle T_0 | T_1 \rangle]$ in contrast to the traditional nomenclature for straight-fiber laminates where the plies are represented by a single angle. In order to cover the complete ply, successive courses need to be placed. Similarly to the conventional laminate nomenclature, a \pm sign means that there are two adjacent layers with equal and opposite variations of the fiber orientation angle. The local reference system $x'y'$ can be rotated with respect to a global reference system xy by an angle ϕ . The reference curve associated with the central path of the AFP head machine is shown in Fig. 2.7a. In addition, different angle combinations obtained by shifting the reference path, are shown 2.7b. A simpler approach, based on circular arcs was developed by the same authors [4], avoids using an iterative nonlinear solver and generates more efficient solutions. Moreover, it also has the advantage of producing courses of constant curvature, which better correspond to manufacturing constraints.

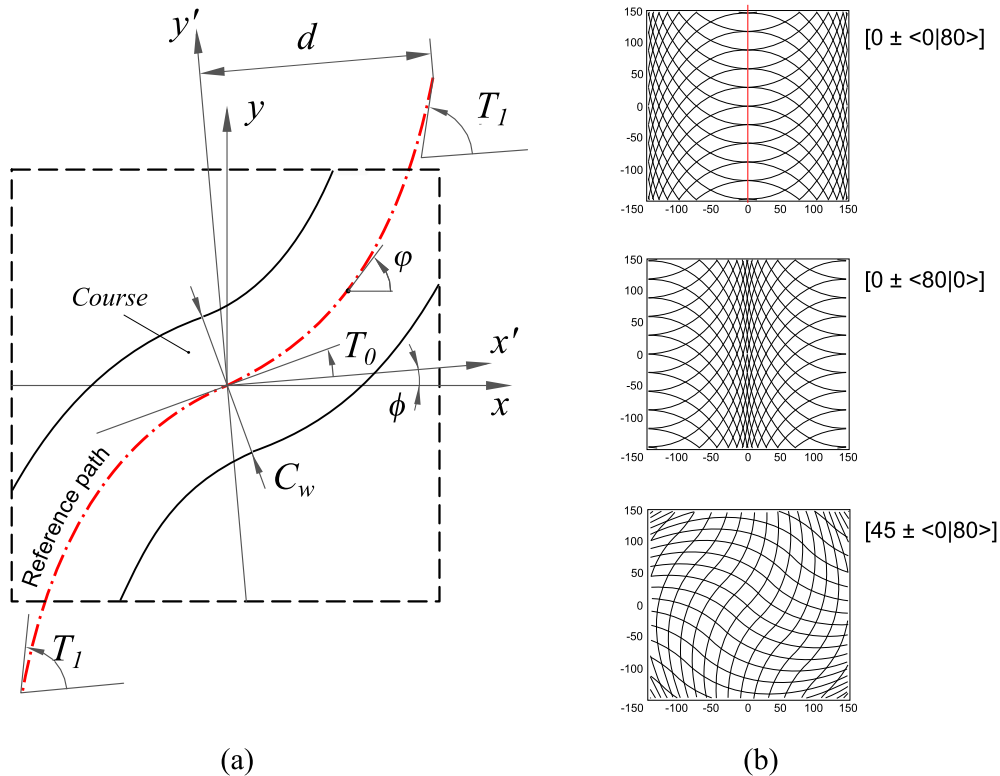


Figure 2.7: (a) Reference path definition. (b) Laminates $[\phi \pm \langle T_0 | T_1 \rangle]$

2.4.2 Development of modeling for VSP

Several approaches have been used to reliably model and predict the mechanical response (in terms of stiffness) and the strength response of variable stiffness laminates. The key contributions are described in the following paragraphs.

One of the main problems in the modeling of VSP is related to the computation of the spatial variation of the fiber orientation. The initial models used the method developed by Gürdal and Olmedo where the fiber direction is assumed to vary only along one of the planar coordinates. The orientation angle is determined by a function which describes the reference path of the AFP machine head. The fiber angle evolves linearly along one direction while, in the perpendicular or shifted direction, it is constant. These models were called the 'idealized' variable-stiffness ply definition and were useful for demonstrating the capabilities of VSP over straight-fiber laminates. With this design, increases of up to 50% in the axial stiffness and up to 80% in the critical buckling load of VSP, were made. The reason for these remarkable results was attributed to the load redistribution from the center of the panels to the over-stiffened edge regions [31, 24].

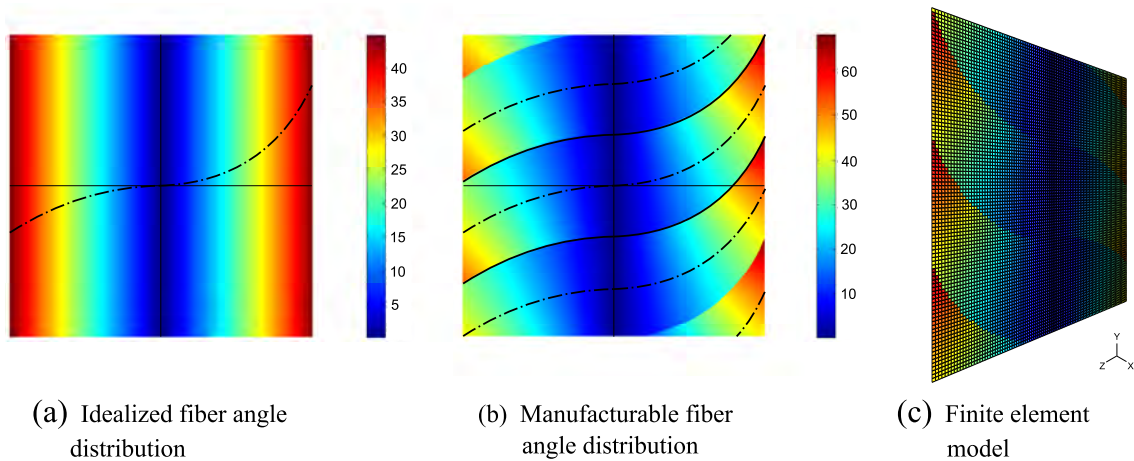


Figure 2.8: Fiber angle distribution: (a) 'Idealized', (b) 'Manufacturable' and (c) VSP modeled for $300\text{mm} \times 300\text{mm}$ tow-steered ply with $T_0 = 0^\circ$, $T_1 = 45^\circ$, $\phi = 0^\circ$. The course on the manufacturable ply includes 32 tows (tow-width of 3.175mm)

Although 'idealized' models were adequate to study the effects of fiber path definitions on the in-plane response characteristics, the theoretical and numerical studies made in some cases through design optimization did not take manufacturing feasibility into ac-

count. An 'idealized' configuration only defines the reference path orientation (the center-line of the AFP machine head course), see Fig. 2.8a. However, in a real environment, the width of each course needs to be taken into account and the thickness variation due to the overlap or gaps zones created during the shifting process have to be considered. The computation of the fiber orientation angles for a manufacturable approach is represented and modeled in Fig. 2.8b and c. A method which provides a representation of the overlap regions and an accurate model of the fiber-orientation angle change throughout the laminate is presented by Langley *et al.* [32]. The finite element modeling method developed in his work involves a discretized reference path and was applied to study the influence of the thickness variation in the overlap zones. However, other defects i.e., gaps, were not addressed in his study.

A theoretical and numerical investigation of the influence of these gap areas on the strength and stiffness of variable-stiffness laminates under compression loading is presented by Blom *et al.* [21]. Their work also included the effects of fiber angle, tow width, laminate thickness and staggering. In addition, their study includes a failure analysis and leads to the conclusion that the onset of damage occurs at tow-drop locations. The strength improvement due to staggering and strength reduction when tows are wider was also demonstrated. The authors recommend other analyses under tension load cases. Consequently, Blom *et al.* expanded their studies from tailored flat panels to cylindrical and conical shells [33, 34] to validate the improvement of the variable stiffness configuration over the traditional straight laminates. In an attempt to improve the capture of the geometry and location of gaps and overlaps, Fayazbakhsh *et al.* [35], present a defect layer method. This method can capture the geometry and distribution of gaps with higher precision and accuracy. However, for the sake of simplification and efficiency, their analyses were modeled using an in-plane stress formulation implemented with shell elements in a regular mesh and the effect of the gap/overlap defects out-of-plane were not studied.

New methodologies are needed to address and include realistic manufacturing constraints in the design of VSP and damage modeling. These new methodologies must be able to predict the mechanical response in terms of failure and damage propagation, applying first-ply failure criteria and continuum damage models to predict the propagation of ply failure mechanisms until structural collapse [36]. Various have been performed to examine the onset of damage in VSP. Lopes *et al.* [37, 38] present a study of buckling and first-ply failure in VSP. In their studie, uncut panels and panels with cutouts are modeled.

In addition, the same authors extended the study to progressive damage analysis of non-conventional laminates with disperse stacking sequence [24]. In all cases, the advantages of VSP over straight-fibre laminates were clearly demonstrated and the critical damage areas were related to the defect zones. During the panel curing process, these tow-drop areas become potential spots for matrix cracking or even delamination initiation, due to the local amplification of interlaminar stresses. Close to these areas, damage occurs as a gradual decrease of stiffness that is associated with energy dissipation in the form of matrix cracks and fiber breakage. Furthermore, an interlaminar stress recovery method using three-dimensional finite elements was developed by Fagiano *et al.* [39, 27] and applied to variable stiffness panels by Diaz *et al.* [40].

In the past, progressive damage models have been applied in variable stiffness panels with good agreement between the failure predictions and experimental results (see Lopes *et al.* [36]). In addition, the studies developed by Lopes *et al.* [24], concluded that the failure of VSP is inevitably affected by the presence of tow-drops. Damage can be triggered by the resin-rich areas, predominately in regions where the angle between the loading vector and fiber orientations is large. The same author points out that in their study the prediction of the occurrence of ply delaminations was neglected altogether. Tow-drop areas are potential spots for the initiation of this failure mode, similar to what occurs in regions of ply drop-offs. Hence, delaminations might actually be the primary and dominant damage mode in VSP configurations constructed by the tow-drop method. The influence of the tow-drop fiber-free areas and of the mismatch angles discontinuities on the damage response in VSP are still a novel fields for researchers. In addition, the continuum damage models for predicting the propagation of ply failure mechanisms, including delaminations, and for studying the influence of defects might require the isolation of defects and their analysis on a sub-level component scale. This approach will be more comparable to the standard approach for conventional laminates and will also lower the computational time spent in the simulations.

Nowadays, studies into in VSP are focused on the damage resistance and damage tolerance under low-velocity impact events. A study of the impact and CAI behavior prediction between fiber orientation, matrix-cracks and delaminations has been presented by Dang *et al.* [41]. In their work, an explicit finite element analysis using bilinear cohesive low-based interface elements is performed to predict and simulate delaminations and crack growth and study the influence of the fiber orientation in a VSP. The authors

conclude that the material with curvilinear path orientation suffers greater damage (mainly in CAI) in comparison to straight fiber laminates because the buckling mechanism in the delaminated area is altered. Good agreement was observed between the results of the study and the experimental data. However, the process-induced defects were not included in the models and, thus, their effect was not specifically analyzed.

Recently, the present author has presented a pre-processing methodology to obtain a parametric VSP modeled in a three-dimensional domain, (described in Chapter 3). This tool contains structured mesh generator possibilities for the capture of gap defects with higher precision in comparison to the existing approach. The methodology allows advanced FE models for reliable analyses of progressive damage and delaminations [42]. With this methodology, damage propagation analyses can be carried out and the inter-laminar behavior can be modeled by means of surface-based cohesive-contact or with cohesive element formulations [43] as shown in Fig. 2.9.

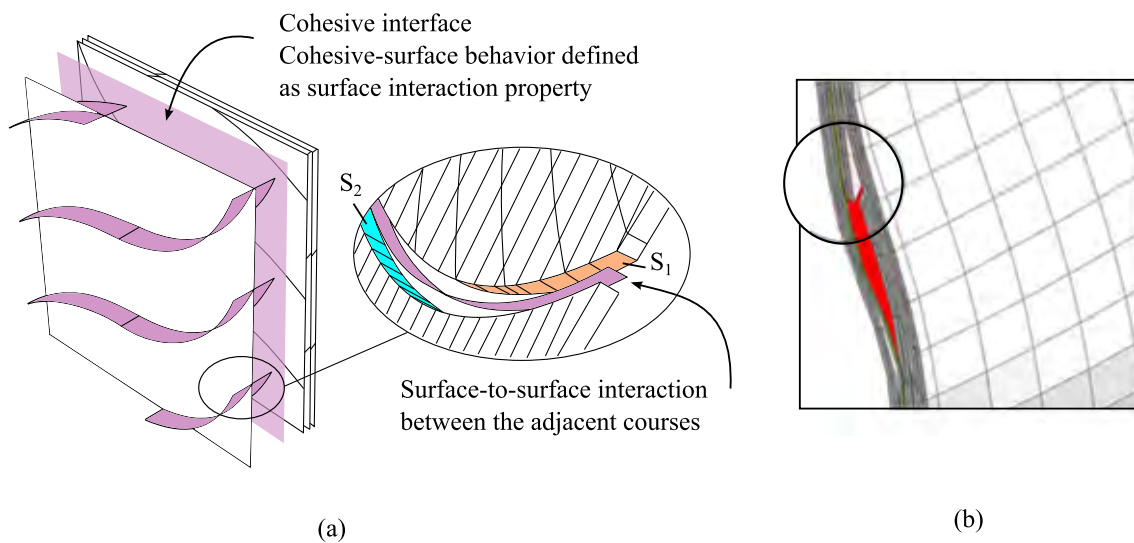


Figure 2.9: (a) Surface-cohesive behavior approach. (b) Delamination damage simulated in *ABAQUS*

In parallel to the simulation tools, experimental campaigns have been carried out. In most cases, the experimental results showed a good agreement with the finite element models, while others can still not be compared with related simulations. In the next section, some of these experimental tests are described.

2.5 Experimental works in VSP

The initial experimental program for the validation of the design and analysis tools for VSP was covered by Gurdal, Tatting, Jegley and Wu [44, 45, 46, 47, 48]. These researchers optimized flat variable stiffness panels for in-plane compression and shear considering the manufacturability aspects. In addition, different specimens were manufactured with the tow-overlap and tow-drop method to analyze mechanical response. The initial objective was focused on the buckling and post-buckling response of plates with and without central holes. Analytically and experimentally, an increase in the buckling load of the panels of up to 100 percent was demonstrated in both cases [48, 49]. The inclusion of non-linear effects and initial imperfections (due to clamping), were analyzed by Wu *et al.* [50, 51, 52]. In addition, experimental tests in square panels under shear loads were performed by Jegley *et al.* [49]. The predictions showed a slight improvement in the buckling load of the variable-stiffness panels in comparison to the straight-fiber panels. Furthermore, compression tests of the variable-stiffness panels proved that the influence of the thermal induced stresses had a considerable positive impact on the buckling load [5, 48].

Other studies applied the curvilinear fiber format to fuselage panels with and without large window cutouts and subjected them to combined out-of-plane pressure loading and in-plane loads [53, 54]. Buckling optimization showed considerable improvement in buckling capability compared to quasi-isotropic laminates, but the strength capacity was lower than the reference counterpart. More recently, NLR has adopted a multidisciplinary approach to its design, construction and testing program for more robust composite window panels with curvilinear paths as a way of implementing this new method of fiber placement into production practices that can be immediately applied in the airline industry [55]. Despite there being many experimental contributions in order to demonstrate and give credibility to the introduction of variable stiffness laminate concepts, the studies were focused mainly on the influence of these geometrical details on the in-plane stiffness and strength of the VSP. In addition, the mechanical response of the specimens has only been analyzed on a structural level. The large dimensions of the specimens needed to validate the influence of the process-induced defects is certainly a deterrent for experimental studies.

In an effort to analyze the effects of the process-induced defects, Croft et al. [56] presented an experimental study quantifying the effect of the main defects that had been manually inserted during specimen manufacture. Their work reveals that the in-plane shear strength decreases along the perpendicular direction to the load when tow-overlapping is present. Furthermore, it was demonstrated that for notched laminates the open hole has a greater influence on failure than that induced by the presence of manufacturing defects. Some experimental studies have been found in the literature for the cases of gap defect influence on damage tolerance under low-velocity impacts. The most critical failure mode for laminates, which drives the design of the majority of aircraft structures is damage tolerance to low-velocity impacts. Several attempts have been made, based on the formulation of new material systems (toughened resins and through-the-thickness reinforcements) to improve the damage tolerance of composite laminates. However, these attempts have had limited success because other key mechanical properties, such as stiffness, are compromised when tougher resins, textile reinforcements or z-pins are introduced. Recently, a new fiber placement architecture called AP-PLY for improved damage tolerance was presented by Nagelsmit *et al.* [57]. Tests show smaller delaminations and higher residual strength for every AP-PLY configuration and lay-up compared to baseline laminates with unidirectional plies.

A physically-based methodology for tailoring ply sequences, ply thicknesses and angle ply orientations is a promising approach to improving damage tolerance in composites without other detrimental effects. However, for a better understanding of the influence of process-induced defects in delamination under drop-weight impact events, more tests are still needed. Rhead et al. [28] present the effect of tow gaps on the impact and compression-after-impact strength of fiber-placed laminates. Their results show that the position, width and depth of tow gaps have a significant effect on damage resistance.

In the present study, experimental work has been done to investigate the effect of the fiber angle discontinuities between different tow courses and the process-induced defects for un-notched and open-hole laminates. The results of tensile strength are analyzed in Chapter 4. In addition, an experimental study into the effects of tow-drop gaps in Variable Stiffness Panels under drop-weight impact events and into the effect of staggering were also performed and are presented in Chapter 5. In both cases, the results are compared with straight-fiber laminates without defects.

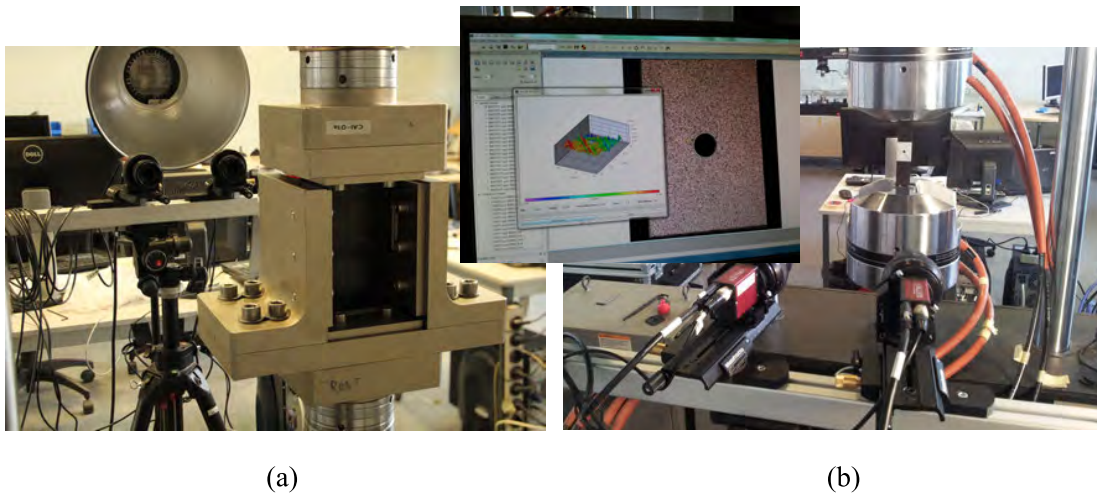


Figure 2.10: Digital Image Correlation (DIC): (a) Setup for Compression After Impact CAI, (b) Setup for Open Hole Tensile

The data was obtained using a *VIC – 3DTM* stereo Digital Image Correlation (DIC) system with two digital cameras. In this test the DIC System was used to measure the full-field displacements and strains. The use of a stereo camera system (Rodagon-WA 60mm lens) allows for three dimensional correlation, providing information on the deformation from the initial geometry to the structural collapse. The experimental setup for both the test and the VIC-3D software are shown in Fig. 2.10.

References

- [1] F.C. Campbell. *Manufacturing Technology for Aerospace Structural Materials*. Elsevier Ltd., 2006.
- [2] D. Lukaszewicz, C. Ward, and K. Potter. The engineering aspects of automated prepreg layup: history, present and future. *Composites Part B: Engineering*, 43:997–1009, 2012.
- [3] D. Evans. Fiber placement. In D. Miracle and S. Donaldson, editors, *ASM Handbook*, volume 21, pages 477–479. ASM International, 2001.
- [4] Z. Gürdal, B. F. Tatting, and K. C. Wu. Tow-placement technology and fabrication issues for laminated composite structures. In *Proceedings of the AIAA/ASME/ASCE/AHS/ASC Structures, 46th Structural Dynamics & Materials Conference*, 2005.
- [5] K. C. Wu, Z. Gürdal, and J. H. Starnes. Structural response of compression-loaded, tow-placed, variable stiffness panels. In *Proceedings of the 43rd AIAA/ASME/ASCE/AHS/ASC Structures, Structural Dynamics and Materials Conference*, Denver, CO, April 2002. AIAA 2002-1512.
- [6] D. Jarvi and T. Oldani. Automated fiber placement using multiple placement heads, replaceable creels, and replaceable placement heads, November 10 2005. WO Patent App. PCT/US2005/013,737.
- [7] L. Izco, J. Isturiz, and M. Motilva. High speed tow placement system for complex surfaces with cut / clamp / and restart capabilities at 85 m/min (3350 ipm). SAE Technical Paper 2006-01-3138, SAE International, 2006.
- [8] R. DeVlieg, K. Jeffries, and P. Vogeli. High-speed fiber placement on large complex structures. SAE Technical Paper 2007-01-3843, SAE International, 2007.
- [9] T. Oldani and D. Jarvi. Performing high-speed events ”on-the-fly” during fabrication of a composite structure by automated fiber placement, October 23 2013. EP Patent 1,787,175.

- [10] T. Oldani. Visual fiber placement inspection, March 20 2013. EP Patent App. EP20,070,101,121.
- [11] Coriolis Composites. The use of robots for fiber placement. <http://www.coriolis-composites.com/technologie.php>, 2014. [Online; accessed 20-February-2014].
- [12] Dassault Aviation. Full-Barrel Composite Fuselage Project (FUBACOMP). http://http://www.aerodays2006.org/sessions/B_Sessions/B3/B31.pdf, 2006.
- [13] D. A. McCarville, J. C. Guzman, and Rotter D. M. Automated material placement - 2008 industry overview. In *In Proceedings of the SAMPE 2008 Conference, Long Beach, CA, USA*, 2008.
- [14] B. Morey. Automating composites fabrication. *Manufacturing Engineering*, 140(4), 2008.
- [15] Defense Advanced Research Projects Agency. Joint strike fighter program. <http://www.jsf.mil/>, 2001. [Online; accessed 20-February-2014].
- [16] Defense Production Act Committee. Integrated advanced composite fiber placement (IACFP). http://http://www.dpatitle3.com/dpa_db/project.php?id=64, 2009. [Online; accessed 20-February-2014].
- [17] R. Pinckney. Fabrication of the v-22 composite aft fuselage using automated fiber placement. In *The First NASA Advanced Composites Technology Conference*, volume 1, pages 385–397, NASA, 1991.
- [18] R. Olmedo and Z. Gürdal. Buckling response of laminates with spatially varying fiber orientations. In *Proceedings of the AIAA/ASME/ASCE/AHS/ASC 34th Structures, Structural Dynamics and Materials Conference, AIAA 93-1567*, pages 2261–2269, 1993.
- [19] G. J. Waldhart, Z. Gürdal, and C. Ribbens. Analysis of tow placed, parallel fiber, variable stiffness composite laminates. In *Proceedings of the AIAA/ASME/ASCE/AHS/ASC 37th Structures, Structural Dynamics and Materials (SDM) Conference*, 1996.

- [20] C. Waldhart. Analysis of tow-placed, variable-stiffness laminates. Master's thesis, Virginia Polytechnic Institute and State University, Blacksburg, VA, 1996.
- [21] A. W. Blom, C. S. Lopes, P. J. Kromwijk, Z. Gürdal, and P. P. Camanho. A theoretical model to study the influence of tow-drop areas on the stiffness and strength of variable-stiffness laminates. *Composite Materials*, 43:403–425, 2009.
- [22] B. C. Kim, K. Potter, and P. M. Weaver. Continuous tow shearing for manufacturing variable angle tow composites. *Composites Part A: Applied Science and Manufacturing*, 43:1347–1356, 2012.
- [23] M. Nagelsmith and W. Guerrits. Influence of steering radius on the mechanical properties of fiber placed composite laminates. In *ICCS17-17th International Conference on Composite Structures Porto, Portugal, June 17-21, 2013*.
- [24] C. S. Lopes. *Damage and Failure of Non-Conventional Composite Laminates*. PhD thesis, Delft University of Technology, 2009.
- [25] A. W. Blom. *Structural Performance of Fiber-Placed, Variable-Stiffness Composite Conical and Cylindrical Shells*. PhD thesis, Delft University of Technology, 2010.
- [26] A. W. Blom, B. F. Stickler, and Z. Gürdal. Design and manufacture of a variable-stiffness cylindrical shell. In *Proceedings of the SAMPE Europe 30th International Conference*, March 2009.
- [27] C. Fagiano. *Computational Modeling of Tow-Placed Composite Laminates with Fabrication Features*. PhD thesis, Delft University of Technology, 2010.
- [28] A T Rhead, T J Dodwell, and R Butler. The effect of tow gaps on compression after impact strength of robotically laminated structures. *CMC: Computers, Materials & Continua*, 35:1–16, 2013.
- [29] T. A. Sebaey, E.V. González, C.S. Lopes, N. Blanco, P. Maimí, and J. Costa. Damage resistance and damage tolerance of dispersed cfrp laminates: Effect of the mismatch angle between plies. *Composite Structures*, 101:255–264, 2013.
- [30] Z. Gürdal and R. Olmedo. In-plane response of laminates with spatially varying fiber orientations - variable stiffness concept. *AIAA J*, 31(4):751–758, 1993.

- [31] Z. Gürdal, B. F. Tatting, and K. C. Wu. Variable stiffness panels: Effects of stiffness variation on the in-plane and buckling responses. *Composites Part A: Applied Science and Manufacturing*, 39:911–922, 2008.
- [32] P. T. Langley. Finite element modeling of tow-placed variable-stiffness composite laminates. Master’s thesis, Virginia Polytechnic Institute and State University, 1999.
- [33] A. W. Blom, P. B. Stickler, and Z. Gürdal. Optimization of a composite cylinder under bending by tailoring stiffness properties in circumferential direction. *Composites Part B: Engineering*, 41:157–165, 2010.
- [34] A. W. Blom, B. F. Tatting, J. M. Hol, and Z. Gürdal. Fiber path definitions for elastically tailored conical shells. *Composites Part B: Engineering*, 40:77–84, 2009.
- [35] K. Fayazbakhsh, N. M. Arian, D. Pasini, and L. Lessard. Defect layer method to capture effect of gaps and overlaps in variable stiffness laminates made by automated fiber placement. *Composite Structures*, 97:245–251, 2013.
- [36] C. S. Lopes, P.P. Camanho, Z. Gürdal, and B. F. Tatting. Progressive failure analysis of tow-placed, variable-stiffness composite panels. *Solids and Structures*, 44:8493–8516, 2007.
- [37] C. S. Lopes, Z. Gürdal, and P.P. Camanho. Variable-stiffness composite panels: Buckling and first-ply failure improvements over straight-fibre laminates. *Computers and Structures*, 86:897–907, 2008.
- [38] C. S. Lopes, Z. Gürdal, and P. P. Camanho. Tailoring for strength of composite steered-fibre panels with cutouts. *Composites Part A: Applied Science and Manufacturing*, 41:1760–67, 2010.
- [39] C. Fagiano, M.M. Abdalla, C. Kassapoglou, and Z. Gürdal. Interlaminar stress recovery for three-dimensional finite elements. *Composites Science and Technology*, 70:530–538, 2010.
- [40] J. Díaz, C. Fagiano, M.M. Abdalla, Z. Gürdal, and S. Hernández. A study of interlaminar stresses in variable stiffness plates. *Composite Structures*, 94:1192–1199, 2012.

- [41] Thi D. Dang and Stephen R. Hallett. A numerical study on impact and compression after impact behaviour of variable angle tow laminates. *Composite Structures*, 96:194–206, 2013.
- [42] O. Falcó, J. A. Mayugo, C. S. Lopes, N. Gascons, A. Turon, and J. Costa. Variable-stiffness composite panels: As-manufactured modeling and its influence on the failure behavior. *Composites Part B: Engineering*, 56:660–669, 2014.
- [43] A. Turon, P.P. Camanho, J. Costa, and J. Renart. Accurate simulation of delamination growth under mixed-mode loading using cohesive elements: Definition of interlaminar strengths and elastic stiffness. *Composite Structures*, 92(8):1857–1864, 2010.
- [44] B. F. Tatting and Z. Gürdal. Design and manufacture of tow-placed variable stiffness composite laminates with manufacturing considerations. In *Proceedings of the 13th U.S. National Congress of Applied Mechanics*, 1998.
- [45] B. F. Tatting and Z. Gürdal. Analysis and design of tow-steered variable stiffness composite laminates. In *American Helicopter Society Hampton Roads Chapter, Structure Specialists' Meeting, Williamsburg, VA, USA: American Helicopter Society*, 2001.
- [46] B. F. Tatting and Zafer Gurdal. Design and manufacture of elastically tailored tow placed plates. Technical Report NASA/CR-2002-211919, NASA, 2002.
- [47] B. F. Tatting and Z. Gürdal. Automated finite element analysis of elastically-tailored plates. Technical report, NASA CR-2003-212679, NASA, 2003.
- [48] D. C. Jegley, B. F. Tatting, and Z. Gürdal. Optimization of elastically tailored tow placed plates with holes. In *Proceedings of the AIAA/ASME/ASCE/AHS/ASC 44th Structures, Structural Dynamics and Materials Conference*, Norfolk, VA, April 2003. AIAA 2003-1420.
- [49] D. C. Jegley, B. F. Tatting, and Z. Gürdal. Tow-steered panels with holes subjected to compression or shear loading. In *Proceedings of the 46th AIAA/ASME/AHS/ASC Structures, Structural Dynamics and Materials*, 2005.

- [50] K. C. Wu and Z. Gürdal. Thermal testing of tow-placed variable stiffness panels. In *Proceedings of the 42nd AIAA/ASME/AHS/ASC Structures, Structural Dynamics and Materials*, 2001.
- [51] K. C. Wu and Z. Gürdal. Variable stiffness panel structural analysis with material nonlinearity and correlation with tests. In *Proceedings of the 47th AIAA/ASME/ASCE/AHS/ASC Structures, Structural Dynamics and Materials*, 2006.
- [52] K. C. Wu. *Thermal and Structural Performance of Tow-Placed, Variable Stiffness Panels*. PhD thesis, Delft University of Technology, 2006.
- [53] A. Alhajahmad, M. M. Abdalla, and Z. Gürdal. Optimal design of a pressurized fuselage panel with a cutout using tow-placed steered fibers. In *Proceedings of the International Conference on Engineering Optimization, Rio de Janeiro, Brazil*, 2008.
- [54] A. Alhajahmad, M. M. Abdalla, and Z. Gürdal. Optimal design of tow-placed fuselage panels with cutouts for maximum strength and buckling performance. In *Proceedings of the 2nd International Conference on Multidisciplinary Design Optimization and Applications, Gijon, Spain*, 2008.
- [55] W. J. Vankan, W. M. van den Brink, R. Maas, and M. Nawijn. Aircraft composite fuselage optimization through barrel and panel level analyses. NLR-TP 427, NLR, 2011. Technical report, , ECCOMAS Composites 2011, Hannover, Germany.
- [56] K. Croft, L. Lessard, D. Pasini, M. Hojjati, J. Chen, and A. Yousefpour. Experimental study of the effect of automated fiber placement induced defects on performance of composite laminates. *Composites Part A: Applied Science and Manufacturing*, 42:484–491, 2011.
- [57] M. H. Nagelsmit, C. Kassapoglou, and Z. Gürdal. A new fibre placement architecture for improved damage tolerance. NLR-TP 2010-626, NLR, 2010. Technical report, NLR-TP-2010-626.
- [58] Open hole tensile strength of polymer composite laminates. Technical report, American Society for Testing and Materials (ASTM), West Conshohocken, PA, USA, 2003. ASTM D 5766/D 5766M-02.

- [59] Standard test method for measuring the damage resistance of a fiber-reinforced polymer matrix composite to a drop-weight impact event. Technical report, American Society for Testing and Materials (ASTM), West Conshohocken, PA, USA, 2012. ASTM D 7136/D 7136M-12.

Chapter 3

Variable-stiffness composite panels: As-manufactured modeling and its influence on the failure behavior

O. Falcó, J.A. Mayugo, C.S. Lopes, N. Gascons, A. Turon and J. Costa. Variable-stiffness composite panels: As-manufactured modeling and its influence on the failure behavior. *Composites Part B: Engineering*, Vol. 56: pp. 660-669, 2014.

O. Falcó, J.A. Mayugo, C.S. Lopes, N. Gascons, A. Turon and J. Costa. "Variable stiffness composite panels: As-manufactured modeling and its influence on the failure behavior". *Composites Part B: Engineering*. Vol. 56 (January 2014) : 660-669

<http://dx.doi.org/10.1016/j.compositesb.2013.09.003>

<http://www.sciencedirect.com/science/article/pii/S1359836813005167>

Received 23 April 2013

Received in revised form 19 July 2013

Accepted 2 September 2013

Available online 11 September 2013

© 2013 Elsevier Ltd. All rights reserved

Abstract

The introduction of tow-steered laminates in structural applications demands reliable design methodologies to predict and simulate their mechanical response. The full details about the mechanisms that lead to damage and failure of these novel panels are not yet known. In this work, a numerical analysis tool has been developed for structural simulations in a three-dimensional domain. This paper presents a comparison between different configurations and modeling approaches of these panels. Finite element analyses are carried out to simulate the first-ply failure of tow-steered panels under tensile load. The simulations show how matrix cracking is affected by discontinuities in the fiber angle between adjacent courses and fiber-free areas resultant from manufacturing effects; whereas fiber tensile failure is directly influenced by the orientation angles of the fiber, whose distribution depends on the chosen course cutting method: on one side, or on both sides.

Keywords

C. Computational modeling; E. Lay-up automated; Variable-stiffness panels

Chapter 4

Variable-stiffness composite panels: Defect tolerance under in-plane tensile loading

O. Falcó, J.A. Mayugo, C.S. Lopes, N. Gascons and J. Costa. Variable-stiffness composite panels: Defect tolerance under in-plane tensile loading. *Composites Part A: Applied Science and Manufacturing*, Submitted Nov. 2013.

Variable-Stiffness Composite Panels: Defect tolerance under in-plane tensile loading

O. Falcó^a, J. A. Mayugo^a, C. S. Lopes^b, N. Gascons^a, J. Costa^a

^aAMADE, Polytechnic School, Universitat de Girona, Campus Montilivi s/n, 17071 Girona, Spain

^bIMDEA Materials - Madrid Institute for Advanced Studies of Materials, c/Eric Kandel, 2, Parque Científico y Tecnológico-Tecnogetafe, 28906 Getafe, Madrid, Spain.

Abstract

Automated Fiber Placement is being extensively used in the production of major composite components for the aircraft industry. This technology enables the production of tow-steered panels, which have been proven to greatly improve the structural efficiency of composites by means of in-plane stiffness variation and load redistribution. However, traditional straight-fiber architectures are still preferred. One of the reasons behind this is related to the uncertainties, as a result of process-induced defects, in the mechanical performance of the laminates. This experimental work investigates the effect of the fibre angle discontinuities between different tow courses in a ply on the un-notched and open-hole tensile strength of the laminate. The influence of several manufacturing parameters are studied in detail. The results reveal that 'ply staggering' and '0% gap coverage' are effective techniques in reducing the influence of defects in these laminates.

Keywords:

A. Carbon fibers; B. Defects; Variable-Stiffness Panels;

1. Introduction

Nowadays, Automated Fiber Placement (AFP) of carbon-fiber-reinforced composites is widely applied in the aerospace industry. The use of this technology permits the manufacture of larger structures, providing more strength and stiffness where needed while ensuring high quality and shorter production times [1]. The AFP process automatically places multiple individual preimpregnated tows onto a mandrel at high speed using a numerically controlled

Email address: ja.mayugo@udg.edu (J. A. Mayugo)

placement head to dispense, clamp, cut and restart each tow during placement. AFP systems make the production of Non-Conventional Laminate concepts (NCLs) possible [2]. Among these concepts are the Variable-Stiffness Panels (VSP), where the fibers follow curved paths, and which are noted not only for their structural performance and versatility, but also for their design complexity [3–6]. The results of compression testing the VSP specimens confirm that they are particularly suitable in resisting buckling, because it is possible to transfer the higher stresses from the interior to the edge of the panels [7]. Also, the VSP are able to improve first-ply failure responses, for example in laminates with a central hole [8]. Despite these potential advantages and the developments of AFP manufacturing over the past two decades, conventional straight-fiber laminates based on 0° , 90° , $\pm 45^\circ$ ply angles are still predominantly used.

Typically, an AFP machine has the capability of placing up to 32 (1/8 in.) fiber tows within a single course width. This means that within each head pass or course, up to 32 tows are placed parallel to each other. A reference path shift occurs discretely at multiples of the course width. Within a given course, the fiber orientation deviates from the reference path which is only followed by the course centreline. The maximum deviation is at the edges of the course, which results in a fiber-angle mismatch between adjacent courses. The wider the courses, the larger this discontinuity is. These geometric discontinuities can be the cause of stress concentrations which in turn, can hinder the performance expected from the idealized structure, i.e. one with a continuous variation of the fiber orientation along one of the planar coordinates.

There are two manufacturing approaches to deal with the converging tows at the VSP course edges: the *tow-overlapping* and the *tow-dropping* methods [9–11]. If the tows overlap, thicker regions are created which can act as stiffeners in the laminate. Conversely, the tow-drop method avoids overlapping zones by cutting the individual tows at their intersection point, so that thickness does not build up. As a result, small defects consisting of resin rich zones without fibers, called *gaps*, are created at the boundaries of the tow-placement course. In both methods, these gap and overlap zones can become potential spots for the initiation of matrix cracking or even delaminations as a result of the local amplification of interlaminar stresses. Different methods have been introduced with the aim of reducing

the influence of these defects on the structural response. Some of which are: the hybrid combination of curvilinear plies with straight-fiber plies (mainly placed at the outer layers), the staggering technique [12], and the variation of the gap coverage parameter [4]. On one hand, the staggering technique avoids the nucleation of the defects that would occur in the same places through-the-thickness of a laminate in plies of the same steering configuration. Staggering reduces the concentration of the resin area (gaps), thus increasing the load transfer effectiveness and making smooth thickness laminates possible. On the other hand, the gap coverage parameter is used to minimize the presence of gaps due to tow-dropping. This parameter determines the degree to which the discrete gaps are covered by fibers, and can vary gradually from 0% to 100% —in which case gaps cease to exist, but small triangle tow-overlaps are created instead.

Several approaches and numerical analyses have been performed to optimize VSP design [13–17]. Other studies —e.g. on buckling response, thermal stresses analyses, strength and stiffness— with the aim of obtaining an adequate understanding of the behavior of these laminates have been developed and validated by experimental work [18–24]. However, the full details of the mechanisms that lead to failure and the mechanical response of a VSP are not yet fully understood, particularly the influence of embedded defects, mainly gaps, overlaps and the fiber angle discontinuities induced by AFP [25, 26]. It is worth mentioning the theoretical and numerical investigation on the influence of the tow-drop areas and staggering on the stiffness and strength of variable-stiffness laminates presented by Blom *et al.*[12]. Additionally, Blom *et al.* expanded their studies from tailored flat panels to cylindrical and conical shells [27, 28]. In the latter cases, the effects of gaps and overlaps were analyzed in a global sub-component level.

The certification of variable-stiffness laminates requires high-level component tests in order to understand the effect of the defects on the mechanical response and failure mechanism of the laminates. Some of these defects have been the object of research [29, 30]. Recently, Nicklaus [31] explored the effect of converging gap defects in the open-hole compressive strength and mode-I fracture toughness. He points out that these ply gaps (resin pockets) produce higher fracture toughness values in the critical stress area adjacent to the hole. Similarly, Croft *et al.* [32], presented an experimental study quantifying the effect of the

main manufacturing-induced defects. Their work reveals the influence of these defects in the mechanical response of composite laminates under tensile, compression and shear loading. It is worth noting that, in that study, the defects were manually inserted during specimen manufacture and were not the result of a real tow-drop or tow-overlap procedure in an AFP machine.

The present work aims to quantify the effects on laminate strength of tow-drop defects found in a real AFP manufacturing environment. Three different configurations were considered: 100% gap coverage (allowing small overlaps), 0% gap coverage and 0% gap coverage with ply staggering. The configurations analyzed have been compared with an equivalent baseline laminate without defects. Initially, the real defect geometry was analyzed using detailed micrographs. Then, these laminate configurations were tested under monotonic tensile loading for un-notched and open-hole specimens. The Digital Image Correlation (DIC) technique has been used to analyze the full strain field and to observe the influence of defects, particularly in those zones prone to damage, just before the final structural collapse. Additionally, the failure mechanisms have been analyzed with the help of high-resolution photography.

2. Specimen design and manufacturing

The test specimens for the experimental work reported in this paper have been designed to represent the ply discontinuities at the edges of adjacent courses in VSP configurations. Accordingly, each specimen represents a sub-domain of a whole panel, as shown in Fig. 1a. The maximum tow-angle mismatch ($\theta_1 - \theta_2$), represented in Fig. 1b for different VSP configurations with linear fiber-angle variations, is dependent on panel dimensions, course width (or number of tows per course, n_t) and fiber angles at the center (T_0) and at the edges of the panel (T_1) [3]. In Fig. 1b only those configurations with $T_0 = 0^\circ$ are considered, as these lead to the worst-case tow-angle mismatch scenarios. Likewise, a panel side of 700 mm in the direction of fiber-angle variation is considered as a limit case. For a panel smaller than this, the maximum variation between T_0 and T_1 would be bounded by the minimum machine turning radius in order to keep an acceptable laminate quality. Hence, a maximum theoretical mismatch angle of 13° is achieved. In reality, the angle $T_1 = 90^\circ$ is never achieved

in practice due to finite tow-width and discrete tow-cutting [25]. For the tensile specimen design in this work, a discontinuity of 12° was been selected as a reasonable approximation to the worst-case scenario.

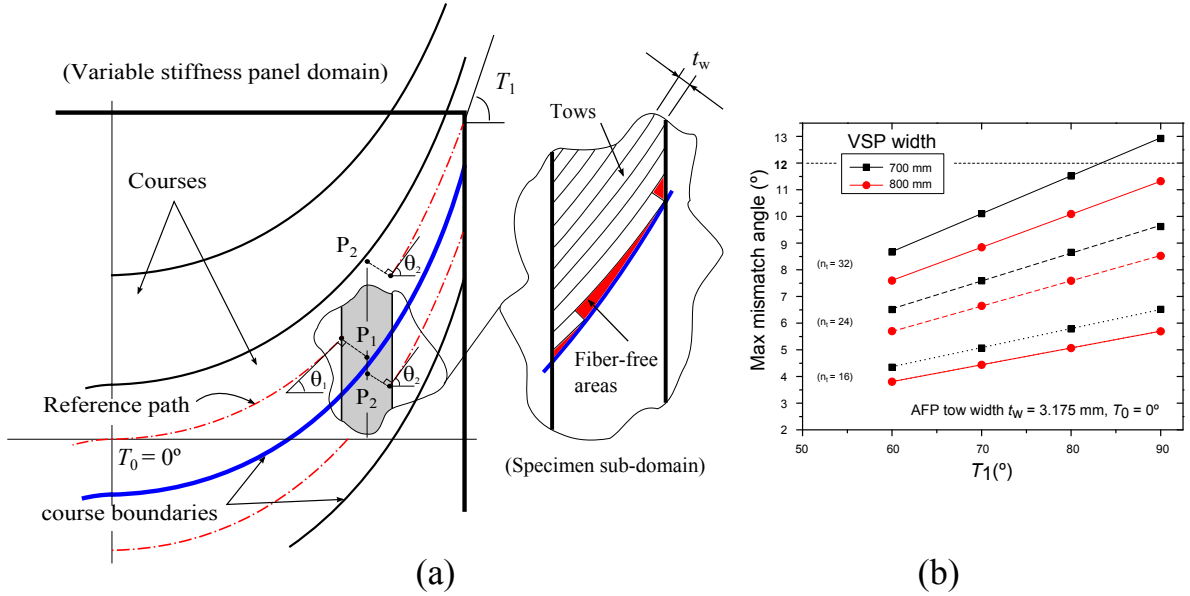


Figure 1: a) Tensile specimen sub-domain definition in a Variable Stiffness Panel. b) Maximum mismatch angle ($\theta_1 - \theta_2$) between the boundary of the courses for panels of 700 mm and 800 mm for $T_0 = 0^\circ$ and different T_1 values.

The specimens consist of straight-fiber layers since, considering the small dimensions of the specimens, there is negligible difference between the actual curved trajectory and a straight one. Some layers in the laminate have one portion with the fibers at 51° and another at 39° , thus creating an angle discontinuity at the specimen mid-length. To avoid more complexity, these plies with angle discontinuity were balanced with plies at -45° . Both the Un-Notched Tensile (UNT) and the Open-Hole Tensile (OHT) specimens have the same outer dimensions: length (L) of 310 mm, width (W) of 32 mm and tab length L_{tab} of 65 mm. The specimen geometry is depicted in Fig. 2a.

The material used in this investigation is the HexPly AS4/8552 pre-impregnated CFRP in 6.35 mm (1/4 in.) wide tows (t_w). The nominal ply thickness after curing is 0.18 mm.

The lay-up analyzed is $[45/0/-45/90/(-45_2/(51|39)_2)_2]_s$. The design of the external plies was constrained to the conventional straight-fiber method to avoid gaps or overlap defects in the outer layers of the laminate. All configurations present the same stacking

sequence (24 plies) with nominal laminate thickness of 4.32 mm. A baseline laminate with a stacking sequence of $[45/0/-45/90/(-45_2/45_2)_2]_s$ has also been analyzed and tested for comparative purposes. The baseline and non-conventional laminates were designed to have similar global stiffness. The elastic properties of the material system are $E_{11} = 138.0$ GPa, $E_{22} = 8.6$ GPa, $G_{12} = 4.9$ GPa, $\nu_{12} = 0.35$.

Three configurations with tow-drop defects have been designed and tested. The configurations are described in Fig. 2b. The difference between the three is in the variation of the gap coverage parameter and the use of the staggering technique. In one configuration, tows are cut avoiding any overlapping, hence generating a triangular fiber gap (0% gap coverage). In another configuration, tows are allowed to overlap by just the required amount to avoid these gaps (100% gap coverage). As a result, right-triangular gaps or overlaps appear in the laminate. The dimension of one leg is the width of the tow and its opposite angle is the discontinuity angle (see Fig. 2b). In our case, the triangle legs are 6.35 mm and 29.9 mm respectively. In these two configurations, gaps and overlaps are co-located through the thickness of the laminate for plies with the same steered configuration. In a third configuration, the co-location of gaps is avoided by staggering the plies in relation to each other. The staggering distance is twice the width of the tow (12.70 mm) along the transverse direction to the 51° tows (see Fig. 2b).

Four plates were manufactured with a Coriolis Fiber Placement Machine in the National Aerospace Laboratory (NLR) in the Netherlands. The material was cured in a two-step cycle — 110°C during 60 min followed by 180°C for 120 min— according to manufacturer specifications for monolithic components. All plates were C-scan inspected to ensure the laminate quality. For the un-notched specimens, tabs are mandatory to avoid excessive stresses near the clamping jaws. E-glass fabric prepreg tabs at $\pm 45^\circ$ were glued to the specimen with epoxy adhesive and tapered with the nominal slope of 1 in 4. After curing the laminates, the specimens were cut using a 2.5 mm thick diamond blade. The central hole of the open-hole tensile specimens was drilled with a 6.3 mm diameter multi-directional drill. The specimens were checked to ensure they were within tolerance and free from delaminations after the cutting process.

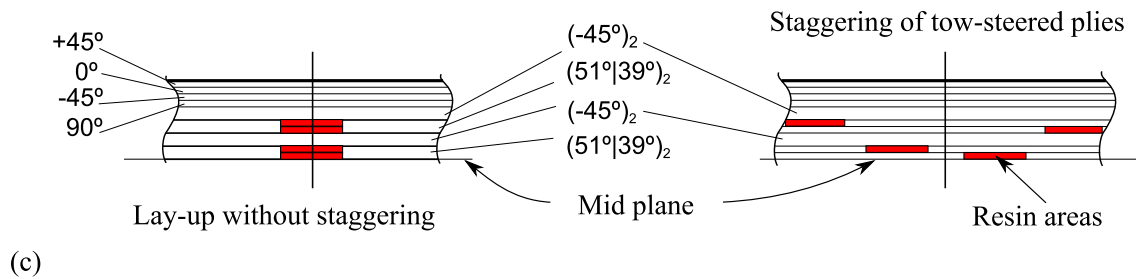
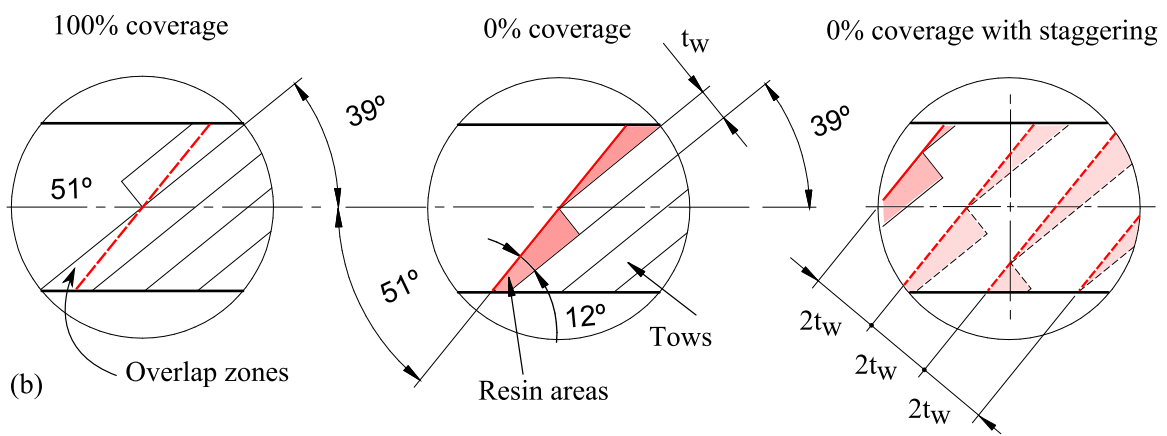
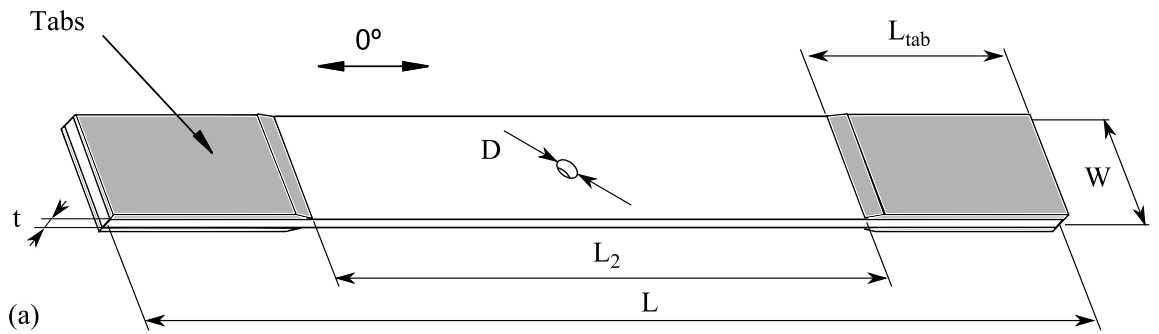


Figure 2: a) Specimen geometry. (b) Tow-drop gap defects (100% gap coverage, 0% gap coverage and 0% gap coverage with staggering). The discontinuity interface in the ply $\langle 51|39 \rangle$ is represented using a red line and resin rich areas are shaded in red. (c) Tow-drop specimen lay-up with and without staggering.

3. Real tow-drop defect geometry

This section scrutinizes the two-drop defects induced in the three configurations through an in-depth analyses of thickness measurements and micrographic images.

The micrographic observation reveals the real size and nature of the gap and overlap

zones. This is essential for a better understanding of the mechanical response of the non-conventional laminates with these types of manufacturing defects.

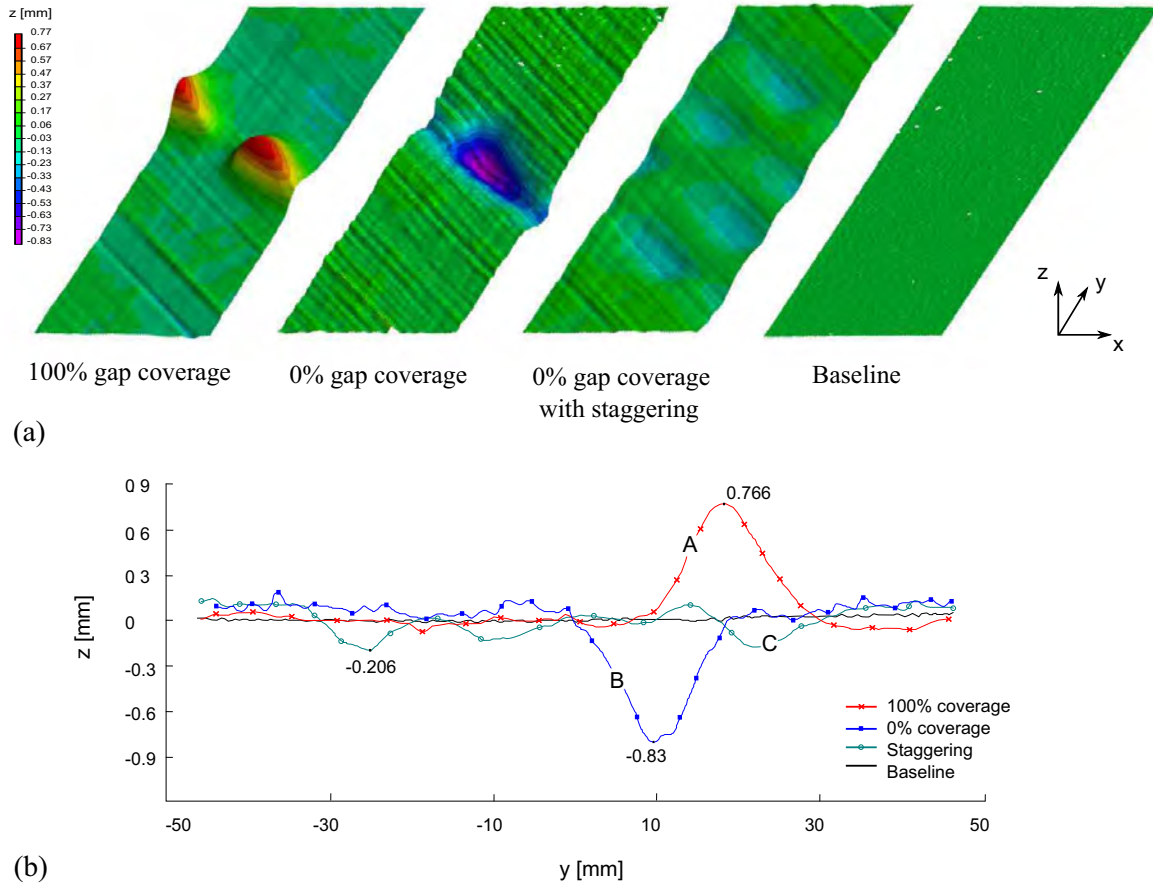


Figure 3: Profile variations on top surface of the different specimens configurations.

The real top-surface profile and dimension measurement for each configuration is precisely obtained with the VIC-3DTM system. A comparison of the surface profile in the top outer layer for each configuration is shown in Fig. 3. The thickness variations along the y -direction of the middle line for the different configurations are compared. For the configurations without ply staggering, the tow-drop defects coincide at the same in-plane location for layers of the same configuration, which produces co-location of overlaps and gaps. For the configuration with 100% gap coverage, the laminate thickness increases by 15% due to the overlapping. Whereas, for the configuration with 0% gap coverage, the maximum thickness reduction is 20%. This thickness reduction is caused by the pressing of gaps in adjacent

layers as a result of the high pressure in the autoclave during the curing process. However, if the staggering technique is applied, the local thickness variation reduced considerable ensuing in a mere 5%. The reason being that staggering reduces the superposition of defects through the laminate thickness.

The micrographic analyses were performed with a Leica DMR-XA compound light trinocular microscope (Bright Field and Fluorescent Imaging) with $50\times$ to $1600\times$ magnification and a resolution of 0.2 microns, together with a ProgRes C14 digital camera.

For the configuration with 100% gap coverage, an external and cut view of the specimens analyzed are shown in Fig. 4. The increase in thickness due to the ply overlapping is remarkable. The curvature of the outer layer is smooth (see Fig. 4a) as a result of the stiffness of the continuous layers during the curing process. The manufactured specimens contain significant areas of overlap, together with small triangular rich resin zones near the tow-drop sections (see Fig. 4b).

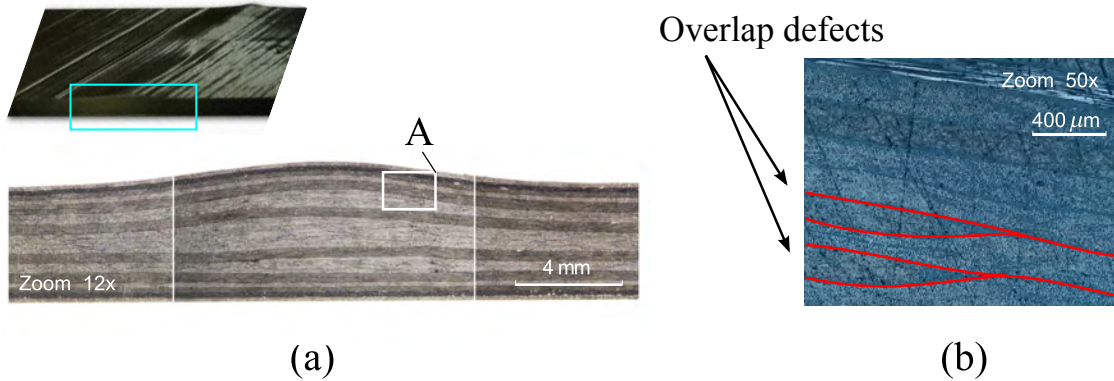


Figure 4: a) Real tow-drop defect for configuration with 100% gap coverage (magnification $12\times$). b) Detailed micrography (magnification $50\times$).

In order to observe the extension of the rich-resin zones in the configuration with 0% gap coverage, three different sections have been analyzed along the specimen (see Fig. 5a). While it is true that, in the section QQ' , small dispersed gaps appear (see Fig. 5c, detail Q), in the sections OO' and PP' , all the gaps are clustered and concentrated. Here, the size of the gap defects is notable (see Fig. 5c, detail O and P), and the waving of the adjacent plies to fill the gap area is evident. The curvature of the plies is similar to the 100% gap coverage

case. Higher angle differences between adjacent layers reduce the waving of the tows.

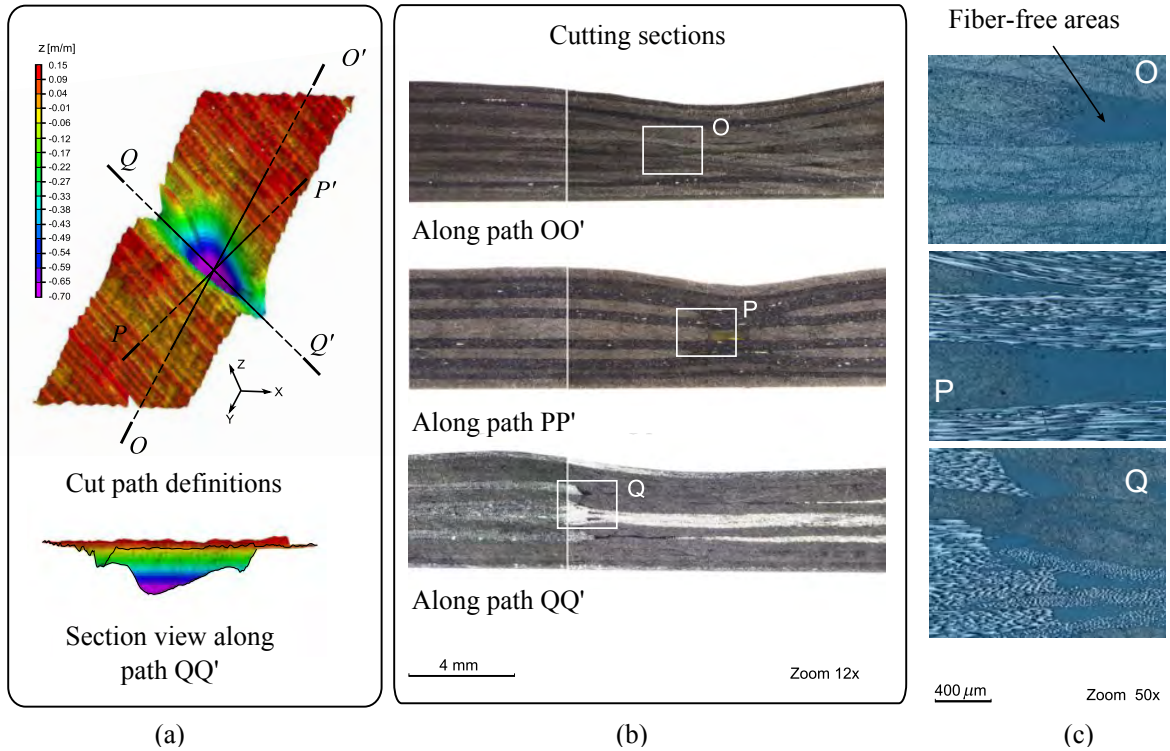


Figure 5: (a) Cut section definitions. (b) Different view for the configuration with tow-drop 0% coverage (magnification 12 \times). (c) Detailed gap micrography (magnification 50 \times).

If the staggering technique is applied to the 0% gap coverage case, the laminate thickness becomes more homogeneous because of the non-coincidence of gaps. A laminate surface similar to the baseline configuration is obtained, as confirmed by microscopic observation (see Fig. 6). Although clustering of defects is avoided, small resin zones still remain as the result of single gaps, as seen in the micrographic detail C in Fig. 6.

The assumption of gap areas totally filled by resin is used mainly for modeling the tow-drop gaps for numerical simulation purposes in order to simplify the analysis. However, this assumption is uncertain according to the observed micrographs. In these simplifications, the effect of the high autoclave pressure on the individual plies in the laminate is neglected. For a better understanding of the failure and damage mechanisms, the real defect geometry needs to be taken into account. This work confirms the results observed by Croft *et al.* [32] with respect to the real defect geometry and its influence on the strength in the non-conventional

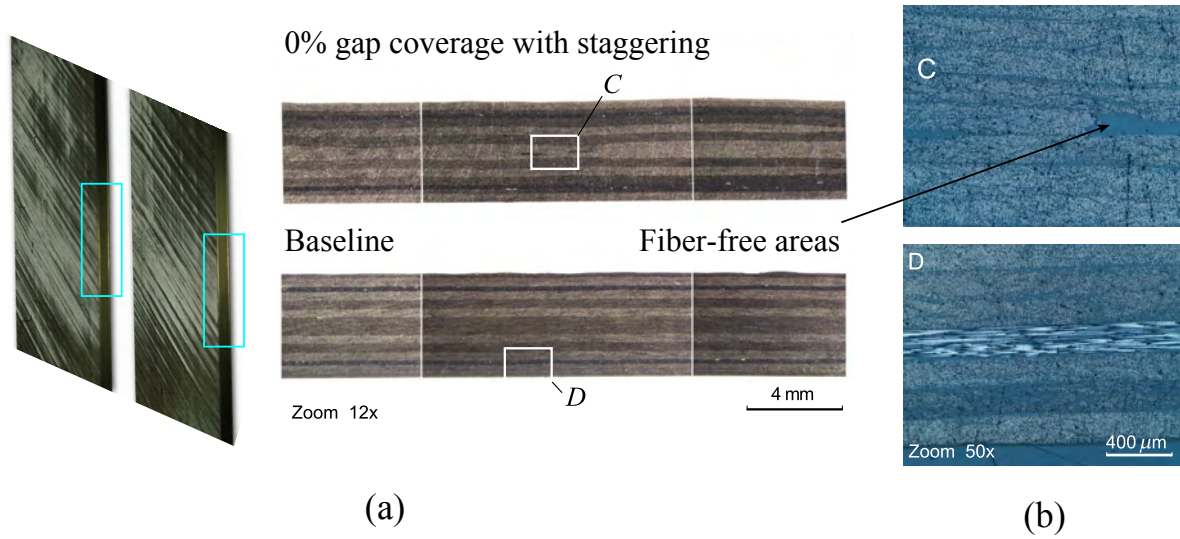


Figure 6: (a) Specimens. (b) Real tow-drop defect for the configuration with 0% coverage with staggering and the Baseline laminate (magnification 12 \times). (c) Detailed defect micrograph (magnification 50 \times).

laminates.

4. Experimental set-up

Un-notched and open-hole specimens were tested using a hydraulic MTS 810 system with a 250 kN load cell. The ASTM standard D 5766 [33] was followed to determine the open-hole tensile strength in multidirectional CFRP specimens. The data acquisition frequency used was 20 Hz.

The VIC-3DTM Measurement System (Correlated Solutions, USA) was used in this test to measure the full-field displacements and strains on the outer 45 $^{\circ}$ ply with Digital Image Correlation (DIC). The DIC system set-up with a pair of stereo-mounted digital cameras is shown in Fig. 7. For real-time analog data acquisitions, the system is connected to the load output of the test frame controller, and records load and displacement data synchronously with the images.

The working distance of the DIC installation was set to 700 mm for the plain tensile test, whereas for the open-hole tensile it was set to 400 mm, for an object facet size of 90 \times 32 mm² and 45 \times 32 mm², respectively. The area of interest was spray painted guaranteeing the quality of the speckle pattern. The selected subset size was 29 (29 \times 29 pixel²) with a

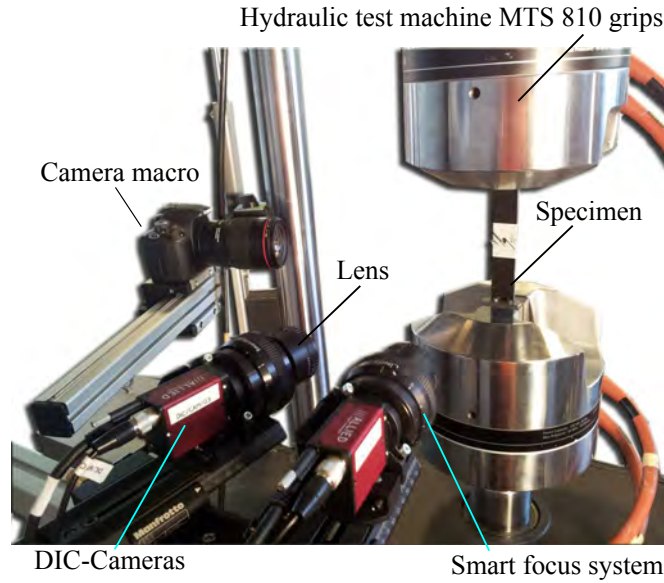


Figure 7: Open-hole tensile (OHT) specimen tensile test set-up with DIC technology included.

7 pixel step size. On the one hand, the subset size has to be large enough to ensure that there is a sufficiently distinctive pattern contained in the area used for correlation, whereas on the other hand, the step size controls the spacing of the points that are analyzed during correlation. The shutter interval time was set to 500 ms to be compatible with an applied displacement rate of $0.5 \text{ mm}\cdot\text{min}^{-1}$. In both cases, a Rodagon WA 60 lens was used with an extension tube [1 \times] joined to a Smart focus system. An additional camera with an EF-100mm macro lens ('camera macro' in Fig. 7) was used to observe the crack propagation on one of the free edge of specimens. All tests were monitored using the VIC-3DTM DIC system on one side. For the plain tests, strain gauges were bonded to the other side. Two strain gauges in the axial and transverse directions were placed in the middle of the specimens, with a gauge factor k of $2.04\pm 1\%$ at 24°C , and resistance of $350\Omega\pm 0.30\%$.

5. Test results and discussion

A total of 24 specimens were tested under tensile load up to final failure, with an average of three specimens for each configuration. The DIC was used to observe the influence of the VSP defects on the strain field until the final structural collapse. The failure is taken as being the first significant load drop in the load-displacement response. The failure mechanisms

and the strength values were analyzed for each configuration. Previous to the failure test, a correlation between the stress-strain responses for one of the specimens was carried out. The results obtained through the DIC system, the axial strain gauge and an extensometer demonstrated very good agreement between the different techniques.

5.1. Un-Notched Tensile (UNT) test

The first analyses were carried out by DIC at the moment just before the final failure of the specimens, in order to observe the influence of tow-drop defects on the strain field and on the out-of-plane displacement. Three specimens with tow-drop defects were selected, one for each configuration, and their behavior was compared. The longitudinal strain (ε_{yy}), transverse strain (ε_{xx}), shear strain (ε_{xy}) of the outer layer at 45° and displacement along the out-of-plane direction (w) throughout the survey area in question are shown in Fig. 8. In all cases analyzed, the load direction and the fiber direction at 0° corresponds to the vertical axis (y-direction). The fibers oriented at 51° are located below the defect zone. The strain variation due to the fiber angle discontinuity of ($51^\circ|39^\circ$) can easily be seen in the DIC representations. The strains concentrate in the vicinity of the defect areas which are critical zones for damage. On the one hand, in the case of 100% gap coverage, the longitudinal strains in the tow-drop area are lower than average strains resulting in overlapping and stiffer zones. On the other hand, in the configurations with 0% gap coverage, the defects result in material zones with lower stiffness and higher strain.

The analysis of the displacement (w) reveals delaminations near the edges of the specimens. In the non-staggered configurations, these delaminations are concentrated in the clustered regions of ply discontinuities. However, in the staggered specimens, the delaminations are less evident and distributed along the edge in different zones (see Fig. 9a).

The results of remote failure stress obtained for the different configurations in plain tensile test are summarized in Table 1. For plain specimens, compared with the baseline lay-up, the configurations with tow-drop defects exhibit lower tensile strength. The specimens with 100% gap coverage show a strength reduction of 10.7%, while the laminates with 0% gap coverage present a more significant strength reduction of about 20.1%. For the configuration

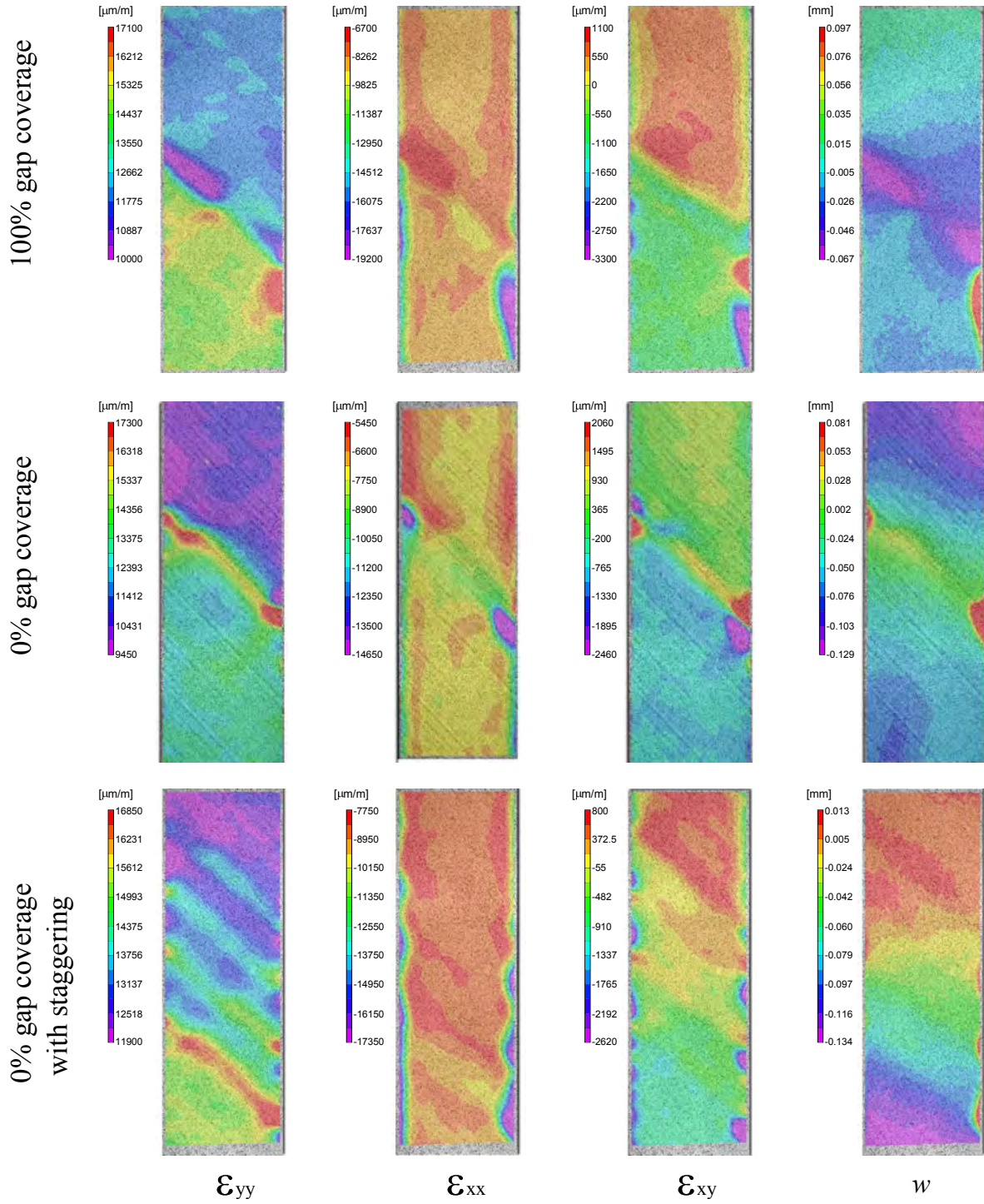


Figure 8: Strain field (ϵ) and out-of-plane displacement (w) comparison for un-notched tensile specimens on the outer layer at 45° just before final failure.

with staggering, the reduction is only 8.6%. The standard deviation of the values is higher in tow-drop specimens due to the different distribution of the defects. The results show an increase of the ultimate strength for the configurations with 100% gap coverage with respect to 0% gap coverage. This can be explained by the reinforcing effect of the overlaps. The results also confirm the expected improvement obtained by means of the staggering technique applied to laminates manufactured by the tow-drop method.

Table 1: Remote failure stress for un-notched tensile (UNT) and open-hole tensile (OHT) specimens (values in MPa). Calculated using the maximum measured stress (P_{\max}) and the values of the specimen thickness (t) and width (w) as: $X^T = P_{\max}/(tw)$.

Configurations	Mean (MPa)	STDV (MPa)	Normalized strength
Un-notched tensile (UNT)			
UNT Baseline	389.2	0.6	1
UNT 100% gap coverage	347.3	12.3	0.89
UNT 0% gap coverage	303.1	21.7	0.78
UNT Staggering (0% coverage)	355.8	9.1	0.91
Open-hole tensile (OHT)			
OHT Baseline	225.6	4.2	1
OHT 100% gap coverage	235.9	6.8	1.04
OHT 0% gap coverage	214.7	1.4	0.95
OHT Staggering (0% coverage)	231.4	6.0	1.02

For comparison purposes, the load-displacement curves for one specimen of each configuration are plotted in Fig. 9. The extensive non-linearity of the load-displacement curves prior to failure confirms a progressive loss of stiffness; probably as a result of both the appearance of matrix cracking in the off-axis layers, and the onset of delaminations across the tow-drop defect zones. Specimen collapse is caused by extensive fiber breakage.

In both of the non-staggered configurations, the edge photographs taken during the test reveal large free-edge delaminations in the zones with defects (Fig. 9a). For example, point O in Fig. 9a identifies the observable delamination onset on the free-edge for the configuration with 100% gap coverage, which advances up to point P where the specimen finally fails. This cracked zone coincides with the defect area. In such areas, the fiber angle discontinuities and the thickness variations increase the interlaminar stresses, which cause delaminations

in the free edges. Such stresses contribute to the weakening of the specimens. Hence, the failure of the plain tensile specimens begins at the edge and propagates along the defect. The staggered laminate configuration presents a structural behavior analogous to the baseline. Both lay-ups present similar observed free-edge delaminations. The crack delaminations are small and uniformly distributed across the edge of the laminate in comparison with the non-staggered configurations. In Fig. 9a, this failure mode is shown in the image taken just before final failure (point Q).

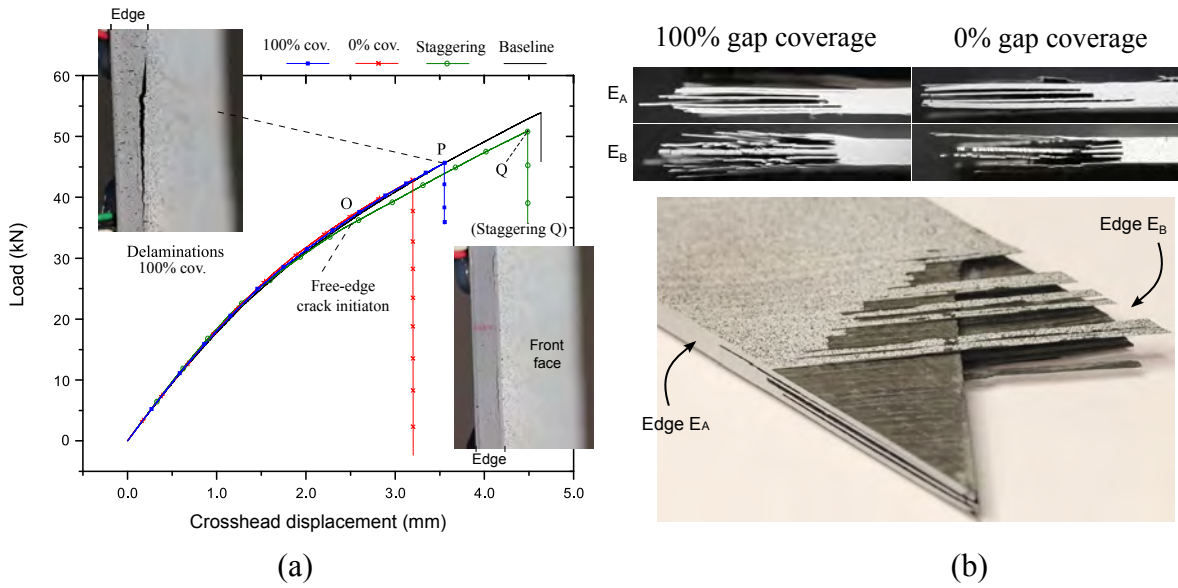


Figure 9: a) Comparison of load-crosshead displacement for different un-notched laminate configurations. (b) Delamination on tested specimen.

Post-failure examination of the specimens shows two main types of failure mechanism: fiber pull-out and delamination. The pull-out failure mechanism is caused by fiber failure mainly at the 0° plies. The delamination analysis reveals that the interlaminar damage always occurs with the same pattern at the sublaminates level. This behavior is common to all the specimens tested. Therefore, this failure mechanism is likely to be more dependant on the lay-up rather than any other factor. To illustrate this, photographs of failed specimens are shown in Fig. 9b. An examination of the fractured edges of specimens (Edge E_A and Edge E_B) reveals large delaminations as a result of the mismatch angles between the plies. Two delaminations appear between the outer layers and the 0° laminae, whereas the other

delaminations occur in the interfaces between the $(-45^\circ)_2$ layers and the $(51^\circ | 39^\circ)_2$ plies.

5.2. Open-Hole Tensile (OHT) test

In contrast to the un-notched specimens where the maximum strain appears in the tow-drop-induced-defect zones, for the open-hole specimens higher strains are produced in the stress concentration spots around the hole. Although all of the OHT specimens tested present a similar fracture behavior, there are small differences between them.

In order to illustrate the longitudinal strain distribution (ε_{yy}), one DIC representation for each configuration has been selected and shown in Fig. 10a. The images depict the critical strain zone just before the crack initiation at the 45° ply; akin to where the onset of damage and the first evident delaminations are observed. When the 100% gap coverage is compared to that of the 0% gap coverage, the first reveals lower strains in the defect direction because of stiff zones caused by the ply overlapping, while in gap zones the strains were higher. For the staggered and baseline configurations, the strain fields are nearly identical. The variations of longitudinal strain (ε_{yy}) along path AA' (see Fig. 10a, baseline) in y-direction for the OHT configurations are plotted in Fig. 10b. As observed, maximum deformation is governed by the increasing stress values in the adjacent zones to the hole where the damage appears, and the manufacturing-induced defects have little relevance in the final failure process.

The longitudinal strain field ε_{yy} for the outer layers at 45° of one test specimen, just before the final catastrophic failure, for each of the configurations tested are shown in Fig. 11. Here, the 45° matrix crack is clearly visible from the hole in the outer ply surface. This external damage is propagated asymmetrically across the width of the specimen to the specimen edges.

The damage mechanisms for the OHT specimen observed in this experiment were similar to those observed by other authors for OHT specimens [34, 35]. Initially, isolated matrix cracking, splitting and delaminations at the hole edge appear (see Fig. 12b). Then, damage propagates across the width of the specimen, leading to final collapse. Fiber breakage in the 0° plies can only be observed after the final catastrophic failure. The failure mechanisms are represented in schematic form in Fig. 11b. Delaminations are controlled by the interlaminar shear stresses, increased by the free edge effect of the hole and the influence of the manu-

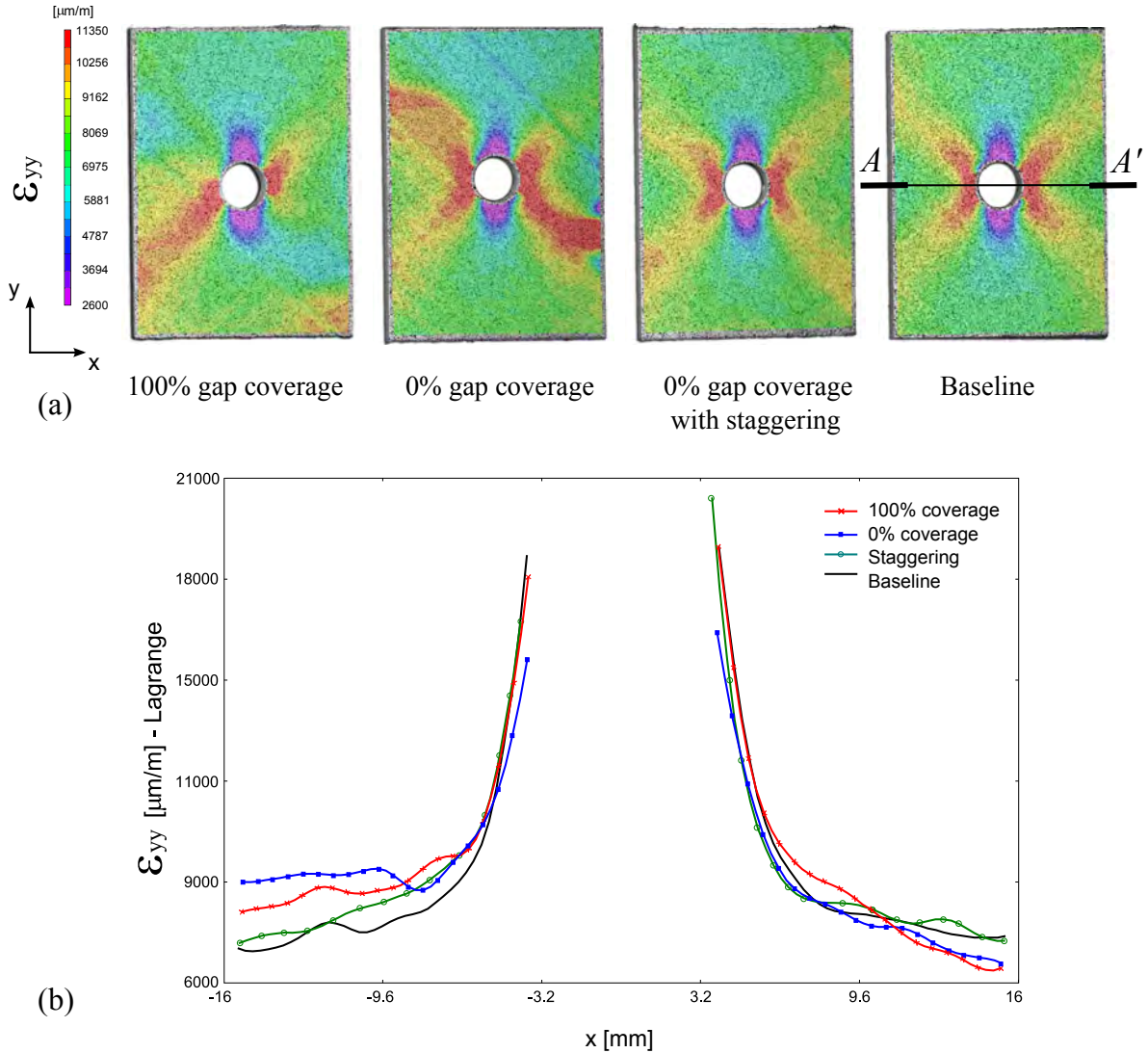


Figure 10: a) Longitudinal strain field for the outer layer of different OHT configurations just before visible crack initiation. b) Plot of the longitudinal strain ϵ_{yy} along path AA'.

facturing induced defects. However, in contrast to the plain specimen, the influence of the open hole is more relevant than the defect itself.

The OHT test load-displacement curves for representative specimens are plotted in Fig. 12a. The results show the similarity between the staggered laminate specimens and the conventional specimens. The load-displacement curves present less non-linearity than those of the un-notched specimens. In these specimens, the structural collapse was also controlled by a pull-out failure mechanism accompanied by delaminations. The post-fracture

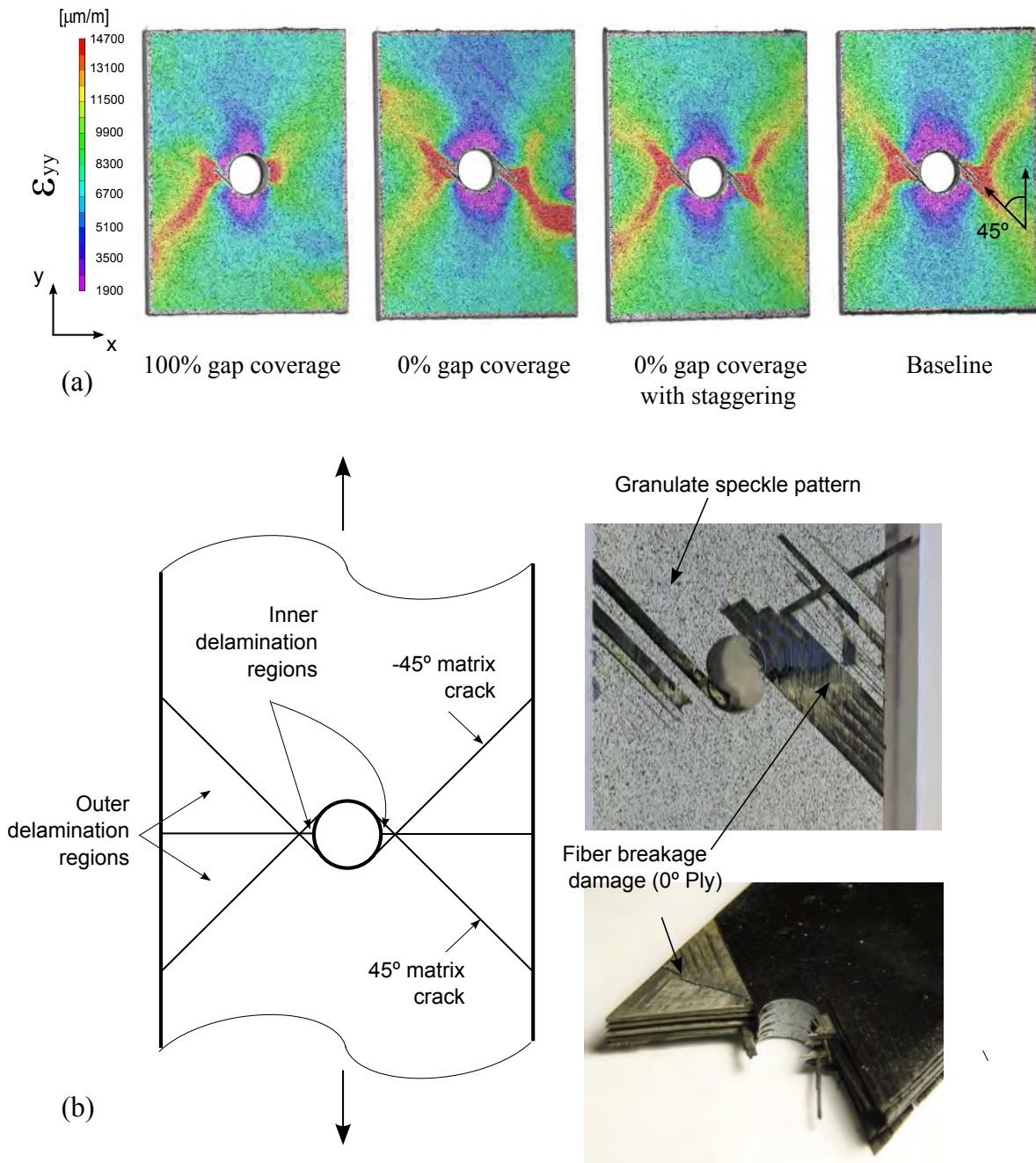


Figure 11: a) Longitudinal strain field for the outer layer of different OHT configurations just before final failure. b) Damage zones associated with the specimens.

analysis and the load-displacement behavior have a good agreement with the observed failure mechanism, as reported by Green *et al.* in [34].

In the outer ply the onset of damage at the hole free edge is propagated parallel to

the fiber orientation of 45° . Similar sub-critical damage mechanisms were observed for all specimens, as shown in Fig. 12b. The zoom on the open-hole region reveals how the damage is initiated in the form of isolated matrix cracks and delamination at the hole edge. This damage is mainly at the interface of the plies with overlap or gaps and conventional plies without fiber angle discontinuities.

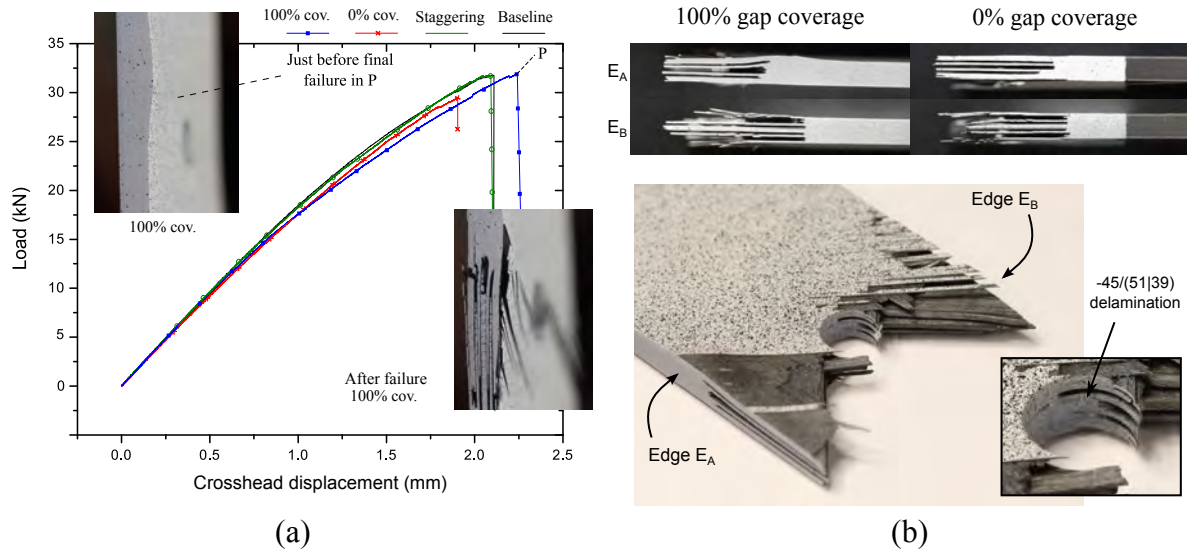


Figure 12: a) Comparison of load-crosshead displacement for different open-hole laminate configurations. (b) Delamination and damage on tested specimen.

The open-hole results present small differences of far-field stress, as specimen failure is strongly driven by the presence of the hole. This means that the stress concentration generated by the hole is little amplified by the manufacturing defects. The results of remote-failure stress obtained for the different configurations in the open-hole tensile test are summarized in Table 1.

6. Conclusions

In the present experimental work, the effect of the fiber angle discontinuities between different tow courses in a ply on the un-notched and open-hole laminates tensile strength was investigated. The influence of the coverage percentage and the staggering technique were studied in detail.

Test specimens were designed and manufactured to represent a sub-domain of a VSP containing a worst-case tow-angle discontinuity, and different practical manufacturing strategies to tackle such discontinuity: i) tow-dropping with 0% gap coverage (gaps); ii) tow-dropping with 100% gap coverage (overlaps); and iii) tow-dropping with 0% gap coverage and ply staggering.

After a geometrical observation of overlapping and gap defects produced by the tow-drop manufacturing method, test specimens were loaded until failure. In comparison with the baseline specimens representing straight-fiber panels without defects, the configuration with 0% gap coverage and no staggering presents the most critical strength reduction; as a results of the clustering of gaps. When the ply staggering technique is applied, these effects are highly mitigated. Therefore, 'ply staggering' and '0% gap coverage' is an effective combination to lessen the influence of defects in VSP.

The experimental results show that the stress concentration, induced by the presence of the hole in OHT specimens, has a higher influence on failure than that induced by the presence of manufacturing defects in un-notched specimens. Additionally, the analysis of failure mechanisms in un-notched specimens reveals that large delaminations initiate in the vicinity of the tow-drop defects, which are then followed by extensive matrix cracking and finally fiber failure. This is probably caused by the amplification of the interlaminar stresses around the defects.

Acknowledgements

The authors acknowledge the financial support of the Ministerio de Economía y Competitividad of Spain under project MAT2009-07918. The first author would also like to thank Generalitat de Catalunya for the FI grant AGAUR, IUE/2365/2009.

References

- [1] Lukaszewicz D, Ward C, Potter K. The engineering aspects of automated prepreg layup: history, present and future. *Composites Part B: Engineering* 2012;43:997–1009.
- [2] Lopes CS. Damage and failure of non-conventional composite laminates. Ph.D. thesis; Delft University of Technology; 2009.

- [3] Gürdal Z, Tatting BF, Wu KC. Variable stiffness panels: Effects of stiffness variation on the in-plane and buckling responses. *Composites Part A: Applied Science and Manufacturing* 2008;39:911–22.
- [4] Gürdal Z, Tatting BF, Wu KC. Tow-placement technology and fabrication issues for laminated composite structures. In: *Proceedings of the AIAA/ASME/ASCE/AHS/ASC Structures, 46th Structural Dynamics & Materials Conference*. 2005,.
- [5] Blom AW, Mostafa , Abdalla M, Gürdal Z. Optimization of course locations in fiber-placed panels for general fiber angle distributions. *Composites Science and Technology* 2010;70:564–70.
- [6] Khani A, IJsselmuiden ST, Abdalla MM, Gürdal Z. Design of variable stiffness panels for maximum strength using lamination parameters. *Composites Part B: Engineering* 2011;42:546–52.
- [7] Lopes CS, Gürdal Z, Camanho P. Variable-stiffness composite panels: Buckling and first-ply failure improvements over straight-fibre laminates. *Computers and Structures* 2008;86:897–907.
- [8] Lopes CS, Gürdal Z, Camanho PP. Tailoring for strength of composite steered-fibre panels with cutouts. *Composites Part A: Applied Science and Manufacturing* 2010;41:1760–67.
- [9] Gürdal Z, Olmedo R. In-plane response of laminates with spatially varying fiber orientations - variable stiffness concept. *AIAA J* 1993;31(4):751–8.
- [10] Tatting BF, Gurdal Z. Design and manufacture of elastically tailored tow placed plates. Tech. Rep. NASA/CR-2002-211919; NASA; 2002.
- [11] Wu KC, Gürdal Z, Starnes JH. Structural response of compression-loaded, tow-placed, variable stiffness panels. In: *Proceedings of the 43rd AIAA/ASME/ASCE/AHS/ASC Structures, Structural Dynamics and Materials Conference*. Denver, CO; 2002,AIAA 2002-1512.

- [12] Blom AW, Lopes CS, Kromwijk PJ, Gürdal Z, Camanho PP. A theoretical model to study the influence of tow-drop areas on the stiffness and strength of variable-stiffness laminates. *Composite Materials* 2009;43:403–25.
- [13] Nagendra S, Kodiyalam S, Davis JE, Parthasarathy VN. Optimization of tow fiber paths for composite design. In: *Proceedings of the AIAA/ASME/ASCE/AHS/ASC 36rd Structures, Structural Dynamics and Materials Conference*, New Orleans, LA. 1995, p. 1031–41.
- [14] Jegley DC, Tatting BF, Gürdal Z. Optimization of elastically tailored tow placed plates with holes. In: *Proceedings of the AIAA/ASME/ASCE/AHS/ASC 44th Structures, Structural Dynamics and Materials Conference*. Norfolk, VA; 2003,AIAA 2003-1420.
- [15] Setoodeh S, Abdalla MM, Gürdal Z. Design of variable-stiffness laminates using lamination parameters. *Composites Part B: Engineering* 2006;37:301–9.
- [16] Blom AW, Stickler PB, Gürdal Z. Optimization of a composite cylinder under bending by tailoring stiffness properties in circumferential direction. *Composites Part B: Engineering* 2010;41:157–65.
- [17] Nik MA, Fayazbakhsh K, Pasini D, Lessard L. Surrogate-based multi-objective optimization of a composite laminate with curvilinear fibers. *Composite Structures* 2012;94:2306–13.
- [18] Nagendra S, Gürdal Z, T. HR. Buckling and failure characteristics of compression-loaded stiffened composite panels with a hole. *Composite Structures* 1994;28:1–17.
- [19] Gürdal Z, Tatting BF. Design and manufacture of tow-placed variable stiffness composite laminates with manufacturing considerations. In: *Proceedings of the 13th U.S. National Congress of Applied Mechanics*. 1998,.
- [20] Wu KC, Gürdal Z. Thermal testing of tow-placed variable stiffness panels. In: *Proceedings of the 42nd AIAA/ASME/AHS/ASC Structures, Structural Dynamics and Materials*. 2001,.

- [21] Jegley DC, Tatting BF, Gürdal Z. Tow-steered panels with holes subjected to compression or shear loading. In: Proceedings of the 46th AIAA/ASME/AHS/ASC Structures, Structural Dynamics and Materials. 2005,.
- [22] Wu KC, Gürdal Z. Variable stiffness panel structural analysis with material nonlinearity and correlation with tests. In: Proceedings of the 47th AIAA/ASME/ASCE/AHS/ASC Structures, Structural Dynamics and Materials. 2006,.
- [23] Lopes CS, Camanho P, Gürdal Z, Tatting BF. Progressive failure analysis of tow-placed, variable-stiffness composite panels. *Solids and Structures* 2007;44:8493–516.
- [24] Setoodeh S, Abdalla MM, IJsselmuiden ST, Gürdal Z. Design of variable-tiffness composite panels for maximum buckling load. *Composite Structures* 2009;87:109–17.
- [25] Falcó O, Mayugo JA, Lopes CS, Gascons N, Turon A, Costa J. Variable-stiffness composite panels: As-manufactured modeling and its influence on the failure behavior. *Composites Part B: Engineering* 2014;56:660–9.
- [26] Nik MA, Fayazbakhsh K, Pasini D, Lessard L. Optimization of variable stiffness composites with embedded defects induced by automated fiber placement. *Composite Structures* 2014;107:160–6.
- [27] Blom AW, Stickler BF, Gürdal Z. Design and manufacture of a variable-stiffness cylindrical shell. In: Proceedings of the SAMPE Europe 30th International Conference. 2009,.
- [28] Blom AW, Tatting BF, Hol JM, Gürdal Z. Fiber path definitions for elastically tailored conical shells. *Composites Part B: Engineering* 2009;40:77–84.
- [29] Sawicki Adan J, Minguet PJ. The effect of intraply overlaps and gaps upon the compression strength of composite laminates. In: Thirty-ninth AIAA structural, dynamics, material conferences, Structural Dynamics and Materials Conference. Long Beach, CA; 1998, p. 744–54.

- [30] Turoski LE. Effects of manufacturing defects on the strength of toughened carbon/epoxy prepreg composites. Master's thesis; Montana State University, Mechanical Engineering, Bozeman; 2000.
- [31] Nicklaus CK. Open hole compressive behavior of laminates with converging gap defects. Master's thesis; Department of Mechanical Engineering, The University of Utah; 2011.
- [32] Croft K, Lessard L, Pasini D, Hojjati M, Chen J, Yousefpour A. Experimental study of the effect of automated fiber placement induced defects on performance of composite laminates. *Composites: Part A: Applied Science and Manufacturing* 2011;42:484–91.
- [33] ASTM. Open hole tensile strength of polymer composite laminates. Tech. Rep.; American Society for Testing and Materials (ASTM); West Conshohocken, PA, USA; 2003. ASTM D 5766/D 5766M-02.
- [34] Green BG, Wisnom MR, Hallett SR. An experimental investigation into the tensile strength scaling of notched composites. *Composites Part A: Applied Science and Manufacturing* 2007;38:867–78.
- [35] Hallett SR, Green BG, Jiang WG, Wisnom MR. An experimental and numerical investigation into the damage mechanisms in notched composites. *Composites Part A: Applied Science and Manufacturing* 2009;40:613–24.

Chapter 5

Effect of tow-drop gaps on the damage resistance and tolerance of Variable Stiffness Panels

O. Falcó, C.S. Lopes, J.A. Mayugo, N. Gascons and J. Renart. Effect of tow-drop gaps on the damage resistance and tolerance of Variable Stiffness Panels. *Composite Structures*, Submitted Feb. 2014.

Effect of tow-drop gaps on the damage resistance and tolerance of Variable-Stiffness Panels

O. Falcó^a, C. S. Lopes^{b,c}, J. A. Mayugo^a, N. Gascons^a, J. Renart^a

^aAMADE, Department of Mechanical Engineering and Industrial Construction, Universitat de Girona, Campus Montilivi s/n, 17071 Girona, Spain

^bIMDEA Materials: Madrid Institute for Advanced Studies of Materials, Getafe (Madrid), Spain.

^cINEGI: Instituto de Engenharia Mecânica e Gestão Industrial, Porto, Portugal.

Abstract

This paper presents an experimental study of the effects of tow-drop gaps in Variable Stiffness Panels under drop-weight impact events. Two different configurations, with and without ply-staggering, have been manufactured by Automated Fiber Placement and compared with their baseline counterpart without defects. For the study of damage resistance, three levels of low velocity impact energy are generated with a drop-weight tower. The damage area is analyzed by means of ultrasonic inspection. Results indicate that the influence of gap defects is only relevant under small impact energy values. However, in the case of damage tolerance, the residual compressive strength after impact does not present significant differences to that of conventional straight fiber laminates. This indicates that the strength reduction is driven mainly by the damage caused by the impact event rather than by the influence of manufacturing-induced defects.

Keywords:

Carbon fiber reinforced polymer; Defects; Variable-Stiffness Panels; Automated Fiber Placement

1. Introduction

Currently, most composite laminates for structural applications in aircraft programs are manufactured using only the traditional straight fibre configurations, which consist mainly of quasi-isotropic layups. As a consequence, neither the full advantage of the Automated Fiber

Email address: ja.mayugo@udg.edu (J. A. Mayugo)

Placement technology (AFP), available since the 1990s, nor the novel laminate concepts are being used efficiently [1]. The increasing trend toward the development of lighter structures based on an optimized use of composites with Non-Conventional Layups (NCLs) is possible by tailoring the direction and placement of fiber laminates —also referred to as variable angle tow composites.

NCLs are defined as disperse stacking sequence laminates [2], or layups, produced by steering tows that follow curved paths. They are also called Variable Stiffness Panels (VSP) [3]. In the past, researchers have studied the advantages of these VSP over conventional laminates and VSP have been proven to be effective in enhancing the buckling and post-buckling response by in-plane load redistribution [4, 5, 6]. Also, VSP showed potential for lessening notch sensitivity and for reducing stress concentration effects [7, 8, 9, 10]. However, a better comprehension of the mechanical response, failure and damage mechanisms in VSP has prevented its extended application. In addition, due to the versatility and design complexity of VSP, the introduction of these advanced concepts will become feasible only if two major issues are considered. Firstly, by developing reliable design methodologies to predict the mechanical response from damage onset up to structural collapse. Secondly, by certifying VSP using high-level component tests in order to understand the process-induced defects.

Nowadays, there are efficient methodologies to design the optimal fiber orientation so as to maximize the structural efficiency of VSP [11, 12, 13, 14, 15], accounting for the manufacturing defects as well [16, 17, 18]. These defects appear during the tow-steering process and are inherent to the AFP head mechanism [3]. The process-induced defects include local tow buckling or wrinkling and thickness change due to tow-drop gaps or overlaps. These defects become potential spots for the initiation of matrix cracking or even delaminations [19], and are key issues which need to be addressed to guarantee performance. Another crucial problem in VSP is related to fiber discontinuities. It is worth mentioning that a novel fiber placement technique called Continuous Tow Shearing (CTS) [20] has been developed to avoid most of the problems mentioned above. This technology relies on the shear deformation capability of dry tows. However, one of its drawbacks is the maximum variation of tow angle.

Experimental tests are needed to evaluate the influence of the gap or overlap defects originated in the real AFP environment. A wide variety of failure and damage mechanisms appear in the NCLs as a result of design complexity and manufacturing process. In order to fully exploit the possibilities of NCLs and their use in composite structures, the effect of process-induced defects requires specific attention. In the past, researchers have studied the effect of converging gap defects [21, 22]. These studies demonstrated that the unnotched tension and compression tests showed significant reductions in strength due to the gaps. Whereas, open hole tension tests were unaffected by the presence of gaps. This was attributed to the hole effect dominating the gap effects. It also was demonstrated that the compression tests are more sensitive to the gap defects than the tension tests are. In addition, failure predictions depended on the gap locations and the number of gaps. Another author, Nicklaus [23], demonstrated that the presence of gaps produce higher fracture toughness values in the areas close to the hole.

Recently, Croft *et al.* [24] presented an experimental study quantifying the effect of the main manufacturing-induced single defects under tensile, compression and shear loading. Their work reveals that the in-plane shear strength decreased when there was tow-overlapping along the perpendicular direction to the load. A further study on the influence of tow-drop gap defects, gap-coverage parameter and the staggering technique under in-plane tensile loading in VSP has been presented by the present authors (Falco *et al.* [25]). That work shows that the configurations where gaps are not covered and plies are not staggered present the most critical strength reduction as a consequence of the clustering of gaps. Large delaminations are initiated in the vicinity of the tow-drop defects, which are then followed by extensive matrix cracking and finally fiber failure. The present contribution deals with a similar sub-domain of VSP, but focuses on the damage resistance and damage tolerance to a drop-weight impact event.

Damage tolerance to low-velocity impacts is a key factor in the design of the majority of aircraft structures due to the low out-of-plane strength of the composites. Such impacts can happen during manufacturing, servicing or maintenance operations. Several experimental investigations have studied the damage response of dispersed laminates to low-velocity impact, and their improvement over conventional laminates [19, 26, 27]. The differences are

related to the effects of bending stiffness, ply clustering and mismatch angle between the plies. It has been demonstrated that the dispersion of ply orientations through the whole $[0^\circ - 90^\circ]$ range has beneficial effects in terms of impact resistance [28]. By reducing the mismatch angles between the adjacent layers, the response is improved in terms of smaller indentation, less damage dissipated energy, delaminations and higher residual strength. In addition, even for laminates with good stiffness properties, the clustering of plies can lead to large delaminations because there are less potential interfaces for delaminations, resulting in a lower damage resistance of the structure [29].

In VSP, all these aspects are combined in a more complex environment which includes process-induced defects. Additionally, mismatch angles appear not only between adjacent layers, but also within the plies, between adjacent shifted courses. Impact events in VSP is a relatively new field of research. Dang *et al.* [30] performed a numerical study on impact and Compression After Impact (CAI) using finite element analysis. Their results conclude that the main reason for the reduction in compressive strength is related to significant delamination. However, their numerical model only considers the effect of fiber steering, while process-induced defects were not considered. Rhead *et al.* [31] present the effect of tow gaps on the compression-after-impact strength of fiber-placed laminates. The results show that the position, width and depth of tow gaps have a significant effect on damage resistance i.e. the tow gaps close to the non-impacted surface can inhibit sublaminates buckling and growth of laminations. However, in the design of their specimens the shape of the tow gaps is continuous and the mismatch angle discontinuities between the courses were omitted. In reality, in the vicinity between two adjacent courses, small triangular fiber-free areas (gaps), are created in order to avoid overlapping. In addition, the proper nature of the course shifting method [3], creates fiber angle discontinuities.

In this work, the aspects mentioned above have been reproduced in a laminate which could be a representative subdomain of a real VSP. The main goal is to study the influence of gap defects on the damage resistance and on the compressive residual strength of three laminates under low velocity impacts. Also, the effect of the staggering technique, used to avoid the co-location of the gaps, has been analyzed. The staggering technique reduces the effect of ply clustering and produces a more uniform distribution of the process-induced

defects. Both configurations, with and without staggered plies, have been compared with a traditional straight fiber laminate. All configurations analyzed present similar bending stiffness in order to avoid misinterpreting the results and reaching ambiguous conclusions.

2. Specimen with tow-drop gaps: Design and manufacturing

The test specimens for the experimental work reported in this paper have been designed to represent the ply discontinuities at the edges of adjacent courses in VSP configurations. Gap-coverage zones have been included in order to study the influence of the process-induced defects and the staggering technique, under drop-weight impact. Each specimen represents a sub-domain of a whole Variable Stiffness Panel at the boundary between the courses. The effects to be studied are very localized, this makes it possible to use relatively small specimens and to use straight-fiber laminates instead of curved trajectories. Some layers in the laminate have one portion with the fibers at 51° and another at 39° , thus creating an angle discontinuity at the mid-length of the specimen. In order to avoid more complexity, these plies with angle discontinuity were balanced with plies at -45° .

Two configurations with tow-drop defects and 0% gap-coverage were designed and tested under low-velocity impact. The configurations are described in Fig 1a. The difference between them is in the use of ply staggering. In the first case, the fiber-resin areas are co-located through-the-thickness. Whereas for the second case, the co-location of gaps is avoided by staggering the plies in relation to each other (see Fig 1b). The thickness variation caused by the pressing of gaps in adjacent layers resulting from the high pressure of the curing process is observed in Fig 1c.

The composite material used in this investigation is the HexPly AS4/8552 pre-impregnated CFRP in 6.35 mm (1/4 in.) wide tows (t_w), with nominal ply thickness after curing of 0.18 mm. The manufacturing process was done in the National Aerospace Laboratory-NLR (The Netherlands), with a Coriolis Fiber Placement Machine which lays courses of up to 8 tows at a time with a total width (C_w) of 50.8 mm per course. The mechanical properties of the material system are $E_{11} = 138.0$ GPa, $E_{22} = 8.6$ GPa, $G_{12} = 4.9$ GPa and $\nu_{12} = 0.35$. The tests are performed on flat rectangular plates of 150×100 mm. The stacking sequence analyzed is $[45/0/-45/90/(-45_2/(51|39)_2)_2]_s$, where the 0° fiber orientation is aligned with the largest

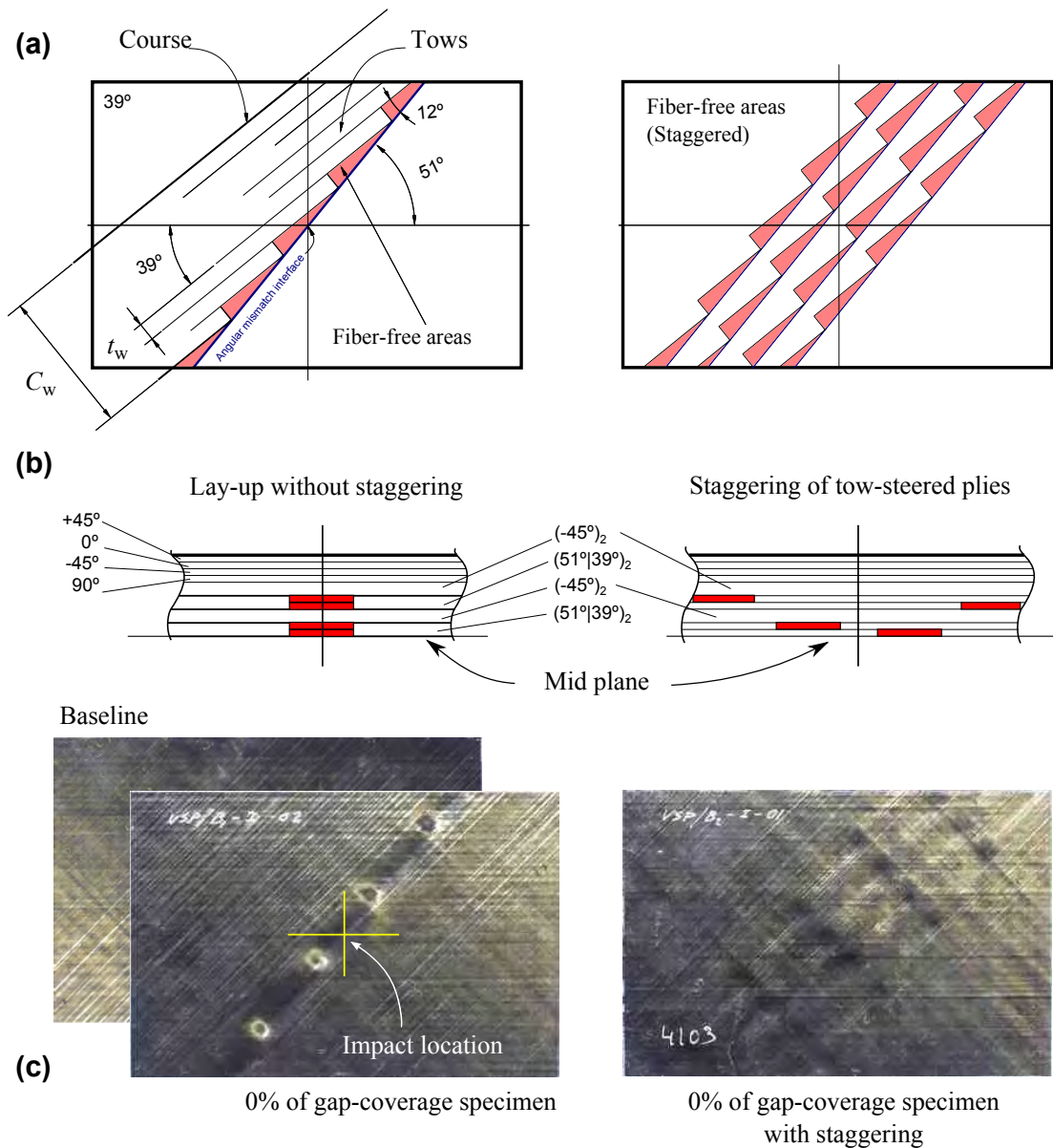


Figure 1: a) Specimen geometry: The discontinuity interface in the ply $\langle 51|39 \rangle$ is represented using a blue line and resin rich areas have been filled. (b) Tow-drop gap defects ('no Staggering' and 'Staggering'). (c) Real specimen with and without staggering.

in-plane dimension. The design of the external plies was constrained to the conventional straight-fiber method to avoid gap defects in the outer layers of the laminate. All configurations present the same stacking sequence (24 plies) with nominal laminate thickness of 4.32 mm. A baseline laminate with a stacking sequence of $[45/0/-45/90/(-45_2/45_2)_2]_s$ has also been analyzed and tested for comparative purposes. The baseline and the non-conventional

laminates were designed to have similar global stiffness.

3. Drop-weight impact and compression after impact tests

The ASTM D7136 [32] standard establishes the method for measuring the damage resistance to a fiber-reinforced polymer matrix composite under a drop-weight impact. In this study, three impact energies (E_i) have been used: 15 J, 30 J and 45 J. The impact mass (M_i) values, the velocity before the impact values ($V_0 = \sqrt{2E_i/M_i}$) and the impact height values ($H_i = E_i/(M_i g)$) are summarized in Table 1. For each impact energy and for each configuration, two specimens with gap defects have been tested. Additionally, two specimens with the baseline configuration are used to assess the non-impacted laminate strength.

Table 1: Impact energies, mass, velocities and drop weight heights.

	Impact energy (J)		
	15	30	45
Impactor mass M_i (kg)	5.0	5.0	5.0
Initial velocity V_0 (m/s)	2.5	3.5	4.2
Impact height H_i (mm)	306	612	917

The impact tests were carried out in a Instron Ceast 9350 (Fractovis Plus, Italy) instrumented drop-weight tower, with a 16 mm diameter hemispherical impactor and an automatic anti-rebound impactor system. The unsupported area of the specimen during the impact is 125 mm by 75 mm. The data recorded are the history of the impactor force, displacement and velocity. After the impact tests and a dent-depth measurement, all specimens were inspected with an Omni-Scan MX (Olympus NDT, USA) ultrasonic system to analyse the resulting delamination area. For the non-staggered specimens the impact location is controlled. For each energy level, one specimen was tested with the impact outside of the defect and the other impacted just inside of the fiber-free area. Conversely, this differentiation is not possible with the other configurations.

The Compression After Impact (CAI) tests were performed using a hydraulic MTS-810 (Material Testing Systems, USA) testing machine of 250 kN load-capacity and with

an anti-buckling fixture support at the specimen edges, according to the ASTM D7137 [33]. The same standard is followed in determining the residual compression after impact strength σ_c of each specimen. The normalized residual compression strength after impact is calculated using the expression: $\sigma_c = P_r/(W \cdot t_n)$, where P_r is the break failure load of the specimen of width (W) and nominal thickness (t_n). In order to monitor the out-of-plane displacements, two displacement transducers are used during the CAI tests. However, for some specimens a more reliable technique, the Digital Image Correlation (DIC) system *VIC – 3DTM* Measurement System (Correlated Solutions, USA) is used. This technology allows out-of-plane displacement and strain fields for the whole surface to be monitored, as well as any possible eccentricities that might occur.

4. Results and discussion

In order to study the influence of tow-drops on damage resistance and damage tolerance, two different configurations with these defects are analyzed and compared with a conventional baseline laminate. Firstly, the results obtained with the impact test are presented. Here, the most relevant features of composite laminates under low velocity impact condition are: the delamination threshold loads, the peak loads, the evolution of the absorbed energies and the projected delamination areas as a result of the impact. Secondly, the residual compressive strengths obtained through CAI tests are analyzed.

4.1. Low velocity impact test results

The corresponding histories of the impact loads as a function of the contact time and of the impactor displacement for the three impact values of energy (15 J, 30 J and 45 J) are shown in Fig 2. For the particular case of the laminate with no staggering, both impacted specimens are represented, because of the differences observed. For the specimens labelled 'no Staggering-side' the impact location is outside the defect zone, and for the specimens 'no Staggering-gap' the impact zone is just inside the fiber-free area. In the other configurations, only one specimen was selected because no significant differences were detected. These impact load evolutions make it possible to determine the delamination threshold load F_d and the peak load F_p . On the one hand, the F_d can be identified as the first significant force

drop in the load impact evolution. F_d represents the initial value at which a significant change in the stiffness properties is detected. Its value is also associated with the development of a first significant delamination [29]. After this point, the response is affected by a large variety of damage mechanisms —matrix cracking, fiber-matrix interface debonding, delamination and fiber breakage. On the other hand, the peak load F_p is the maximum force recorded during the impact process.

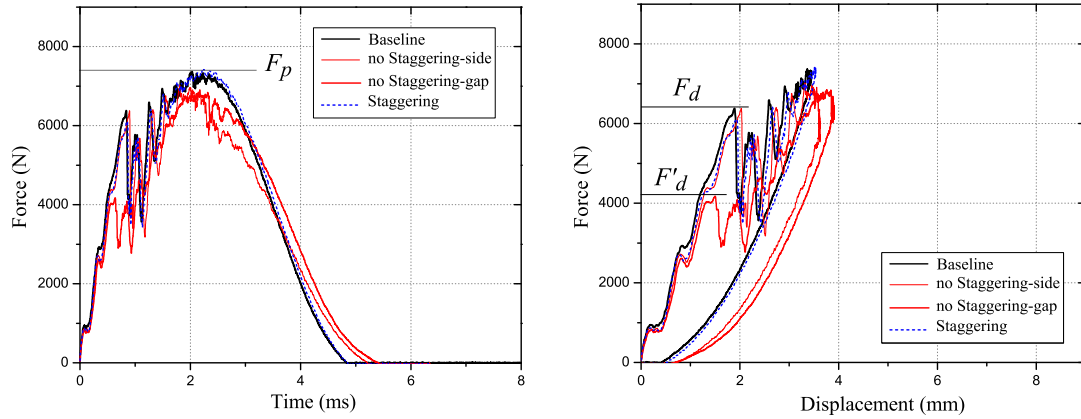
The threshold load F_d has similar values for impact energies of 15 J, 30 J and 45 J. Excluding the tests labelled as 'no Staggering-gap', the delamination threshold load F_d for the all configurations analyzed had similar values. Therefore, this agrees with other experimental works [29] where the F_d value is independent of the impact energy. Note that the 'no Staggering-gap' tests were carried out on specimens impacted in the gap defect. For this configuration, a reduction of about 30% in F_d was observed for all impact energies.

The delamination threshold loads are on average 6.4 kN, 6.1 kN and 6.0 kN for the configurations 'baseline', 'no Staggering' and 'staggering', respectively. The corresponding energy levels for these configurations are 6.2 J, 6.1 J and 5.8 J. In comparison, in the cases when the impact occurs inside the fiber-free area, the average of the threshold load is 4.3 kN, occurring at energy levels of 3.1 J.

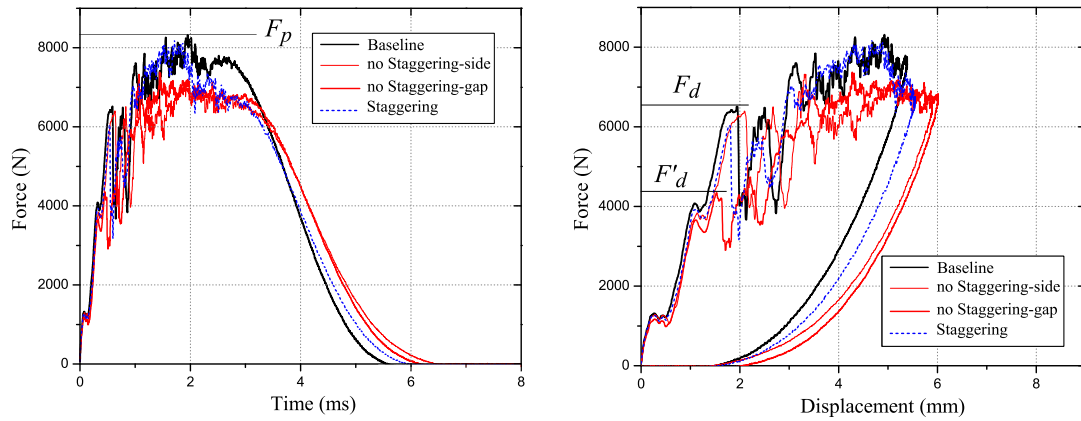
As expected, the peak load F_p and the total impact time increase by intensifying the impact energy. The value of F_p for the baseline and staggered configurations have similar values. For the configuration without staggering, a slight reduction of F_p of 6.8%, 11.2% and 8.7% is observed for impact energies 15 J, 30 J and 45 J, respectively. This is probably as a result of different damage mechanisms depending on the co-location of the fiber-free areas.

The absorbed energy value represents how the impactor kinetic energy is transferred to the specimen by means of different failure mechanisms, mainly in the form of delaminations. The evolution of the absorbed energy for each tested laminate and its corresponding impact energy are shown in Fig 3.

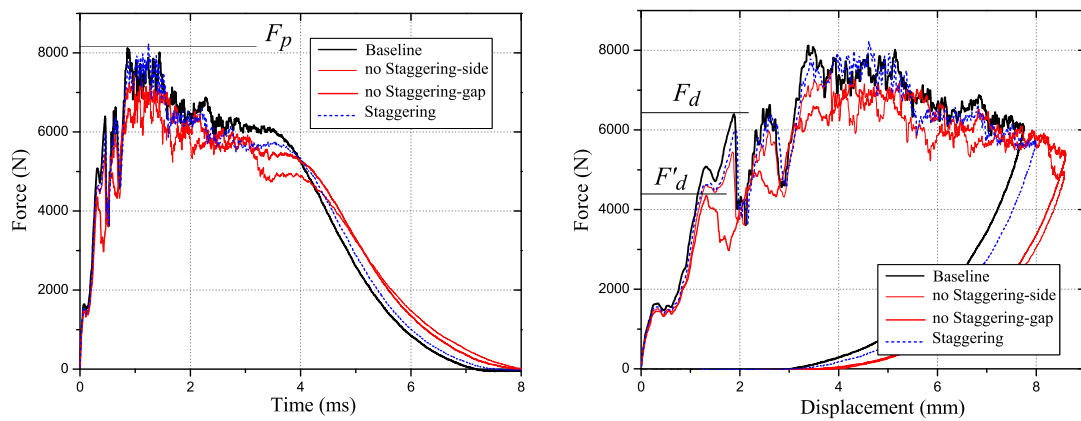
The analyses of the dissipated energy shows very similar behavior between the configuration baseline and the configuration with staggered fiber-free areas. The non-staggered configuration shows a higher energy dissipation. This means that the clustered fiber free-areas (gap-defects) are more prone to damage. In addition, if the staggering technique is



(a) Configurations tested at 15 J impact energy



(b) Configurations tested at 30 J impact energy



(c) Configurations tested at 45 J impact energy

Figure 2: Impact load evolution and in function of displacement for the configurations 'Baseline', 'no Staggering' and 'Staggering' tested at: (a) 15 J, (b) 30 J and (c) 45 J. The values F_p and F_d for the baseline configuration are marked for each impact energy by a horizontal line.

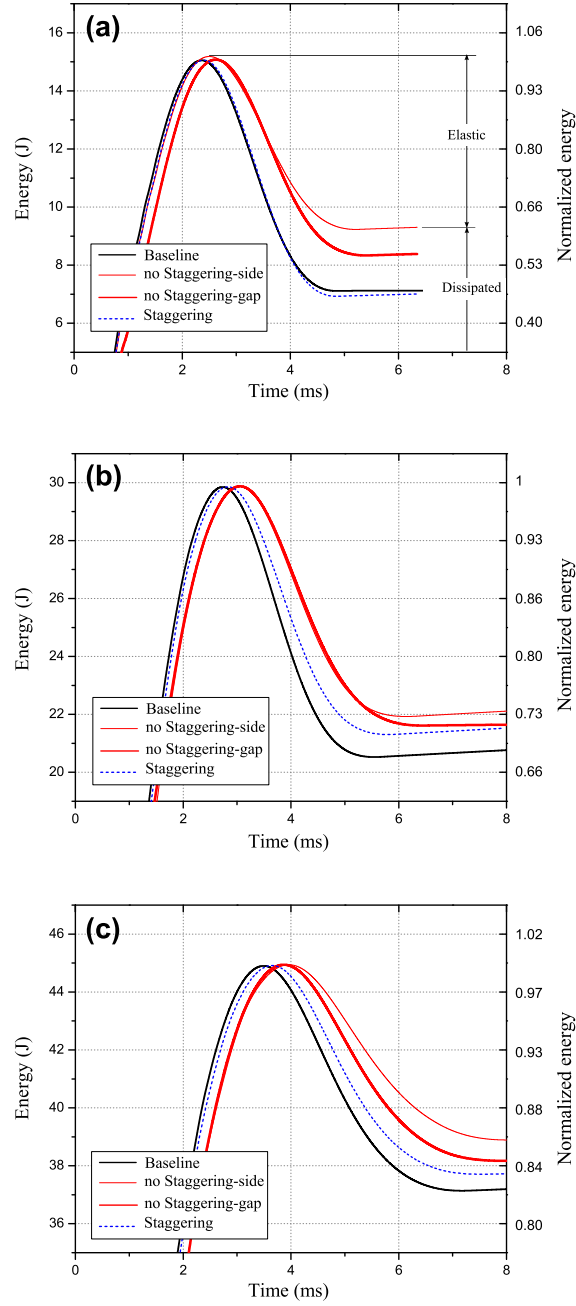


Figure 3: Evolution of the absorbed energies of configurations 'Baseline', 'no Staggering' and 'Staggering': (a) 15 J, (b) 30 J and (c) 45 J. The elastic energy and the energy dissipated are represented in the plot (a).

applied, the dissipated energy values are close to the baseline configuration in comparison to the other configurations. Therefore, results indicate that the influence of the gap defects in the dissipated energies is more representative in low values of the impact energy. For higher

energy levels, the gaps lose influence, and this is probably indicative of failure mechanisms occurring at higher energies, such as fiber failure, are not so influenced by the resin-rich gaps defect. This behavior for the lower impact energy is clearly observed in the normalized dissipated energies E_a , depicted in Fig. 6a. In these diagrams the results of all the impacted specimens are included. As expected, the dissipated energy increases when increasing the impact energy. Lower dispersion of the absorbed energy values is observed between the configurations analyzed at higher impact energies.

The projected delamination areas as identified by C-Scan inspections are shown in Fig. 4. The shape of the projected delamination area for the configuration with staggering and baseline configuration subjected to 15 J impact is almost circular. In comparison, for the configuration without staggering, the shape follows a more irregular pattern, influenced by the orientation of the gap zones. However, for high values of the impact energy, the shape of the areas does not present significant differences. With the C-Scan, the location of the 'tow-drop effect' (or 'gap defect') is clearly observed. For impact energy values of 30 J, a large delamination is observed at the interface furthest away from the impact point with a dominant propagation angle of 45° . The delamination axis is more aligned with the ply angles than with the defect angles.

A comparison of the ply splitting on the non-impacted face is shown in Fig. 5. In spite of having similar delamination areas, more splitting is observed in the no staggering configuration.

A graphical summary of the delamination area in function of the impact energy is represented in Fig. 6b. Here, the delamination area, A_d , is normalized by the unsupported area during the impact ($125 \text{ mm} \times 75 \text{ mm}$). Linear interpolation trends are also represented in the same graphs. The positive slope for all configurations is mainly due to the increasing delamination of the back face of the specimen. It is observed that the distribution of A_d is similar for the baseline and for the staggered configurations. Besides the slight differences observed, in general the effect of the gap defect has little influence on the normalized delamination areas A_d . Nonetheless, a more irregular trend is observed for the configuration without staggering. It could be reasoned that, at lower energies fiber gaps trigger relatively larger damage, whilst at higher energies, gaps tend to concentrate damage in a narrower

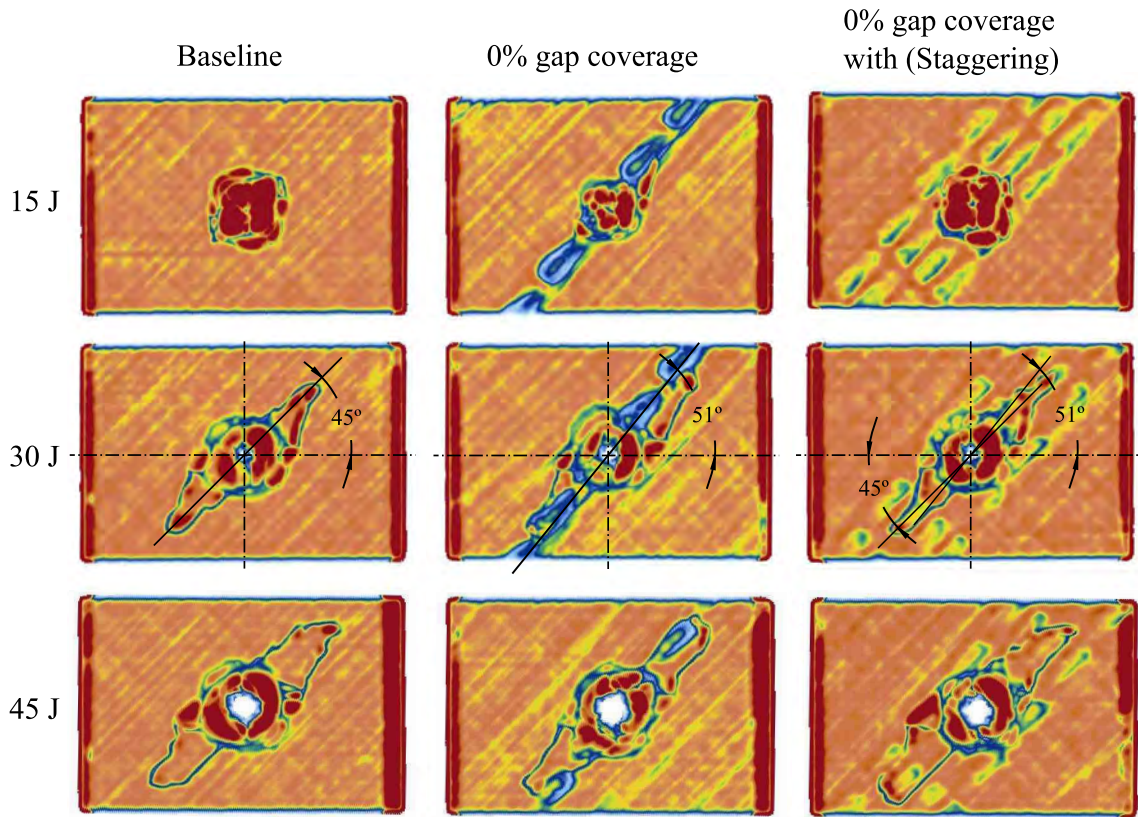


Figure 4: C-scan inspection for the laminates.

gap.

4.2. Compression after impact results

The contour plots of the longitudinal ε_{yy} and shear ε_{xy} strain for the three configurations impacted at 15 J are compared in Fig. 7. In the strain field analyses, the differences between each configuration are observed. It is also possible to observe the strain differences due to the mismatch angle discontinuities in the inner layers for the configurations without staggering and for the configuration with the staggered gaps—the discontinuity is identified by a dashed line in Fig 7. As expected, the region with higher strain values is the zone with layers with the fiber angle orientation of 51° .

The results obtained with the compression after impact test on all configurations are compared in Fig. 8 in order to assess the effect of the impact damage on the residual

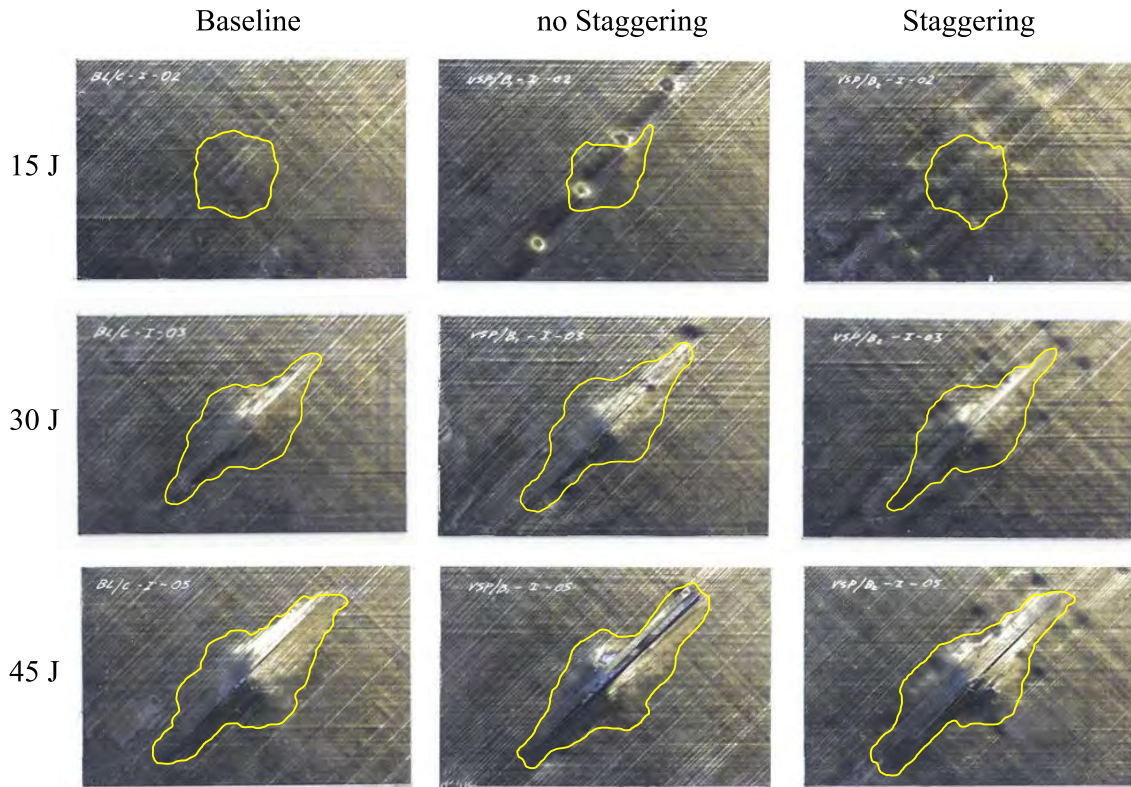


Figure 5: Visual inspection of non-impacted face for the configuration tested.

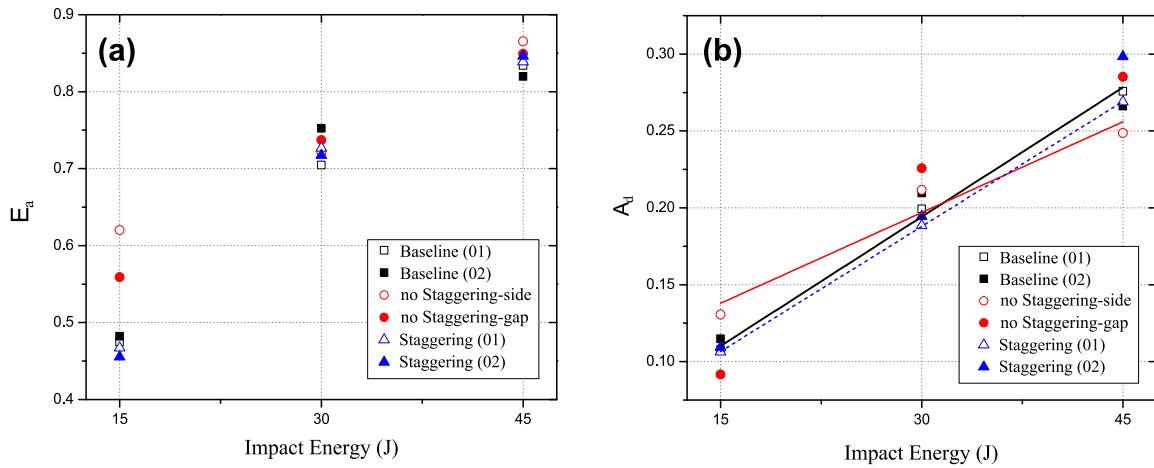


Figure 6: (a) Dissipated energy normalized, and (b) normalized projected area according to the impact energy of configurations 'Baseline', 'no Staggering' and 'Staggering'.

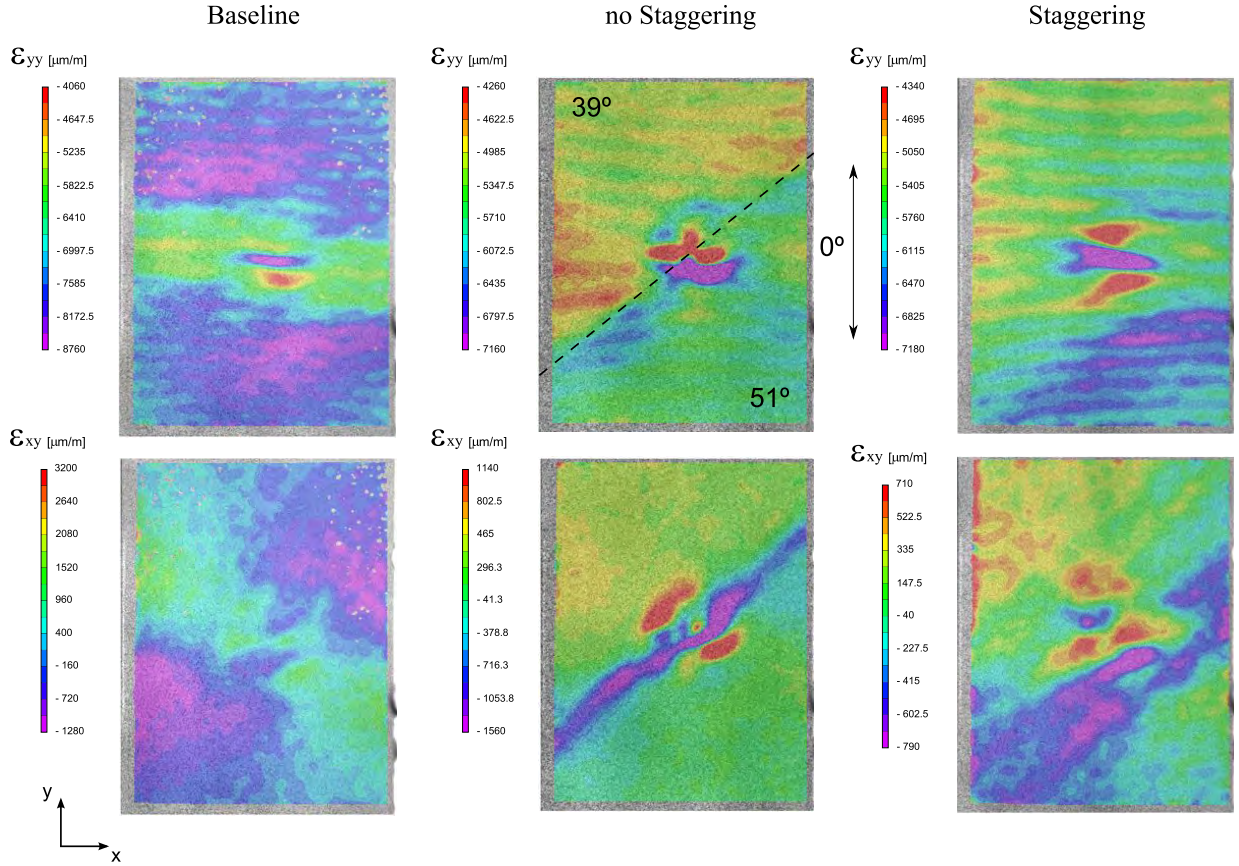


Figure 7: DIC contours of longitudinal field strain ε_{yy} , shear field strain ε_{xy} and out-of-plane displacement w for the configurations: 'Baseline', 'no Staggering' and 'Staggering' at impact energy of 15 J and compression load value of 81.1 kN, 64.0 kN and 68.0 kN, respectively.

compressive strength (σ_c). As expected, the maximum residual compressive load values for all laminate configurations decreases for all laminates when the impact energy increases. All configurations present a similar behavior of the residual compressive loads, although for the particular case of the specimen 'no Staggering-gap' and for all impact energy values, a slightly higher reduction of the maximum compressive load is observed, as well as of the stiffness reduction. Fig 8 also includes the results for two non-impacted baseline specimens. The numerical values for the residual compressive strengths are shown in Table 2. Akin to the impact results, the greatest dispersion of the residual value occurs for the lowest value of the impact energy (15 J). The differences in the residual strength between the different configurations at each impact energy level are relatively small.

Table 2: Residual compressive strengths (σ_c) in MPa.

Impact energy (J)	Configurations					
	Baseline		no Staggering		Staggering	
	(01)	(02)	(side)	(gap)	(01)	(02)
0	289.2	308.7	n/a	n/a	n/a	n/a
15	207.0	205.6	184.4	201.4	194.0	189.9
30	165.9	162.3	152.3	n/a	156.5	157.7
45	143.9	142.4	139.9	134.2	140.8	142.8

It can be concluded that the gaps do not attract such a large amount of damage as in conventionally laminates so as to significantly reduce the residual strength of the laminates. Therefore, the influence of staggering is negligible. This was also observed in the results obtained for variable stiffness specimens with gaps in previous experimental tests under an in-plane loading condition for notched specimens with open-hole [25].

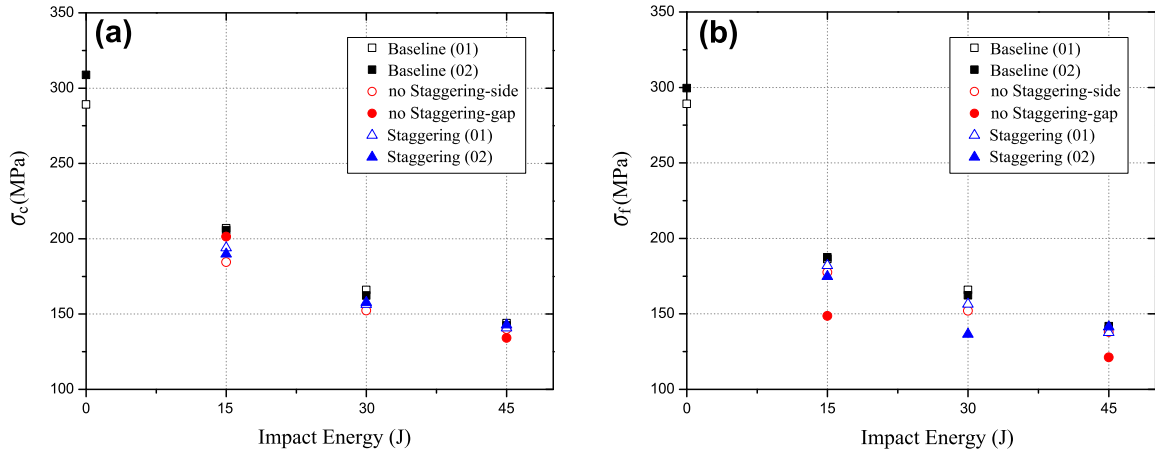


Figure 8: (a) Residual compressive strength (σ_c), versus the impact energy for the configurations: 'Baseline', 'no Staggering' and 'Staggering'. (b) Damage onset stress (σ_f).

In addition, the local buckling onset stress (σ_f) is plotted in Fig 8b. The analysis of (σ_f), reveals that for small impact energies their values are significantly lower than the residual strength (σ_c). Whereas, for higher energies the values of local buckling onset and values of ultimate stress are much more similar.

5. Conclusions

The main goal of this work was to study the influence of gap defects on the damage resistance and damage tolerance of VSP under low-velocity impacts. Two configurations with tow-drop defects and 0% gap-coverage have been designed and tested. The difference between them consists in the use of ply staggering. Both configurations have been compared with a traditional straight fiber laminate.

The study of the damage resistance, with three levels of low velocity impact energy, indicates that the influence of the gap defects is relevant only under small impact energy values, and is more relevant on impact resistance than on impact damage tolerances. The damage tolerance, represented by the residual compressive strength after impact, does not present significant differences. This indicates that the strength reduction is driven mainly by the damage caused through the impact, rather than by manufacturing-induced defects. However, in order to confirm these assertions, further tests at lower impact energies would be necessary.

Acknowledgements

The authors acknowledge the financial support of the Ministerio de Economía y Competitividad of Spain under the project MAT2009-07918. The first author would like to thank the Generalitat de Catalunya for the FI pre-doctorate Grant 2010FI_B00658. The third author gratefully acknowledges the funding from the Portuguese Foundation for Science and Technology (FCT) through the project PTDC/EME-TME/111004/2009. The authors also thank Dr. Engineer Martin Nagelsmit of National Aerospace Laboratory for his assistance in the manufacturing process of the non-conventional laminates.

References

- [1] Lukaszewicz D, Ward C, Potter K. The engineering aspects of automated prepreg layup: history, present and future. *Composites Part B: Engineering* 2012;43:997–1009.
- [2] Sebaey TA, González EV, Lopes CS, N. B, J. C. Damage resistance and damage

- tolerance of dispersed CFRP laminates: Design and optimization. *Composite Structures* 2013;95:569–76.
- [3] Gürdal Z, Tatting BF, Wu KC. Tow-placement technology and fabrication issues for laminated composite structures. In: *Proceedings of the AIAA/ASME/ASCE/AHS/ASC Structures, 46th Structural Dynamics & Materials Conference*. 2005,.
- [4] Gürdal Z, Olmedo R. In-plane response of laminates with spatially varying fiber orientations - variable stiffness concept. *AIAA J* 1993;31(4):751–8.
- [5] Gürdal Z, Tatting BF, Wu KC. Variable stiffness panels: Effects of stiffness variation on the in-plane and buckling responses. *Composites Part A: Applied Science and Manufacturing* 2008;39:911–22.
- [6] Lopes CS, Gürdal Z, Camanho P. Variable-stiffness composite panels: Buckling and first-ply failure improvements over straight-fibre laminates. *Computers and Structures* 2008;86:897–907.
- [7] Nagendra S, Gürdal Z, T. HR. Buckling and failure characteristics of compression-loaded stiffened composite panels with a hole. *Composite Structures* 1994;28:1–17.
- [8] Lopes CS, Gürdal Z, Camanho PP. Tailoring for strength of composite steered-fibre panels with cutouts. *Composites Part A: Applied Science and Manufacturing* 2010;41:1760–67.
- [9] Tatting BF, Gurdal Z. Design and manufacture of elastically tailored tow placed plates. *Tech. Rep. NASA/CR-2002-211919*; NASA; 2002.
- [10] Jegley DC, Tatting BF, Gürdal Z. Tow-steered panels with holes subjected to compression or shear loading. In: *Proceedings of the 46th AIAA/ASME/AHS/ASC Structures, Structural Dynamics and Materials*. 2005,.
- [11] Blom AW, Mostafa , Abdalla M, Gürdal Z. Optimization of course locations in fiber-placed panels for general fiber angle distributions. *Composites Science and Technology* 2010;70:564–70.

- [12] Duvaut G, Terrel G, F. L, Verijenko VE. Optimization of fiber reinforced composites. *Composite Structures* 2000;48:83–9.
- [13] Khani A, IJsselmuiden ST, Abdalla MM, Gürdal Z. Design of variable stiffness panels for maximum strength using lamination parameters. *Composites Part B: Engineering* 2011;42:546–52.
- [14] Setoodeh S, Abdalla MM, IJsselmuiden ST, Gürdal Z. Design of variable-stiffness composite panels for maximum buckling load. *Composite Structures* 2009;87:109–17.
- [15] Nik MA, Fayazbakhsh K, Pasini D, Lessard L. Surrogate-based multi-objective optimization of a composite laminate with curvilinear fibers. *Composite Structures* 2012;94:2306–13.
- [16] Blom AW, Lopes CS, Kromwijk PJ, Gürdal Z, Camanho PP. A theoretical model to study the influence of tow-drop areas on the stiffness and strength of variable-stiffness laminates. *Composite Materials* 2009;43:403–25.
- [17] Nik MA, Fayazbakhsh K, Pasini D, Lessard L. Optimization of variable stiffness composites with embedded defects induced by automated fiber placement. *Composite Structures* 2014;107:160–6.
- [18] Falcó O, Mayugo JA, Lopes CS, Gascons N, Turon A, Costa J. Variable-stiffness composite panels: As-manufactured modeling and its influence on the failure behavior. *Composites Part B: Engineering* 2014;56:660–9.
- [19] Lopes CS. Damage and failure of non-conventional composite laminates. Ph.D. thesis; Delft University of Technology; 2009.
- [20] Kim BC, Potter K, Weaver PM. Continuous tow shearing for manufacturing variable angle tow composites. *Composites Part A: Applied Science and Manufacturing* 2012;43:1347–56.
- [21] Sawicki Adan J, Minguet PJ. The effect of intraply overlaps and gaps upon the compression strength of composite laminates. In: *Thirty-ninth AIAA structural, dynamics,*

- material conferences, Structural Dynamics and Materials Conference. Long Beach, CA; 1998, p. 744–54.
- [22] Turoski LE. Effects of manufacturing defects on the strength of toughened carbon/epoxy prepreg composites. Master's thesis; Montana State University, Mechanical Engineering, Bozeman; 2000.
- [23] Nicklaus CK. Open hole compressive behavior of laminates with converging gap defects. Master's thesis; Department of Mechanical Engineering, The University of Utah; 2011.
- [24] Croft K, Lessard L, Pasini D, Hojjati M, Chen J, Yousefpour A. Experimental study of the effect of automated fiber placement induced defects on performance of composite laminates. *Composites: Part A: Applied Science and Manufacturing* 2011;42:484–91.
- [25] Falcó O, Mayugo JA, Lopes CS, Gascons N, Costa J. Variable-stiffness composite panels: Defect tolerance under in-plane tensile loading. *Composites Part A: Applied Science and Manufacturing*, Submitted Nov 2013;.
- [26] Sebaey T, González E, Lopes C, Blanco N, Costa J. Damage resistance and damage tolerance of dispersed CFRP laminates: The bending stiffness effect. *Composite Structures* 2013;106:30–2.
- [27] Sebaey T, González E, Lopes C, Blanco N, Costa J. Damage resistance and damage tolerance of dispersed CFRP laminates: Effect of ply clustering. *Composite Structures* 2013;106:96–103.
- [28] Sebaey T, González E, Lopes C, Blanco N, Maimí P, Costa J. Damage resistance and damage tolerance of dispersed CFRP laminates: Effect of the mismatch angle between plies. *Composite Structures* 2013;101:255–64.
- [29] González E, Maimí P, Camanho P, Lopes C, Blanco N. Effects of ply clustering in laminated composite plates under low-velocity impact loading. *Composites Science and Technology* 2011;71:805–17.

- [30] Dang TD, Hallett SR. A numerical study on impact and compression after impact behaviour of variable angle tow laminates. *Composite Structures* 2013;96:194–206.
- [31] Rhead AT, Dodwell TJ, Butler R. The effect of tow gaps on compression after impact strength of robotically laminated structures. *CMC: Computers, Materials & Continua* 2013;35:1–16.
- [32] ASTM. Standard test method for measuring the damage resistance of a fiber-reinforced polymer matrix composite to a drop-weight impact event. Tech. Rep.; American Society for Testing and Materials (ASTM); West Conshohocken, PA, USA; 2012. ASTM D 7136/D 7136M-12.
- [33] ASTM. Standard test method for compressive residual strength properties of damage polymer matrix composites plates. Tech. Rep.; American Society for Testing and Materials (ASTM); West Conshohocken, PA, USA; 2012. ASTM D 7137/D 7137M-12.

Chapter 6

Conclusions and Future Work

6.1 Introduction

The present thesis covers the analysis of the process-induced defects on steered-fiber laminates. In accordance with the main goal, the influence of the process-induced defects on the damage resistance and damage tolerance of Variable Stiffness Panels was investigated. In order to accomplish this objective, two specific tasks were addressed. Initially, a methodology for modeling variable stiffness panels which takes into account the tow-drop defects was developed. This tool is useful for elasticity and failure analyses as well as progressive damage-analysis with delamination. The proposed methodology considers the effect of mismatch angle discontinuities of fiber orientation, as well as the effect of fiber-free areas that occur during manufacture.

Secondly, experimental works were performed to investigate the effects of different process-induced defects. The in-plane response analysis of laminates with some overlap/gap defects was carried out under tensile loading testing. For damage tolerance analyses, low-velocity impacts tests were made. Both tests provide designers with a better comprehension of the damage mechanisms in those laminates with defects included. The main conclusions obtained and the future challenges associated with the variable stiffness laminates are discussed in the following paragraphs.

6.2 Conclusions

6.2.1 Methodology for modeling variable stiffness panels taking into account manufacturing constraint

A state-of-the-art overview on variable-stiffness panel technology was developed. The advantages of Automated Fiber Placement systems and the limitations for manufacturing of tow-steered laminates were addressed. In addition, the main process-induced defects and their influence on the mechanical response of these laminates were also described. The literature survey identifies the fields of interest remain for investigation. For instance, predicting the occurrence of ply delaminations was neglected altogether, the damage and failure analyses performed in previous studies for VSP under in-plane loads. Along similar lines, although some models take into account defects such as overlaps/gaps, these analyses were performed using only an in-plane stress formulation implemented in shell elements and, as a consequence, interlaminar stress analysis and delaminations in variable stiffness panels is still being investigated.

This present work contributes a methodology to model tow-steered panels in a three-dimensional domains. This approach opens up the following possibilities:

- In design and/or manufacturing terms, different configurations and modeling strategies can be simulated. Reference paths for constant curvature or paths with linear variation of the fiber orientation are possible. In both cases, the modeling strategy can take into account that the panels are manufactured by cutting the tows on one or both sides of the course. The methodology also allows for the inclusion of tow-angle discontinuities and the implementation of ply-staggering.
- For modeling and/or simulation, a structured mesh generator for the design and parametric modeling of steered fiber panels for FE analysis was developed. With a structured mesh strategy, a more accurate location of the fiber-free areas (gap-defects), can be achieved. Therefore, a better representation, which includes the manufacturing constraints in comparison to the ideal-ply approach, has been achieved. In addition, for accurate retrieval of the interlaminar stress distribution, it is also possible to refine the mesh in the through-the-thickness direction.
- With the three-dimensional FE model developed for flat tow-steered laminates,

advanced simulation for failure and damage propagation can be addressed. Although the models with a structured mesh approach add complexity and create non-conforming meshes, they allow for the prediction of delamination and of the intralaminar response between the adjacent courses, by means of surface-based cohesive-contact interactions. For failure analyses and progressive damage simulation where the local effects are important, a detailed 3D domain might be required, whereas for stiffness and buckling assessment, idealized 2D analyses are recommended.

- For failure predictions, a three-dimensional failure criterion, which takes into account all components of the stress tensor for fiber-reinforced, laminates was applied. For comparison purposes, four models were analyzed under in-plane tension loading with different modeling approaches. While not significant, differences in global stiffness were found. Different modeling approaches resulted in different first-ply failure results. The fiber tensile failure index for longitudinal tensile failure shows a significant dependence on the fiber orientation angles.

6.2.2 Manufacturing and experimental testing

The baseline and the variable-stiffness composite panels were manufactured using a Coriolis advanced fiber placement machine. Four plates were manufactured, a baseline without overlap/gap defects as well as three plates: i) one with tow-drop gap-coverage of 100%; ii) one with gap-coverage of 0% without staggering and iii) one with the tow-drop gap defects staggered. Before cutting for the laboratory coupons, C-scan inspections were carried out to detect any manufacturing flaws in the plates. The specimens were manufactured taking the American Standard Test Method for open hole tensile strength as a reference (Chapter 2, reference [58]). The impact specimens were manufactured according to the American Standard Test Method for drop-weight impact on laminated composite plates (Chapter 2, reference [59]).

In both experimental campaigns and in order to monitor the complete strain fields and the out-of-plane displacements, a Digital Image Correlation (DIC) system, VIC-3D™ Measurement System (Correlated Solutions, USA) was used. This technique was very useful for observing the difference in strain because the mishmash-angle discontinuities and the tendency of the crack propagation drive for the process-induced defects. The main conclusions of the experimental results from the variable stiffness coupons and their comparison with conventional laminates are addressed below:

Defect tolerance under in-plane tensile loading

- The effect of two principal defect types, namely gap and overlap, on the ultimate strengths for variable stiffness laminates was investigated. In addition, the effect of the fiber angle discontinuities between different tow courses in a ply on the un-notched and open-hole laminates tensile strength was analyzed. Tests were performed in specimens which represent a sub-domain of a variable stiffness panel. Then, each test was compared with the equivalent baseline configuration exempt from defects.
- In comparison with the baseline for un-notched specimens, the configuration with 0% gap-coverage (gaps), presents the most significant strength reduction (of about 20.1%), because the collocations of the gap-defects through the thickness. For the configuration with 100% gap-coverage (overlaps), the strength reduction was about 10.7%. For both coupons with gap and overlap defects, large delamination were observed in the defect zones due to the higher interlaminar stress concentration around the defects. With respect to the staggered coupons, the results show that the staggering is effective in reducing the influence of defects. This technique avoids the collocations of defects and provides a similar response to conventional laminates without defects. For these staggered configurations the strength reduction was only 8.6%. Therefore, the configuration with 0% gap coverage and no staggering presents the most critical strength reduction; as a result of the clustering of gaps. When the ply staggering technique is applied, these effects are highly mitigated. The combination of 'ply staggering' and 'full gap coverage' is the most effective in reducing the influence of defects in VSPs.
- With regards to the influence of the process-induced defects on coupons with open-

hole, the experimental results show that the un-notched specimens more influenced by the defects than that of the notched specimens. In general, this occurs independently of the defect type or the use of staggering. Insignificant differences of the remote failure stress between the specimens tested were observed.

Damage resistance and tolerance in variable stiffness laminates with tow-drop gap defects

- For the study of the damage resistance in variable stiffness laminates, low-velocity impact tests, with three levels of the impact energy, were performed. Two sets of specimen 'no-staggered' and 'staggered' were analyzed and their results were compared with a conventional laminate. The results show that the influence of gap defects is relevant only under small impact energy values, and is more relevant on impact resistance than on impact damage tolerance.
- The damage tolerance, represented by the residual compressive strength after impact, does not present significant differences. This indicates that the strength reduction is driven mainly by the damage caused through the impact, rather than by process-induced defects. In order to observe a more determinant influence of the defects, further tests at lower impact energies would be recommended.
- A study of the effect of tow-gaps with respect to the location of the impact, on a gap or on the side of a gap, was performed. The results show that the threshold load, F_d , remains constant in the face of changes in the impact energy, albeit with the exception for the particular case when the impact is just on the gap-defect.

6.3 Future Work

The following improvements are suggested for future research for the effective development and application of variable stiffness laminates.

Numerical analysis including damage propagation for in-plane and impact events can be carried with the developed numerical tool. The predicted results would be validated with the experimental results obtained in the present work. The tested coupons can be modeled with the different approaches addressed in the Chapter 3 of this thesis.

The proposed methodology needs to be extended to modeling other types of defects such as overlaps in a three-dimensional domain. In addition, VSP models with the novel Automated Fiber Placement manufacturing approach such as Continuous Tow Shearing described in Chapter 2, could be implemented.

For more advanced progressive damage simulations the inclusion of interlaminar and intralaminar damage models for CRFP system material and for resin-rich regions need to be considered. In the simulations performed in this thesis, only the influence of gap-defects on the failure prediction were considered, however, the damage sustained inside the resin zones was excluded.

Additionally, the numerical tools for the simulation of the impact and the CAI tests in the VSP, besides the suitability of the formulated constitutive models, the process-induced defects need to be included for an accurate prediction of the results, as the resin is expected to sustain damage at higher applied strain in comparison to CRFP.

Experimental testing to study the influence of the process-induced defects on the mechanical response of notched and un-notched specimens under compression and shear loading needs to be addressed. In the present work, the defect tolerance in-plane tensile loading was studied (Chapter 4). Under compression loading, more complex damage mechanisms would be expected as the result of the likelihood of buckling.

Finally, despite acceptable coupons as a representative part or sub-domain from a large variable stiffness plate with gap-defects being used for experimental purposes, the influence of the process-induced defects was not isolated completely. The free-edges, due to the small dimensions of the specimens, also influenced the damage results. Hence, future analyses on VSP should take into account the occurrence of delamination without the influence of outside conditions. Furthermore, future research should focus on the influence of other types of defects and more realistic experimental coupons with curved fibers should be designed.